SYNTHESIS AND CHARACTERIZATION OF BIOPOLYMER NANO-APATITE COMPOSITE ELECTROSPUN BIOACTIVE SCAFFOLD: A POTENTIAL APPLICATION FOR GUIDED TISSUE/BONE REGENERATION

BY

MUHAMMAD NADEEM

A thesis submitted in fulfilment of the requirements for the degree of

Doctor of Philosophy

at the Faculty of Dentistry
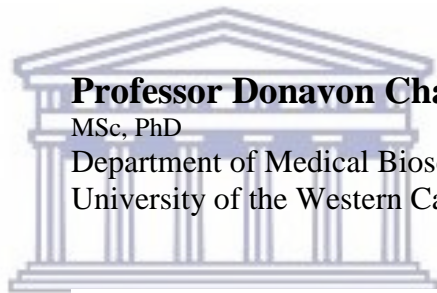University of the Western Cape

FEBURARY 2019

i

Promoters: **Professor Lawrence Stephen**
BChD, PhD
Head of Diagnostic Cluster
Faculty of Dentistry
University of the Western Cape

Professor Donavon Charles Hiss
MSc, PhD
Department of Medical Biosciences
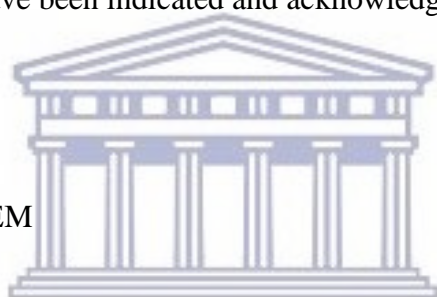University of the Western Cape

Dr. Abdul Samad Khan
BDS, MSc, PhD, MADM
Associate Professor Dental Materials
Interdisciplinary Research Centre in Biomedical Materials
(IRCBM)
COMSATS University, Islamabad Lahore Campus
Lahore, Pakistan

DECLARATION

I, the undersigned hereby declare that "*Synthesis and characterization of biopolymer nano-apatite composite electrospun bioactive scaffold*: *A potential application for guided bone/periodontal tissue regeneration*" is my own original work; that it has not been submitted before for any degree or examination in any university, and that all the sources I have used or quoted have been indicated and acknowledged by complete references.

MUHAMMAD NADEEM

FEBURARY, 2018

Signed: ------------------------------

ACKNOWLEDGEMENTS

thankful that in the midst of all her other responsibilities, she always spared time to help me with my project.

It is a pleasure to express my gratitude to Dr. Atif Javaid, polymer Department, UET, Lahore Pakistan, for his help and support in conducting the mechanical testing.

I convey special acknowledgment to Dr. Sheer Zaman, IRCBM COMSAT University Islamabad, Lahore Campus for his help to run the cell studies.

My family and friends have always understood and encouraged my academic endeavours. I am really grateful to them all especially to my wife Dr. Faiza Amjad who helped and encouraged me to compile this thesis.

Lastly, I am very grateful to all those who supported me in any respect during the completion of the project.
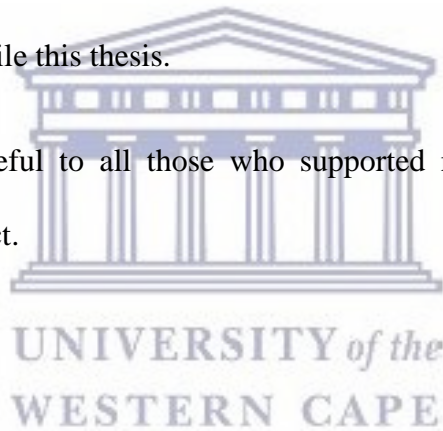
DEDICATION

This thesis is dedicated to my mother Razia khatoon, who passed away during my PhD project; she has always been a source of inspiration to me. Whatever I have achieved in life is because of her prayers.

&

To my supervisors

TABLE OF CONTENTS

LIST OF FIGURES

LIST OF TABLES

UNIVERSITY *of the*
WESTERN CAPE

LIST OF ABBREVIATIONS

ABM: Anorganic Bovine Derived Hydroxyapatite Matrix

AD: AlloDerm

ADM: AcellularFreezed Dried Dermal Matrix

AGEs: Advanced Glycation End products

ATR: Attenuated Total Reflectance

Ba: Barium

BG: Bioactive Glass

BCP: Biphasic Calcium Phosphate

BMP: Bone Morphogenetic Protein

Ca: Calcium

CAL: Clinical Attachment Loss

CAF: Calcium Alginate Films

CAF: Coronally Advanced Flap

CaO: Calcium Oxide

$[Ca(NO_3)_2 . 4H_2O]$:   Calcium Nitrate

CTAB: Cetyltrimethylammonium Bromide

CM:	Collagen Membranes
CPI:	Community Periodontal Index
CPC:	Calcium Phosphate Cement
CO_3:	Carbonate
COOH:	Carbonyl Group
DD:	Degree of Deacetylation
DDM:	Demineralized Dentine Matrix
DFDBA:	Demineralized Freezed Dried Bone Allograft
DHT:	De Hydrothermal Treatment
d-PTFE:	High density Polytetraflouroethylene
e-PTFE:	Expanded Polytetraflouroethylene
ECM:	Extracellular Matrix
EDC:	1-ethyl-3-(3- dimethylaminopropyl) Carbodiimide Hydrochloride
EDS:	Energy-Dispersive X- rays Spectroscopy
EDTA:	Ethylene Di-amine Tetra Acetic acid
EMD:	Enamel Matrix Derivatives
Er:YAG:	Erbium-doped:yttriumaluminiumgarnet

F: Flouride

FDBA: Freezed Dried Bone Allograft

FGF: Fibroblast Growth Factor

FGM: Functionally Graded Membrane

FTIR: Fourier Transform Infrared Spectroscopy

GA: Glutaraldehyde

GCF: GinigivalCrevicular Fluid

GBR: Guided Bone Regeneration

GTR: Guided Tissue Regeneration

H: Hydrogen

HA: Hydroxyapatite

HCA: Hydroxyl Carbonate Apetite

HFD: Horizontal Furcation Depth

HCl: Hydrochloric acid

IGF: Insulin like Growth Factor

K^+:   Potassium

KCl: Potassium Chloride
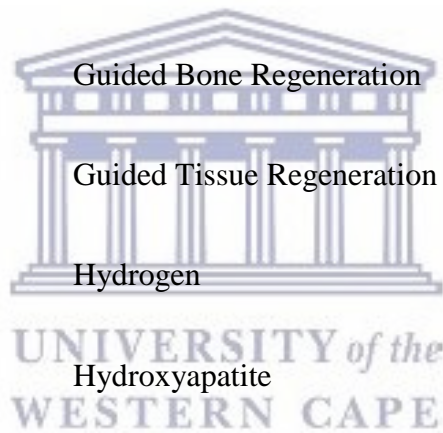
KOH:	Potassium Hydroxide
Mg:	Magnesium
MEM:	Minimum Essential Medium
MTT:	3-(4,5-dimethylthiazol-2-yl)-2, 5-diphenyl tetrazolium bromide
N:	Nitrogen
Na^+:	Sodium
Na –Alg:	Sodium Alginate
Na_2O:	Sodium Oxide
NaOH:	Sodium Hydroxide
NHS:	N Hydroxysuccinamide
NMP:	N-Methyl 2 Pyrolidone
$[(NH_4)_2HPO_4]$:	DiAmmonium Hydrogen Phosphate
OFD:	Open Flap Debridement
OH:	Hyrdoxyl
ORS:	Osseous Resective Surgery
P:	Phosphorus
PD:	Probing Depth
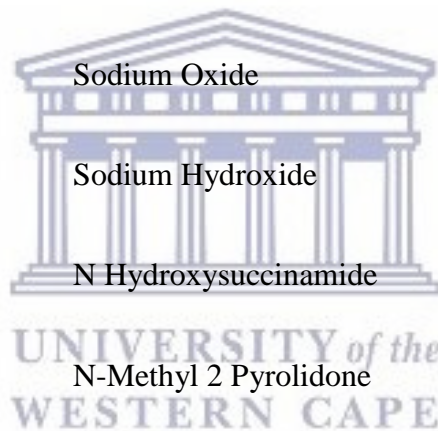
PBS: Phosphate Buffered Saline

PDLLCL: Copolymers of Lactic acid and Poly (ε-caprolactone)

PDS: Poly Dioxanon

PLA: Poly Lactic acid

PGA: Poly Glycolic acid

PCL: Poly(ε-caprolactone)

PDGF: Platelet Derived Growth Factor

PLGA: Poly Lactic-co-Glycolic Acid

PLLA: Poly (L-lactic acid)

PMMA: Polymethyl Methacrylate

PHEMA: Polyhydroxylethlmethacrylate

PO4:   Phosphate

P$_2$O$_5$:   Phosphorus Pentoxide

RTM: Regenerative Tissue Matrix

SEM: Scanning Electron Microscopy

SF: Silk Fibroin

Si: Silicon
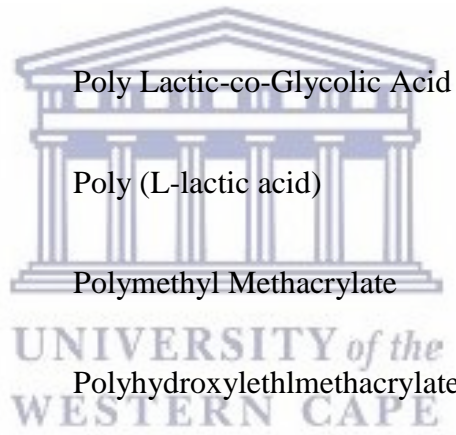
Si-HA: Silicon Substituted Hydroxyapatite

SiO_2:   Silicon Oxide

Sr: Strontium

TCP: β Tricalcium Phosphate

TEMED: Tetramethylethylenediamine

Ti-RPTFE: Titanium Reinforced Polytetraflouroethylene

UTM: Universal Testing Machine

UV: Ultraviolet

Zn: Zinc

CHAPTER 1

SCOPE OF THESIS
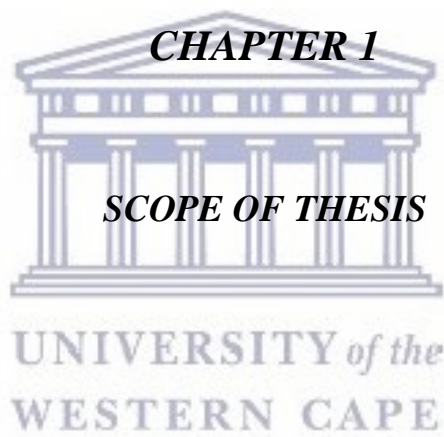
Search for an ideal scaffold for guided tissue/bone (GTR/GBR) regeneration continues as till now none of the commercially available GTR/GBR membrane fulfils the desired criteria. Currently, a variety of new materials and techniques have been investigated all over the world to improve the properties of GTR/GBR membranes. In the recent past three dimensional bioactive scaffolds composed of natural polymers have gained enormous popularity as potential future GTR/GBR devices. Electrospinning has emerged as one of the relatively simple, cost effective and efficient technique to fabricate three dimensional nanofibrous scaffolds in the field of tissue engineering. The rationale of this project is to investigate the natural polymers based bioactive nanofibrous scaffolds for GTR/GBR applications in the field of Periodontology.

The thesis consists of 6 chapters in total. The 2nd chapter gives an insight into periodontal diseases and treatment modalities used to treat such conditions. The literature review gives a broad overview of the concept of GTR and shed some light on the past, present and future of GTR/GBR scaffolds.

Chapter 3 outline the main aims and objectives of the current project.

Chapter 4 explains the materials and methods used for the synthesis and characterization of the nanofibrous scaffolds.

Chapter 5 consits of the results of all the characterization of membranes and nanofibrous scaffolds

Chapter 6 comprises of discussion about the results and conclusions made on the basis of the results.

CHAPTER 2

GUIDED TISSUE REGENERATION
PAST, PRESENT & FUTURE
(REVIEW OF LITERATURE)

2.1. INTRODUCTION

Periodontal diseases are highly prevalent and affect children, adolescents and adults in some form. Plaque induced gingival diseases are the most common type of periodontal diseases, while non-plaque induced gingival diseases are less prevalent and caused by specific bacteria, viruses, fungi or trauma. Gingival diseases are usually confined to gingiva and do not cause destruction of the tooth supporting structures. These conditions are completely reversible by the removal of bacterial plaque and improving the oral hygiene practices of the patient (Albandar & Tinoco, 2002).

On the other hand, periodontitis is a destructive form of periodontal diseases which is not reversible and results in the loss of tooth supporting structures including connective tissue attachment, cementum and bone (Kinane, 2001). The ultimate goal of the periodontal therapy is to gain the lost support of the teeth. Various treatment modalities have been advocated starting from simple non-surgical periodontal treatment including scaling and root planing to advance resective and regenerative surgical techniques (Claffey et al., 2004).

In the last three decades, regenerative periodontal therapy has gained immense popularity and Guided Tissue Regeneration (GTR) has emerged as an effective mode of treatment to gain the lost periodontal tissues. Following the same principles, this treatment modality is also used to regenerate bone around dental implants and termed as Guided Bone Regeneration (GBR). GTR/GBR works on the concept of isolating the periodontal defect by applying some barrier membrane to block the invasion of non-osteogenic cells (Villar & Cochran, 2010). Both non-resorbable and resorbable barrier membranes have been

4

used for this purpose. However, there are some limitations associated with each type and overall results with them have been modest (Scantlebury & Ambruster, 2012).

Till now, all the commercially available resorbable and non-resorbable membranes are bio-inert. There is need of the time to develop barrier membrane with better mechanical properties and bioactivity to enhance the bone growth. Therefore, the aim of the present study is to develop and characterize a *biopolymer nano-apatite composite electrospun bioactive GTR/GBR scaffold* with better physical properties and ability to release growth factors at defect site.

2.2: PERIODONTAL DISEASES

Any acquired or developmental disorder of the tissues supporting the teeth is defined as periodontal disease. The etiology of these disorders could be inflammatory, traumatic, neoplastic, genetic or metabolic. However, the most common type of periodontal diseases is inflammatory in nature, which is caused by accumulation of dental plaque on tooth surfaces and phenomenon of dysbiosis (Philstorm et al., 2005; Hill & Artis, 2011). The inflammatory periodontal diseases are termed as Gingivitis and Periodontitis.

2.2.1: GINGIVITIS

Gingivitis is the inflammation confined to the gingival tissues around a tooth usually intiated by accumulation of dental plaque. Gingivitis can occur in teeth with no signs of attachment loss as well as around periodontitis-affected teeth with previous attachment loss (Armitage, 1999). According to current classification system gingivitis is broadly classified as dental biofilm induced and non-dental biofilm induced gingival inflammation (Caton et al., 2018). Gingivitis is characterized by redness and edema of

5

gingival tissue, commonly painless, rarely causes spontaneous bleeding and is often present subtle clinical changes. In most instances patients are unaware of the disease or incapable to recognise it (Trombelli et al., 2018).

Plaque induced gingivitis is a consequence of interaction between bacterial plaque and host defense system. This interaction can be modified due the presence of local or systemic factors, medications and malnutrition. Local contributing factors such as calculus, malocclusion, faulty restoration and anatomical variations retain plaque and prevent its removal by routine oral hygiene measures (Armitage, 1999). The most common system factors that contribute to gingivitis are associated with endocrine hormones changes during puberty, pregnancy and ellitus (Figuero et al., 2013). Exaggerated inflammatory response in gingival tissues during pregnancy has been established by scientific evidence that these hormones may alter the tissue response to bacterial plaque and thus play an indirect role in the expression of periodontal diseases (Mealey & Moritz, 2003; Figuero et al., 2013). Alterations in the composition of sub-gingival plaque also occur due to high concentrations of estrogen and progesterone during pregnancy. Some bacterial species such as *Prevotella intermedia, Bacteroides* and *Campylobacter rectus* flourish in sub-gingival plaque of pregnant women, because they use estrogen as a substrate instead of vitamin K, all of which have a potential to cause periodontal damage (Armitage, 2013).

Non-plaque induced gingivitis is often a manifestation of systemic conditions; however, it may also correspond to pathological changes confined to gingival tissues (Holmstrup et al., 2018). Dental plaque is not a primary cause of inflammation in such type of

gingivitis and its removal does not cure the condition however, presence of dental plaque can increase the severity of clinical manifestations (Holmstrup, 1999).

2.2.2. PERIODONTITIS

Periodontitis is an infectious disease characterized by microbially –associated, host-mediated inflammation within the tooth supporting structures causing irreversible damage of periodontal ligaments, disrupting its attachment to cementum and bone. This is detected as clinical attachment loss (CAL) by circumferential measurement of the erupted dentition with a standardized periodontal probe (Tonetti et al., 2018).

Classification of the periodontitis has been revised extensively over the last 3 decades. According to current classification system the periodontitis is divided into three main categories (Armitage, 1999; Caton et al. 2018).

1. Necrotizing Periodontal disease
2. Periodontitis as a manifestation of systemic diseases
3. Periodontitis

Necrotizing ulcerative gingivitis (NUG) and Necrotizing ulcerative periodontitis was collectively referred to as necrotizing periodontal diseases (NPD) in 1999 classification of periodontal diseases (Armitage, 1999). Recently, it has been agreed upon that both NUG and NUP were associated with diminished systemic resistance to bacterial infections. In addition it was also reported that patients constantly exposed to a severe systemic compromise have a higher risk of developing NPD with faster and more severe progression (Herrera et al., 2018).

Many systemic disorders and some medications can affect the periodontium and cause loss of attachment and alveolar bone. Although most of these disorders are rare, they frequently cause considerable loss of periodontal apparatus by influencing periodontal inflammation or through mechanism distinct from periodontitis. Innate mechanisms are responsible for most of these disorders; however, some are acquired via environmental factors or life style (Albandar et al., 2018).

Chronic and aggressive periodontitis are similar in many clinical aspects it has been observed that chronic and aggressive forms of periodontitis have significant clinical differences including age of onset of the disease, rates of progression and pattern of bone destruction at affected sites, clinical signs of inflammation and its relevance with the amount of plaque and calculus present (Armitage & Cullinan, 2010).

In spite of extensive research on aggressive periodontitis since the 1999 workshop there is presently insufficient proof to consider aggressive and chronic periodontitis as two pathophysiologically different diseases (Tonetti et al., 2018). Therefore, in current classification system chronic and aggressive periodontitis has been described as periodontitis (Caton et al., 2018).

Although it is clear at this point that localized aggressive periodontitis (LAgP) demonstrate a distinctive phenotype but a more comprehensive understanding of the differences among events leading up to loss of bone in LAgP as compared chronic periodontitis need to wait for a more clear explanation of early events (Fine et al., 2018).

8

2.3. TREATMENT OF PERIODONTAL DISEASES

A broad range of treatment modalities exist in periodontics suitable for different conditions. Generally the periodontal treatment includes the following steps.

- Patient education regarding maintenance of oral hygiene and counseling on control of risk factors

- Removal of supra and sub-gingival bacterial plaque and calculus by means non-surgical periodontal therapy including scaling and root planing and correction of osseous deformities by surgical procedures.

- Finishing procedures such as reevaluation and reinforcement of oral hygiene practices

The following modes of treatment may be indicated during the course of treatment:

- Local or systemic delivery of chemotherapeutic agents to reduce, eliminate or change the quality of periodontal pathogens

- Resective periodontal procedures to reduce or eliminate periodontal pockets. Soft tissue resective procedures include gingivoplasty, gingivectomy and different flap procedures while hard tissue resective procedures comprises of ostectomy, osteoplasty, root resection, hemisection and odontoplasty

- Regenerative procedures include soft and hard tissue grafts, guided tissue regeneration, ridge augmentation, ridge preservation, implant site development and sinus grafting

- Periodontal plastic surgery for correction of gingival recession and other soft tissue defects

9

- Occlusal therapy to reduce trauma from occlusion

- Preprosthetic periodontal surgery to facilitate restorative or prosthetic procedures

- Extraction of teeth or roots

- Procedures to facilitate orthodontic movements such as tooth exposure, frenectomy, fiberotomy, gingival augmentation and implant placement

- Management of perio-systemic inter-relationship

(Position paper, 2001; Claffey et al., 2004)

2.3.1. NONSURGICAL PERIODONTAL THERAPY

Non-surgical periodontal therapy conventionally consists of sub-gingival debridement along with patient education to improve oral hygiene. Similar degree of sub-gingival debridement can be achieved with manual, sonic or ultrasonic instruments. However, operator skills and experience is one of the most important factors in the effectiveness of treatment (Claffey et al., 2004; Ishikawa & Baehni, 2004; Drisko, 2001). In addition to mechanical instrumentation supra and sub-gingival irrigation, local delivery and systemic antibiotics and host modulation may be employed as adjuncts to improve the outcomes (Greenstein, 2000; Drisko, 2000; Walker et al., 2004; Fritoli et al., 2015; Keestra et al., 2015; Jepsen & Jepsen, 2016).

However, none of the above mentioned methods can completely eradicate the periodontal microbes due to anatomical complexity of roots which may contain concavities and furcation area especially in deep periodontal pockets (Takasaki et al., 2009). Therefore, lasers and photodynamic therapy was introduced during 1990's in an attempt to achieve the complete elimination of periodontal pathogens (Lisa et al., 2013). Most commonly

10

used lasers are erbium-doped:yttrium-aluminiumgarnet (Er:YAG). Lasers possess efficient bactericidal properties by thermal denaturation or direct destruction of bacterial cells (Takasaki et al., 2009). Photodynamic therapy works on the principal that a photosensitizer substance which binds to target cell can be activated by light of suitable wavelength to produce singlet oxygen and other very reactive agents that are highly toxic to bacteria. Many studies show significant reduction in bacterial load with the use of lasers and photodynamic therapy alone or in combination of scaling and root planning however, complete eradication of periodontal pathogen is not possible (Aoki et al., 2004; Lisa et al., 2013; Meisel & Kocher, 2005; Pires et al., 2011; Sgolastra et al., 2013; Petelin et al., 2015).

2.3.2. SURGICAL PERIODONTAL THERAPY

Surgical techniques for the treatment of periodontitis are broadly classified as resective and regenerative periodontal therapy. Soft or hard tissue resective procedures are done at the expense of tissue in an attempt to control the disease and correct the anatomical deformities produced during the course of disease while the regenerative techniques are aimed at the gain of lost tissue (Lisa et al., 2013).

2.3.2.1. RESECTIVE SURGICAL PROCEDURES

 Pocket elimination was considered to be the most desirable outcome of periodontal therapy. Supra-bony and false pockets can be predictably treated with gingivectomy while shallow intra-bony pockets require osseous resctive surgery with or without apically repositioned flaps (Aimetti et al., 2015; Wang & Greenwell, 2001).

11

2.3.2.1. a. GINGIVECTOMY

Gingivectomy procedure is aimed at the removal of thick fibrotic soft tissue wall of the pocket (Claffy et al., 2004). It is indicated for the treatment of supra-bony pockets when the pocket is not extending to or beyond the mucogingival junction. This technique is also used to treat the gingival overgrowth caused by inflammatory periodontal diseases or due to the use of some drug (Camargo et al., 2001). Generally, this procedure is not indicated for the elimination of intra-bony pockets which require osseous surgery. Inadequate band of attached gingiva, acute inflammation, interference of frenal or muscle attachment and long clinical crowns also limit the use of this technique (Wang & Greenwell, 2001). Figure 2.1 shows the surgical technique of gingivectomy.

Fig: 2.1. Surgical technique of gingivectomy: Presence of false pockets, each pocket is marked at several points with pocket marker. Initial external bevel incision is performed with Kirkland's knife, interproximal incision is made by Orban's knife, pocket wall is removed, all the granulation tissue and residual calculus is removed with the help of curettes, gingivoplasty is performed with the help of electrosurgery or diamond bur. Area is covered with periodontal dressing. (Adapted from Camargo et al., 2001)

12

2.3.2.1. b. OSSEOUS RESECTIVE SURGERY

Osseous resective surgery (ORS) involves modification of alveolar bone around teeth to reestablish the morphology to resemble normal bone with positive architecture. The earliest myth for osseous surgery was that the bone surface was considered necrotic or infected due to periodontal infections and it should be removed (Carnevale & Kaldahl, 2000). ORS is indicated for the treatment of shallow intra-bony defects (≤3mm) not suitable for regenerative procedures. The outcomes of the ORS are reduced probing depths and gingival contours that enhance good self-performed oral hygiene (Carnevale & Kaldahl, 2000; Aimetti et al., 2015).

ORS has certain clinical limitations such as opening of the furcation especially in interproximal area of two maxillary molars. In addition compromised aesthetic in anterior region and sensitivity of the exposed roots are other major concerns (Carnevale & Kaldahl, 2000). Figure 2.2 shows the osseous resective surgery of interproximal defects.
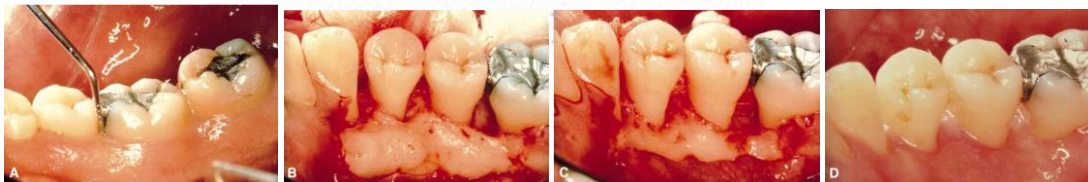
Fig: 2.2: Osseous resective surgery for interproximal defects (Carnevale & Kaldahl, 2000)

2.3.2.2. REGENERATIVE PROCEDURES

Regeneration means reproduction or reconstruction of a damaged or lost part of body in such a way that morphology and function of damaged or lost tissues are fully restored. The ideal goal of regenerative periodontal treatment is to restore the morphology and

13

function of all components of periodontium including gingiva, periodontal ligaments, root cementum and alveolar bone (Susin & Wikesjö, 2013). On the other hand, periodontal repair implies healing of the periodontium without reconstruction of lost tooth attachment apparatus. Healing most commonly occurs with the formation of long junctional epithelium (Bosshardt & Sculean, 2009). Periodontal regenerative procedures includes soft tissue grafts, autogenous bone and bone substitutes grafts, biomodification of root surfaces, guided tissue regeneration (GTR) and any combination of these techniques (Position paper, 2005).

2.3.2.2. a. BONE GRAFTS

Bone grafts are the second most commonly transplanted tissue after the blood. Annual frequency of bone replacement procedures is more than 500,000 in the United States and 2.2 million worldwide for repair of bone defects in the field of orthopaedic, neurosurgery and dentistry (Giannoudis et al., 2005). These materials have been widely used to enhance bone formation in order to correct the periodontal osseous defects. Bone graft materials offer a structural scaffold for clot formation, maturation and remodeling that favors bone formation in bony defects (Sculean & Jepsen, 2004). Ideally bone grafts should be non-toxic, nonantigenic, easily malleable, freely available and resistant to infection. It must be capable of stimulating new attachment apparatus including bone, cementun and periodontal ligaments. It is assumed that these materials facilitate the regeneration through their osteogenic, osteoinduction and osteoconduction properties (Nasr et al., 1999; Zimmermann & Moghaddam, 2011; Reynolds et al., 2010).

14

The bone grafting and replacement materials are categorized into four main groups namely: (Bayerlein et al., 2006)

- Autogenous bone grafts

- Allogenic grafts

- Xenogenic grafts

- Alloplastic grafts

2.4. GUIDED TISSUE/BONE REGENERATION (GTR/GBR)

At present time, the ultimate goal of periodontal therapy is not only to arrest the inflammatory disease progression but also to regenerate the lost supporting structure of the teeth including cementum, periodontal ligament and bone. GTR is a procedure employed to regenerate lost periodontal tissue through differential tissue response. The technique involves meticulous debridement of the bone defect and root surface followed by selective cell repopulation of the area by means of a cell occlusive membrane (AAP Position paper, 2005).

Melcher, (1976) was the first to present the idea of compartmentalization. He divided the periodontium into four compartments namely the lamina propria of the gingiva, periodontal ligament, cementum and the alveolar bone. He postulated that the cells from these compartments can grow into periodontal defect and can repopulate the root surface after periodontal therapy. The nature of the attachment that will form after treatment will be defined by the type of cells that will occupy the defect space. Therefore, it is believed that the migration of gingival epithelial cells which grow at a faster rate compared to mesenchymal cell is the major factor that hampers the periodontal regeneration after

15

conventional therapy. In addition growth of gingival connective tissue on root surface results in connective tissue attachment and root resorption. Melcher's hypothesis was tested in a series of studies and led to the development of rationale of GTR (Gottlow et al., 1986; Nyman et al., 1982; Gottlow et al., 1984). Figure 2.3 shows the four compartments of periodontium.
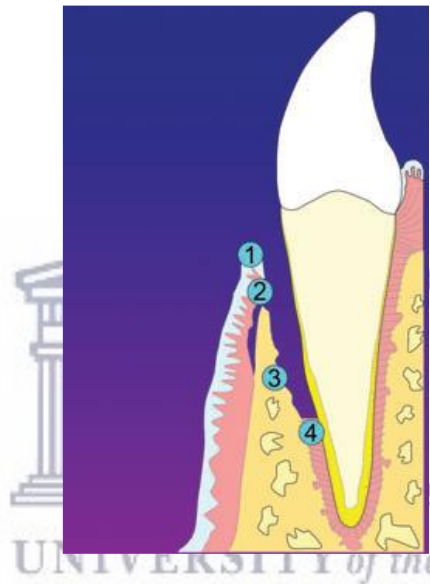
Fig: 2.3. Schematic drawing illustrating the four compartments of periodontium: (1) oral gingival epithelium; (2) gingival connective tissue; (3) bone from the alveolar process; and (4) periodontal ligament. (Adapted from Bosshardt & Sculean, 2009)

The biologic rationale of GTR is based on the concept that placing a physical barrier prevents downwards migration of gingival epithelial and connective tissue cells and provides exclusive space for the inward migration of mesenchymal cells on exposed root surface from periodontal ligaments which support periodontal regeneration (Villar & Cochran, 2010; Cortellini & Tonetti, 2000; Karring et al., 1993). Figure 2.4 shows the normal healing process while figure 2.5 illustrates the rationale of GTR.

16
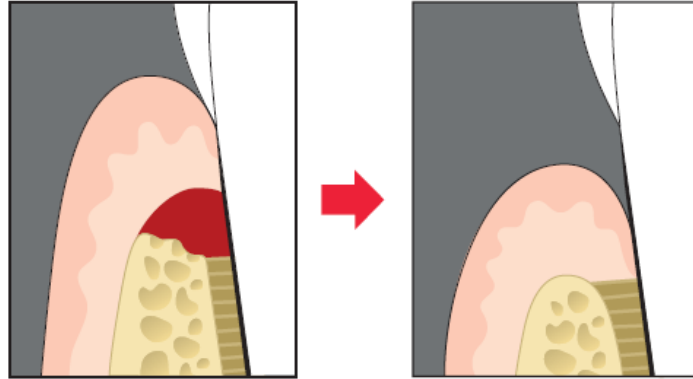
Fig: 2.4. Normal healing process following adaptation of periodontal flap with significant reduction of the attachment apparatus (Adapted from Ramseier et al., 2012)
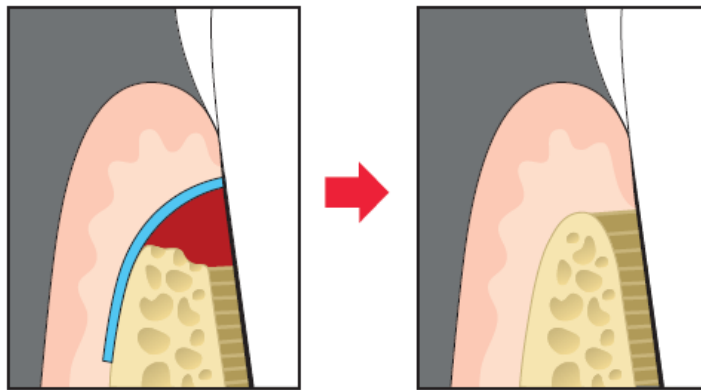
Fig: 2.5. Guided Tissue Regeneration: A barrier membrane is placed to stop downgrowth of gingival epithelium (GTR), prevent long junctional epithelium formation (Adapted from Ramseier et al., 2012)

In the light of the compartmentalization hypothesis Nyman et al., (1982) conducted the first clinical study using non-resorbable Millipore filters in an effort to achieve new attachment and demonstrated that periodontal regeneration could be achieved by preventing the epithelial cells and fibroblasts from the gingival tissue to repopulate into periodontal defects. During the same time, Dahlin et al. (1889) published the landmark study describing a reconstructive technique to create new bone around exposed parts to dental implants following the principals of GTR. This surgical method was later termed as guided bone regeneration (GBR).

17

Both GTR and GBR rely on a physical barrier in the form of a membrane to isolate the defect from overlaying soft tissues in order to block the fast growing gingival cells to repopulate the area. The barrier membranes are of prime importance in the outcome of GTR/GBR techniques (Scantlebury & Ambruster, 2012).

2.4.1 PRINCIPLES OF GTR/GBR

Success of the GTR/GBR is dependent of the following principles:

Cell exclusion: the fast growing gingival tissue cells are blocked to gain access to the defect site and forming fibrous connective tissue.

Tenting: the barrier is applied in such a way that a space is created and defect is completely isolated. In order to achieve good isolation the edges of barrier are extended 2 to 3 mm beyond the margins of defect.

Scaffolding: the space produced by tenting becomes occupied with a fibrin clot, which act as a scaffold for the growth of progenitor cells.

Stabilization: the barrier stabilizes and protects the newly formed clot form being disturbed during healing due the movement of the overlaying tissue. For this purpose the barrier membranes are usually fixed into position with the help of sutures, mini screws or bone tacks.

18

Framework: in non-space maintaining defects the barrier must be supported to avoid collapse. For this purpose autogenous bone or bone replacement grafts are used which also act as framework for regeneration (Hitti & Kerns, 2011; McAllister & Haghighat, 2007)

2.4.2. GTR/GBR MEMBRANES

The barrier membrane used for GTR/GBR can be broadly classified into three groups.

First generation barrier membranes: are non-resorbable membranes. Expanded polytetrafluoroethylene (e-PTFE) was the first barrier membrane specially designed for periodontal regeneration which was further modified by embedded bendable titanium struts. Such titanium reinforced ePTFE membrane open new horizons for vertical ridge augmentation.
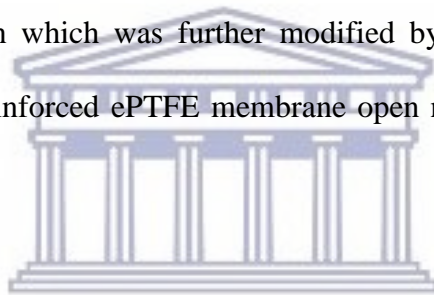
Second generation barrier membranes: are resorbable or biodegradable. There are two main categories of resorbable membranes: natural and synthetic. Natural membranes are produced from natural polymers such as collagen and chitosan while synthetic are made from aliphatic polyesters and their copolymers.

Third generation barrier membranes: are based on the concept of tissue engineering which not only acts as barrier but also as delivery devices. They are capable of releasing specific agents such as drugs, growth factors and adhesion molecules at the defect site in order to enhance the periodontal regeneration.

(Scantlebury & Ambruster, 2012; Sam & Pillai, 2014)

19

2.4.3. IDEAL PROPERTIES OF GTR/GBR MEMBRANES

A GTR/GBR membrane should possess the following properties to achieve the best results:

Biocompatibility: should integrate with the host tissue without eliciting any inflammatory response or immune reaction

Cell-occlusiveness: should have capability to exclude undesirable cell types from entering the isolated space adjacent to the root surface

Biodegradability: should have suitable degradation profile that could match new tissue formation

Mechanical stability: should have adequate mechanical and physical properties to allow its adaptation

Space making: should be able to maintain space adjacent to the root surface

Sustained strength: should have sufficient sustained strength to avoid membrane collapse during healing

Clinical manageability: should be easy to manipulate clinically

Osteoinduction: should have the ability to release bioactive proteins and interact with cells to promote cell adhesion, proliferation, migration and differentiation

(Taba et al., 2008; Sculean et al., 2008; Chen & Jin, 2010; Sam & Pillai, 2014)

2.4.4. FIRST GENERATION BARRIER MEMBRANE

(NON-RESORBABLE MEMBRANES)

The first commercial membrane for GTR/GBR was created from Teflon (PTFE) by W.L. Gore and Associates (Flagstaff, AZ, USA). Based on its structure PTFE can be divided into two types: expanded-PTFE (e-PTFE) and high density-PTFE (d-PTFE) (Scantlebury & Ambruster, 2012; Rakhmatia et al., 2013).

e-PTFE membrane (Gor-Tex®) has two parts: a collar portion having open microstructure with internodal distance of 25 µm which helps in clot formation and collagen fiber attachment while blocks epithelial migration; and an occlusive portion with internodal distance of less than 8 µm which covers root surface and avert flap tissues contact with the root surface. These small pores allow nutrient inflow while inhibit the penetration of tissue cells (Rakhmatia et al., 2013; Scantlebury & Ambruster. 2012; Hitti & Kerns, 2011; Gottlow 1993).

High density PTFE (d-PTFE) membranes (TefGen, Cytoplast) were designed to lessen the bacterial contamination associated with e-PTFE membrane. These membranes are non-porous, non-permiable, non-expanded and dense produced from 100% pure medical grade bio inert PTFE. The thickness of different commercially available d-PTFE membranes varies from 0.2 to 0.3 µm. In addition it was claimed that they can be removed with gentle tug in a way comparable to that used for suture removal, thus, eliminating the need of second stage surgery for membrane removal (Sam & Pillai, 2014; Marouf & El-Guindi, 2000).

Keeping in view, the critical need of space maintenance during regenerative healing researcher explored the potential for reinforced preformed or shapeable e-PTFE

membranes for the treatment of large defects. To meet this need titanium reinforced membranes were developed that incorporate laminated component of commercially pure titanium. Such membranes have the same structural properties of non-reinforced e-PTFE membrane with additional capacity to be shaped and provide and maintain space in situations where bone morphology is not conducive to support non-reinforced membranes (Sam & Pillai, 2014; Hardwick et al., 1995).

Several investigators have reported good efficacy of non-resobable membranes in the treatment of periodontal and peri-implants defects. Cortellini et al., (1993) evaluated the osseous healing response of 40 intrabony defects with 1-2 and three wall combination component of 6.1 ± 2.5 mm depth treated using non-resorbable membrane (Teflon). Intrasurgical baseline clinical measurements were compared with clinical measurements after one year surgical re-entry. A substantial bone regeneration of 4.3 ± 2.5 mm was observed however there was a 0.4 ± 1.9 mm resoption of osseous crest with net gain of 4.7mm. Similarly, Pontoriero et al., (1988) reported complete resolution of grdae II furcation defects in 90 % of mandibular molars treated using e-PTFE. However, the results of GTR treatment of class III furcation defects with e-PTFE were not promising and Pontoriero & Lindhe, (1998) observed that although there was some reduction in probing pocket depths but none of the furcation defects was healed and retained the characteristics of grade III furcation.

Figure 2.6 shows the use of e-PTFE membrane for GTR.
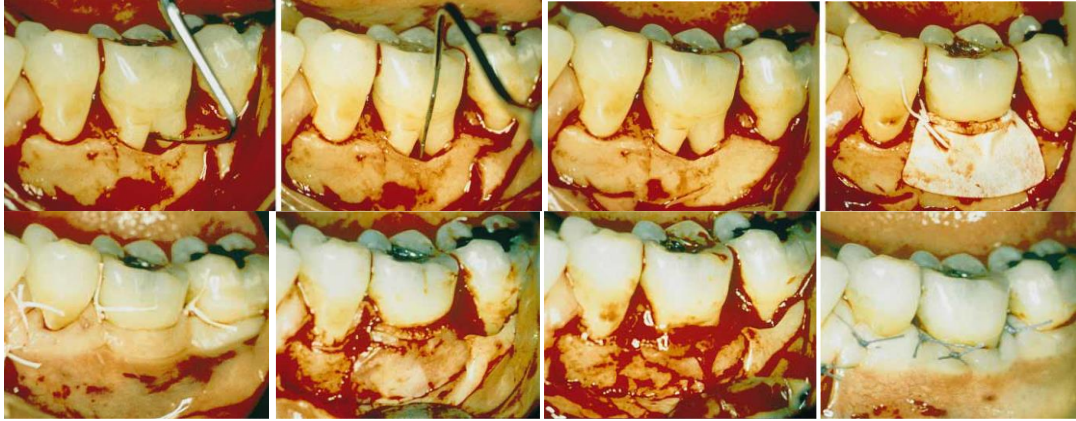
Fig: 2.6. Use of e-PTFE membrane for GTR: grade II furcation defect on buccal aspect of left mandibular molar treated with GTR using e-PTEF. Surgical re-entry shows complete fill of defect (Adapted from Sanz & Giovannoli, 2000)

High density PTFE (d-PTFE) membranes were also investigated by many researches. Carbonell et al., (2014) in a literature review on the potential of d-PTEF in GTR/GBR concluded that d-PTFE may be a promising barrier but scientific evidence is limited. d-PTFE has been shown to be superior compared to resobable membrane but no significant difference was found when compared to e-PTFE. Marouf & El-Guindi, (2000) compared the clinical efficacy of e-PTFE and d-PTFE. They found that d-PTFE membranes were easy to remove while e-PTFE showed firm adherence to the bone. A greater speed and quality of bone regeneration was observed in osseous defects covered with e-PTFE. Therefore, they suggested that semipermiable membrane (e-PTFE) is more effective than occlusive d-PTFE membrane. While Lee et al., (2010), in their comparative study using two different non-resobable membranes found that there is no significant difference in bone regeneration potential between e-PTFE and d-PTFE. Bartee, (1995) reported that d-PTFE membranes can be predictably used in situations where primary closure is not possible and membrane is exposed. Such exposure does not cause any significant adverse effect on healing. Barber et al., (2007) conducted a study using d-PTFE without

23

achieving a primary closure and concluded that d-PTFE offer an ideal treatment options for large defects where primary closure is difficult to achieve with added advantages of predictable regeneration of bone and soft tissue and preservation of keratinized tissue. Figure 2.7 illustrates the use of d-PTFE membrane for GTR.

Fig: 2.7. Use of d-PTFE membrane for GTR: Flapless and atraumatic extraction of the fractured premolar, immediate implant in the extraction socket bone grafted and d-PTFE membrane positioned over the graft and implant with no attempt to achieve primary closure, three weeks later, the membrane remaining exposed, week 6, the membrane removed and a consolidated layer of osteoid tissue present, thick keratinized tissue at the surgical, 4 months after implant placement., flapless uncovering of the implant in the presence of thick keratinized tissue (Adapted from Barber et al., 2007)

Titanium-reinforced PTFE (Ti-PTFE) membranes have also been tested for their GTR/GBR potential in many clinical studies. Cortellini et al., (1995) conducted a controlled clinical trial to compare the regenerative potential of Ti-PTFE, e-PTFE and flap procedure for the treatment of intrabony defects and reported that a significantly greater clinical attachment gain was observed in Ti-PTFE group. Similarly, many studies have demonstrated excellent results using Ti-PTFE membranes to repair osseous defects around dental implants and vertical ridge augmentation procedures (Tinti & Benfenati, 2001; Simion et al., 2007; Canullo & Malagnino, 2008; Merli et al., 2007). Figure 2.8 shows vertical and horizontal augmentation using Ti-PTFE.

24

Fig: 2.8. Vertical and horizontal augmentation using Ti-PTFE vertical and horizontal defect around implants, Ti-PTFE membrane adapted, membrane removal all space under membrane filled with bone (Adapted from Tinti & Benfenati, 2001)

Titanium meshes ((Cytoflex® Mesh and Cytoplast™ Osteo-Mesh TM-300) composed of pure titanium are another form of non-resobable barrier and has been used for alveolar ridge augmentation with admirable results (Assenza et al., 2001). Titanium mesh offer excellent mechanical properties which help to stabilize the bone grafts. Its rigidity helps to maintain the space and good stability prevents graft displacement. In addition the smooth surface of the titanium mesh makes it less vulnerable to bacterial contamination on exposure during healing (Levine et al., 2014; Roccuzzo et al., 2004; Proussaefs & Lozada, 2006). Figure 2.9 shows the use of titanium mesh for GBR around dental implant.

Fig: 2.9. Titanium mesh used for GBR around implant: second stage surgery after 4 months, mesh removal shows good bone formation around implant (own pt)

Major disadvantage of non-resobable membranes is the need of a second stage surgery for membrane removal which may interfere with healing and cause damage to newly formed tissue. Exposures of the membrane during healing and bacterial contamination are

other concerns associated with their use which may lead to the premature removal of membrane and jeopardize success (Sam & Pillai, 2014; Rakhmatia et al., 2013; Zhang et al., 2013).

2.4.5. SECOND GENERATION BARRIER MEMBRANES
    (RESORBABLE MEMBRANES)

In order to avoid the need of second stage surgery for membrane removal resorbable barriers were introduced in the early 1990's. Vicryl mesh (Johnson and Jhonson) was the first resobable barrier launched commercially. However, the product was not largely adopted because it was not purposely designed for GTR (Scantlebury & Ambruster, 2012). A double-layered membrane (Guidor® Guidor, Sunstar Americas, Inc, Chicago, IL) was the first resobable membrane particularly designed for GTR. It was made of polylactic acid (PLA) treated with acetyltributylcitrate to achieve flexibility to improve barrier adaptation to the bone (Scantlebury & Ambruster, 2012; Aurer & Jorgić-Srdjak, 2005).

Histological animal studies shows that the barrier function was maintained for at least six weeks and complete resoption of membrane occurred in 6-12 months. However, foreign body reaction characterized by the presence of macrophages and multinuclear cell in histological sections was reported. Although clinical studies advocated membrane efficacy in various type of periodontal defects, the membrane vanished from the market for unknown reasons (Gottlow et al., 1994; Falk et al., 1997).

A large verity of resobable membranes are commercially available in the market and broadly classified into synthetic and natural depending upon the type of material used to develop the membrane. Tables 2.1 and 2.2 shows the currently available resobable

26

membranes (Bunyaratavej & Wang, 2001; Rakhmatiaet al., 2013; Gentile et al., 2011; Almazrooa et al., 2014; Soheilifar et al. 2014).

Membrane	Commercial Name	Material	Properties
Synthetic resorbable membranes	Resolut	Poly-DL lactid/ Co-glycolid	Resorption: 8- 10 weeks Good space maintainer Good tissue integration
	Vicryl	Polyglactin 910 Polyglicolid/ polyl actid 9:1	Resorption: 4–12 weeks well adapted Four preformed shapes
	Atrisorb	Poly-DL lactide and Solvent	Resorption: 36–48 Weeks Soft Well-adaptable Interesting resorptive Characteristics
	Epi-Guide	Poly-DL lactic Acid	Resorption:6–12 weeks 3-layer technology Self-supporting
	Vivosorb	DL-lactide-ε-caprolactone (PLCL)	Anti-adhesive barrier Maintains its mechanical properties for up to eight weeks
	OsseoQuest	Hydrolyzable Polyester	Resorption:16–24 weeks Good tissue integration
	Biofix	Polyglycolic Acid	Resorption: 24–48 weeks Isolate the space from cells from soft tissue and bacteria
	Mempol	Polydioxanon	Experimental membrane bilayer structure first layer is nonpermeable

Table: 2.1. Synthetic Resorbable membranes

Membrane	Commercial Name	Material	Properties
Natural resorbable membranes	Bio-Gide	Xenogenic collagen Type I & III form porcine skin	Resorption: 24 weeks Usually used in combination with filler materials
	Bio-mend	Xenogenic collagen Type I form bovine tendon	Resorption: 8 weeks Fibrous network modulate cell activities
	Biosorb Membrane	Xenogenic collagen Type I form bovine	Resorption:26–38 weeks Provided stable fixation Good tissue integration
	Neomem	Xenogenic collagen Type I form bovine	Resorption: 26–38 weeks Double-layer product used in severe cases
	OsseoGuard	Xenogenic collagen Type I form bovine	Resorption:24–32 weeks Improves aesthetic outcome
	Ossix	Xenogenic collagen Type I form porcine	Resorption: 16–24 weeks Increase the woven bone
	AlloDerm	Collagen type I derived from cadaveric human skin	Resorption: 16 weeks Biocompatible with good tissue integration
	Paroguide	Type I horse collagen: 96 - 98%; Glycosaminoglycanes (chondroitin sulphate): 2 - 4%.	Resorption: 8 to 12 weeks Allow cellular selection
	Periogen	Xenogenic collagen Type I & III form bovine dermis	Resorption: 4-8 weeks

Table: 2.2. Natural Resorbable membranes

2.4.5.1 SYNTHETIC RESORBABLE MEMBRANES

Synthetic resorbable membranes are synthesized mainly from polyesters such as poly (glycolic acid) (PGA), poly (lactic acid) (PLA), poly (ε-caprolactone) (PCL), poly (hydroxyl valeric acid), poly (hydroxyl butyric acid) and their co-polymers. Under strict controlled settings aliphatic polyesters can be prepared reproducibly (Gentile et al., 2011). The broad range of polyesters materials allows for the manufacture of large variety of membranes with diverse physical, mechanical and chemical properties. In addition these polymers have the ability to degrade completely through hydrolysis. The degradation products are completely eliminated from body through natural pathways. PGA is transformed into metabolites and PLA can be cleared through the tricarboxylic acid cycle (Zhang et al., 2013; Gentile et al., 2014).

Synthetic resorbable membrane Resolute® consists of an occlusive layer of glycolide and lactic copolymer and a porous mesh of polyglycolide fiber. The compact film prevents cell ingrowth and porous network enhance tissue integration. The membrane maintains its structure for 4 weeks and complete degradation occurs in 5 to 6 months (Aurer & Jorgić-Srdjak, 2005).

Cortellini et al., (1997) conducted the clinical trial comparing resobable membrane (Resolute®) with conventional non-resorbable membrane (e-PTFE) and access flap. Results indicated that both resorbable and non-resorbable membranes showed significantly higher clinical attachment gain than access flap procedure. While the CAL gain was not significantly different between resorbable and non-resorbable groups. Histological study by Hürzeler et al., (1997) showed that membrane was resorbed completely in 5 months with no apparent adverse effect on healing. Histologic

29

observation indicated a reparative healing with long junctional epithelium with limited cementum and bone formation in control group (with no membrane) while test specimens (with membrane) exhibited significantly more deposition of cementum and bone.

Fibers of polyglactin 910, a copolymer of glycolide and L-lactide (9:1 wt/wt) were used to create snugly woven mesh (Vicryl Periodontal Mesh®) (Fleischer et al., 1998). The polyglactin 910 is biocompatible elicit no antigenic reaction and maintain its physio-chemical properties during first 3-4 weeks. Although lack of tissue integration and formation of recession defects has been reported in animal studies, clinical observations advocate effectiveness equal to that of other GTR membranes (Zybutz et al., 2000; Aurer & Jorgić-Srdjak, 2005).

Copolymers of lactic acid and ε-caprolactone (PDL-PCL) have also been used to develop GTR/GBR membranes and demonstrate a slower degradation time as compared PLA membranes. PCL is characterized by higher hydrophobicity and low water solubility than PGA, PLA and their co-polymers. A commercially available product (Vivosorb®, consisting of poly(DL-lactide-co-ε-caprolactone) primarily used as nerve guide, has been reported to have GBR potential. It retains its mechanical properties up to 8 weeks and shows biocompatibility occlusiveness and space maintenance (Hoogeveen et al., 2009; Gentile et al., 2011).

Atrisorbs® (DL-lactide polymer) was introduced in 1996, and composed of 37% of a liquid polymer of lactic acid that is dissolved in 63% N-methyl-2- pyrrolidone (NMP) (Bogle et al., 1997). Atrisorb® membrane is the first liquid product adapted directly at the surgical site. An irregular membrane is produced when polymer is placed in 0.9% saline solution for 4–6 min in a special cassette. The resultant membrane is 600-750 μm thick

30

and can be trimmed into desired shape. It can easily be adapted into the defect by applying moderate pressure. Complete resorbption of the membrane takes 6 to 12 months. Histological and clinical studies proved its efficacy in the treatment of periodontal defects (Gentile et al., 2011; Hou et al. 2004).

Epi-Guide® is a three layered membrane composed of D-L polylactic acid designed to stop the downgrowth of epithelial cells and fibroblasts. The structure and function of the membrane remains intact for 5 months with a complete bioresorption after one year. The porous layer is kept in contact with gingival tissue to promote fibroblast infiltration and attachment while the layer facing towards the bone has limited porosity that favors fluid uptake, helps adherence to tooth surface and inhibit fibroblast penetration. Finally, the inner labyrinth layer creates pathways, while internal chambers facilitate collateral circulation and flow of interstitial fluid in the membrane (Aurer & Jorgić-Srdjak, 2005; Gentile et al., 2011).

Mempol® is a bilayered experimental membrane synthesized from polydioxanon (PDS), a dioxanon polymer. The first layer is fully impermeable covered with PDS loops 200 μm long and is faced towards gingival tissue for integration with connective tissue. Frequent recession of gingival tissue has been experienced during testing of membrane. However, the clinical efficacy has been reported to be comparable to that of PLA membranes (Christgau et al., 2002; Lang et al., 1994).

In addition to polyester, organic polymer polyurethane containing urethane group -NH-CO-O- with diverse properties has also been tested for the production of GTR/GBR membranes. Polyether urethanes are degraded through enzymatic and oxidative degradation and membrane has been found to be present in tissues after 8 weeks of

31

implantation. Animal studies have reported that polyurethane membranes have a tendency to swell up after placement. Inflammation at the flap margins and recession has also been observed which is more pronounced compared to with that polylactic membrane (Aurer & Jorgić-Srdjak, 2005; Pinchuk, 1994; Ratner et al., 1988).

2.4.5.2. NATURAL RESORBABLE MEMBRANES

Among the various resorbable materials which were investigated for their potential application as GTR/GBR barriers, collagen appeared to be the most favorable choice and was considered to fulfill the majority of the requirements expected from bioresorbable membrane (Ferreira et al., 2012). Collagen is the most abundant protein in human body. Until now almost 28 types of collagen have been identified among these, type 1 collagen is the most common type present in the extracellular matrix (ECM) (Hitti & Kerns, 2011). Collagen has great potential as biomaterial for tissue engineering due to its certain inherent properties such as biocompatibility, hemostastic function through its ability to aggregate platelets which may aid in early clot formation and stabilization, chemotactic properties which may facilitate fibroblast migration, high porosity, abundant availability, easy processing, hydrophilicity, low antigenicity, clinical manageability and controlled biodegradability induced by cross-linking reagents (Ferreira et al., 2012; Hitti & Kerns, 2011; Bunyaratavej & Wang, 2001; Owens & Yukna, 2001).

Native collagen undergoes relatively quick degradation, hence does not offer the required stability desirable for a barrier membrane for GTR/GBR (Tal et al., 2008). Extended stability by decreasing the degradation of collagen has been achieved through cross-linking techniques. A number of cross-linking techniques have been developed to extend

32

membrane resoption and boost biodurability such as ultraviolet and gamma irradiation, treatment with glutaraldehyde, diphenylphosphorilazide or diphenyl-phosphoryl-azide and ribose (Ghanaati, 2012; Patino et al., 2002; Brunel et al., 1996; Tanaka et al., 1988).

Membranes based on natural materials are typically derived from human skin (Alloderm®), porcine skin (Bio-Gide®) and bovine achilles tendon (BioMend®) consisting of either type I or a combination of type I and type III collagen (Zhang et al., 2013; Bottino & Thomas, 2015; Patino et al., 2002). The Alloderm® regenerative tissue matrix (RTM) is an acellular freeze dried dermal matrix (ADM) of type I collagen derived from cadaveric human skin and is used for soft tissue applications such as root coverage, gingival augmentation, soft tissue ridge augmentation and soft tissue augmentation round dental implants (Batista et al., 2001; Núñez et al., 2009).

AlloDerm GBR® RTM is produced utilizing the same process. Thickness of the matrix ranges from 0.5 mm to 0.9 mm and is used as GTR/GBR barrier membrane especially in situation where primary closure is difficult to achieve (de Andrade et al., 2007; Griffin et al., 2004; Borges et al., 2009; Bottino et al., 2012). Figure 2.10 shows the morphology and clinical use of Alloderm.
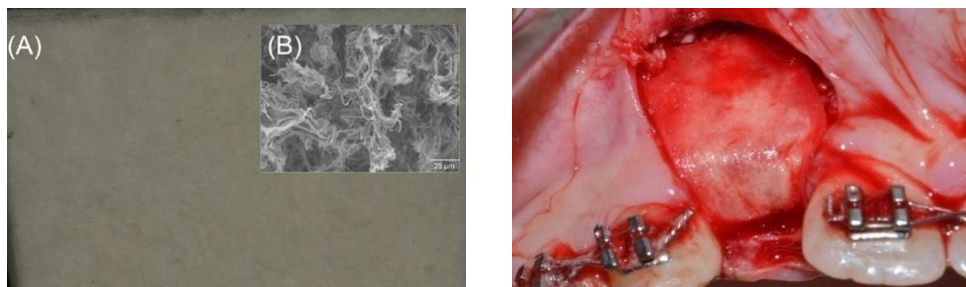
Fig: 2.10. Alloderm: (A). Macrophotograph of AlloDerm® (AD). AD is a minimally processed, non-crosslinked, freeze-dried acellular dermal matrix collagen-based graft. (B). SEM image shows the fibrous nature and highly porous graft morphology (Bottino et al., 2012), Alloderm adapted for GBR around dental implant. (Own patient)

The most popular commercial collagen membrane is Bio-Gide® which is synthesized from xenogenic type 1 collagen of porcine skin. The membrane has a bi-layered structure with a dense and a porous layer. The smooth surface of compact layer stops epithelial cell infiltration while the porous layer enhances integration of newly formed bone (Owens & Yukna, 2001; Zhang et al., 2013). Figure 2.11 shows the structure of Bio-Guide.

Fig: 2.11. Structure of Bio-Gide®, scanning electron microscopy (SEM) at magnifications of 100x and 400x (adapted from Zhang et al., 2013; Scantlebury & Ambruster, 2012)

BioMend® is produced from 100% type I collagen derived from bovine deep flexor (Achilles) tendon. The membrane is semipermeable with a pore size of 0.004 μm and degrades in four to eight weeks (Patino et al., 2002; Aurer & Jorgić-Srdjak, 2005; Gentile et al., 2011).

A systematic review conducted by Stoecklin-Wasmer et al., (2013) analyzed the outcomes of GTR with collagen membranes (CM) as compared to open flap debridement (OFD) without any other type of membrane. The meta-analysis showed that, in infrabony defects, GTR with bioabsorbable CM, either alone or in combination with bone substitutes, yielded more beneficial effects than OFD in terms of CAL gain.

The GTR/GBR potential of resorbable membranes has also been compared with non-resorbable membranes. Eickhilz et al., (2006) reported significant CAL gain in class II furcation defects with both non-resorbable and resorbable membrane and results were stable after 10 years. There was no significant difference in stability between the groups.

34

Pretzl et al., (2008) conducted a ten year follow up study to compare the long terms results of GTR therapy with non-resorbable and resorbable membranes in the treatment of intra-bony defects and observed that there was no significant difference in CAL gain in both groups and results were stable in 12 of 16 sites after 10 years. Parrish et al., (2009) reviewed the clinical efficacy of non-resobable and resorbable membranes in guided tissue regeneration techniques and concluded that non-bioabsorbable membranes without graft material, collagen membranes with graft material were found to be superior to OFD with or without graft material.

The major drawback of bioresorbable membrane is the lack of space maintaining properties particularly collagen membranes. Therefore, use of bone graft materials leads to improved clinical outcomes. Unpredictable degradation behavior which can significantly alter the bone formation is another limitation of bioresorbable membrane. If membrane becomes exposed the enzymatic activity of macrophages and neutrophils cause rapid degradation of membrane hence affecting the structural integrity which results in compromised barrier function and less bone regeneration. Possible disease transmission from animal is another concern (Rakhmatia et al., 2013; Dimitriou et al., 2012).

2.4.6. THIRD GENERATION BARRIER MEMBRANES

(BIOACTIVE MEMBRANES)

Currently available GTR/GBR membranes act as a physical barrier to avoid epithelial and connective tissue down-growth thus favoring the regeneration of periodontal tissues in GTR procedures and bone formation around dental implants in GBR techniques. These conventional membranes possess many structural, mechanical and bio-functional limitations therefore; the ideal membrane for GTR/GBR has yet to be developed (Bottino et al., 2012).

As the concept of tissue engineering has gained popularity, third-generation membranes have evolved based on the model of tissue engineering to overcome the critical drawback associated with both 1st generation (non-resorbable) and 2nd generation (bioresorbable) membranes. Third generation membranes are supposed to not only act as barriers but also as delivery devices to release specific agents such as growth factors, drugs and signaling molecules at the defect sites in order to orchestrate and direct natural wound healing in an enhanced way. That is why 3rd generation membranes are considered bioactive (Sam & Pillai, 2014).

The notion of tissue engineering was proposed by Langer and Vacanti in the early 1990's to regenerate the lost or damaged human tissues and organs. According to Langer and Vacanti, (1993) tissue engineering is an interdisciplinary field that applies the principles of engineering and the life sciences toward the development of biological substitutes that restore, maintain, or improve tissue function. The principles of tissue engineering are based on the combination and interplay of three major essentials such as scaffolds or membranes, regenerative cells or stem cells, and cell signaling molecules or

36

growth factors. All over the world researchers are working on the development of new tissues and organs both in vitro and in vivo following the principles of tissue engineering with very encouraging results (Bottino & Thomas, 2015). Figure 2.12 represents the 3 major component of tissue engineering.
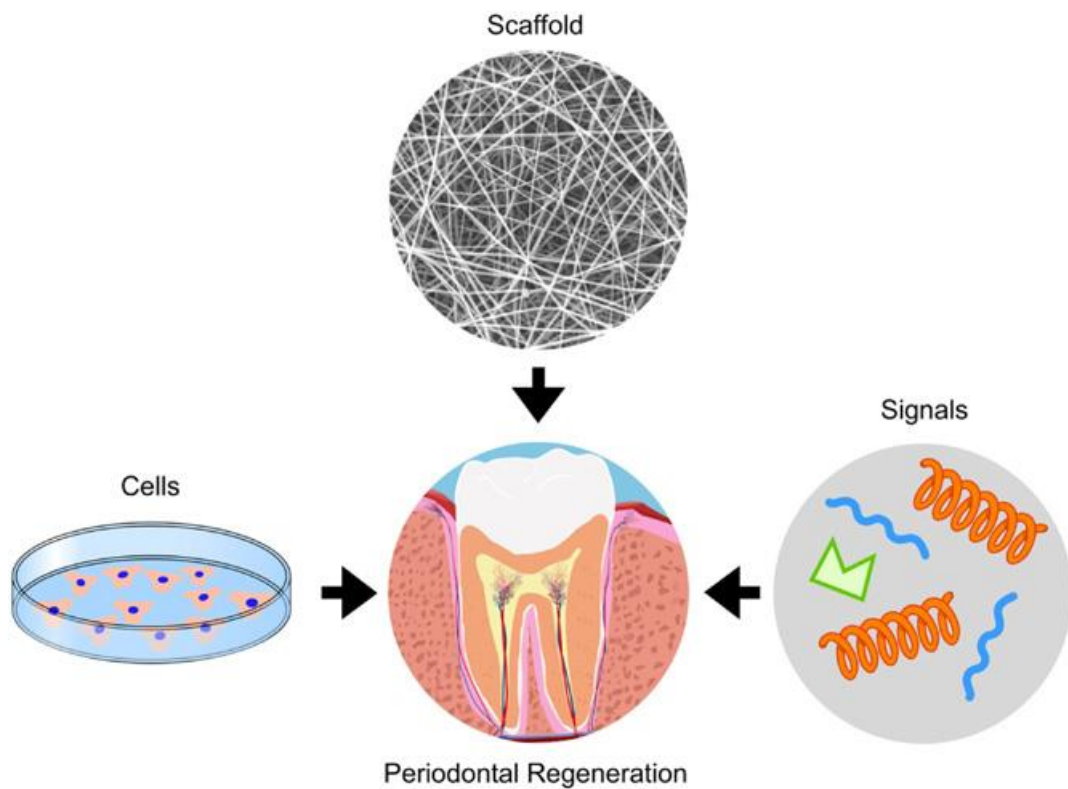
Fig: 2.12. Schematic representation of the three major components involved in dental and craniofacial tissue engineering: (1) signaling molecules (e.g. bone morphogenetic proteins), (2) progenitor/stem cells (e.g. dental pulp stem cells) and (3) extracellular-matrix mimicking scaffolds. (Adapted from Bottino & Thomas, 2015).

2.5. RECENT ADVANCES IN THE DEVELOPMENT OF GTR/GBR MEMBRANES

Recently, there has been huge emphasis on the need of both bioactive and multilayered GTR/GBR membranes in order to not only meet the basic requirements of satisfactory mechanical properties and degradation profile, but, more importantly to deliver biomolecules such growth factors, drugs and/or stem cells in order to amplify the regenerative potential (Bottino & Thomas, 2015).

For this purpose, many new natural polymers have been investigated for their potential as GTR/GBG membrane materials such as chitosan, alginate, silk fibroin and gelatin. Moreover, blending of natural and synthetic polymers has also been attempted in order to overcome the week mechanical properties and unpredictable degradation behavior of collagen membranes (Wang et al., 2016). Inorganic fillers such as Hydroxyapatite (HA), β-Tricalcium Phosphate (TCP), Bioactive Glasses (BG) have also been incorporated into polymers to make composites. Addition of inorganic fillers increases mechanical flexibility of the scaffold under wet conditions which assures easy handling in clinical situations (Gentile et al., 2014).

There have been major advances in the field of nanotechnology which led to the development of GTR/GBR scaffolds with 3 dimensional configurations using a range of different techniques. Of these, electrospun nanofibrous scaffolds which closely resemble the extracellular matrix (ECM) have gained tremendous interest (Bottino & Thomas, 2015). The spatially designed and functionally-graded (FGM) bioactive scaffolds have been developed with this technique and loaded with growth factors, antibiotics and

adhesion molecules in order to enhance bone formation and reduce the detrimental microbial influences on periodontal regeneration (Gentile et al., 2014; Jang et al., 2009).

2.5.1. POTENTIAL FUTURE MATERIALS FOR GTR/GBR

A number of synthetic and natural biodegradable polymers have been comprehensively explored as scaffold materials for tissue engineering applications. The synthetic polymers being investigated include polycaprolactone, poly (lactic-co-glycolic acid), poly (ethylene glycol), poly (vinyl alcohol), and polyurethane. The natural polymers gained popularity are chitosan, alginate, gelatin and silk fibroin. The naturally derived polymers are of exceptional interest due to their biological and chemical similarities to natural tissues (Kim et al., 2008).

CHITOSAN: In the past two decades chitosn has been revealed to be a fascinating candidate material for GTR/GBR scaffolds due to its superior biocompatibility, non-antigenicity, suitable degradation profile to harmless products, hemostatic ability, manageability in wet environment, antimicrobial, fungistatic and wound healing potential (Kim et al., 2008; Wnag et al., 2016).

Chitosan is a linear polysaccharide, composed of glucosamine and N-acetyl glucosamine units linked by β (1–4) glycosidic bonds. The content of glucosamine is known as the degree of deacetylation (DD) which is defined as the average number of *N*-acetyl-D-glucosamine units per 100 monomers expressed as a percentage (Dash et al., 2011). Figure 2.13 shows the chemical structure of chitosan.
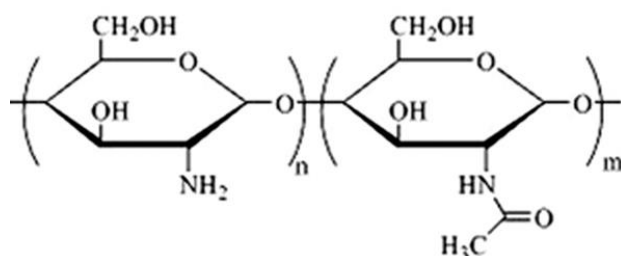
Fig: 2.13. Structure of chitosan (adapted from Dash et al., 2011)

The molecular weight of chitosan may range from 300 to over 1000 Daltons with degree of deacetylation (DD) from 30% to 95% depending upon the source, method of preparation and physiological conditions (Dash et al., 2011). Chitosan is obtained from chitin which is widely distributed in nature and believed to be the second most abundant biomaterial after cellulose (Kumirska et al., 2010). Major sources of chitin are crustaceans (shrimps, crabs, lobsters, krill, etc) insects and certain fungi (Majeti & Kumar, 2000). Crustacean shells consist of proteins (30–40%), calcium carbonate (30–50%), chitin (20–30%) and pigments (astaxanthin, canthaxanthin, lutein or β-carotene). These proportions vary from species to species and from season to season (Aranaz et al., 2009). The most common method for chemically extracting chitin from crustacean shells involves demineralization (elimination of calcium carbonate) and deproteinization in aqueous NaOH or KOH. Flow chat below and figure 2.14 shows the steps of extraction of Chitosa (Dutta et al., 2004).

Crustacean shells → Size reduction → Protein separation → (NaOH) → Washing Demineralization (HCl) → Washing and Dewatering → Decolouration → Chitin → Deacetylation (NaOH) → Washing and Dewatering → Chitosan

Scheme of chitosan extraction from crustacean shells (Adapted from Dutta et al., 2004)
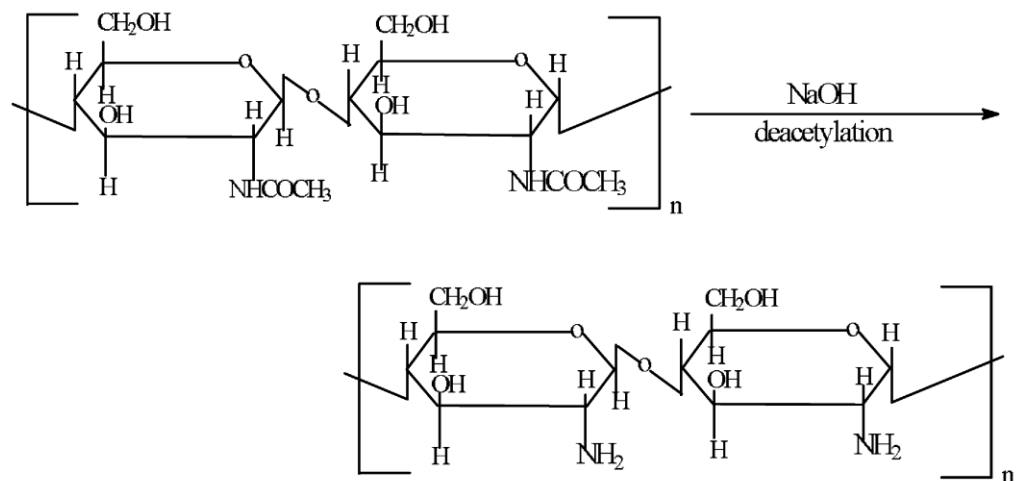
Fig: 2.14. N-deacetylation of chitin (Adapted from Majeti & Kumar, 2000)

A large variety of biomedical application for chitin and chitin derivatives have been reported in literature (Lin et al., 2015; Tseng et al., 2013). A number of studies have shown the use of chitosan scaffolds and membrane in the treatment of burns and deep wounds. It is believed that the wounding healing properties are due the ability of chitosan to stimulate fibroblast production by affecting the fibroblast growth factor (Jayakumar et al., 2011; Ong et al., 2008). Another important biomedical application of chitosans is the development of drug delivery systems such as nanoparticles, hydrogels, microspheres, films and tablets (Bernkop-Schnürch & Dünnhaupt, 2012; Agnihotri et al., 2004; Bhattarai et al., 2010). Chitosan has also been investigated as bone, cartilage, nerve and organ regenerative material with promising results (Costa-Pinto et al., 2011; Suh & Matthew, 2000; Haipeng et al., 2000; Yuan et al., 2004; Park et al., 2003).

Although to date the chitosan based GTR/GBR membranes are still in the animal trial phase, however, the results show great potential of this material in GTR/GBR procedures (Xu et al., 2012; Wang et al., 2016). Unique bioproperties of chitosan make it an

41

attractive candidate for tissue engineering. One of the most important properties is the antibacterial effect of chitosan on both Gram negative and Gram positive bacteria (Li et al., 2010; Liu et al., 2004). In addition chitosan has been reported to have antifungal, antitumor and antioxidative activity (Kong et al., 2010). The exact mechanism for antibacterial activity of chitosan is not yet entirely understood but has been assumed to involve cell lysis, breakdown of the cytoplasmic membrane and chelation of trace metal cations essential for microbial growth (Aranaz et al., 2009; Benhabiles et al., 2012). However, research on its antibacterial application in GTR/GBR is insufficient (Kong et al., 2010; Wang et al., 2016).

Chitosan is considered a non-toxic and biocompatibale polymer. Toxicity has been reported to be dependent on DD and molecular weight. At lower DD toxicity is less prominent and less related to molecular weight. No significant cytotoxic effects have been found in both in vitro and in vivo studies (Baldrick, 2010; Zhuang et al., 2003; Kean & Thanou, 2009; Xu et al., 2011; Bavariya et al., 2014).

A number of in vitro and animal studies have evaluated the regenerative potential of chitosan based membranes. Hong et al., (2007) prepared asymmetric gradational-changed porous membranes of chitosan for GTR by means of immersion-precipitate phase inversion technique and reported that membranes had excellent biocompatibility and adequate degradation rate. Ho et al., (2010) developed the asymmetric chitosan membranes for GTR by using the two-step phase separation process. These membranes exhibited strong antimicrobial activities. The osteoblastic cells cultured with the asymmetric chitosan membrane also expressed higher cellular activity and in the drug release experiment, the membrane was proven to be suitable for the multi-staged delivery

(Yeo et al., 2005). Animal study conducted also concluded that the chitosan membrane appeared to be of great promise for application in GTR (Kuo et al., 2006)

ALGINATE: Alginates have gained particular interest in medical and pharmaceutical industries due to their usefulness in specific applications and ability to form hydrogels under comparatively mild pH and temperature (Sun & Tan, 2013). Alginates are generally considered non-toxic, biocompatible, biodegradable, non-antigenic, less expensive and abundantly available in nature. In addition, alginates meet the important requirement of being amenable to sterilization and storage (d' Ayala et al., 2008).

Commercially available alginate is classically extracted from brown algae (*Phaeophyceae*), including *Laminaria hyperborea, Laminaria digitata, Laminaria japonica, Ascophyllum nodosum,* and *Macrocystis pyrifera* by treatment with aqueous alkali solutions, typically with NaOH. The extract is filtered and in order to precipitate alginate either sodium or calcium chloride is added to the filtrate. This alginate salt can be converted into alginic acid by treatment with dilute HCl. After additional refinement and alteration, water-soluble sodium alginate powder is produced (Rinaudo, 2008; Lee & Mooney, 2012). Another source of alginates is bacterial biosynthesis which provides alginate with more defined chemical structure and physical properties. Bacterial alginate can be produced from *Azotobacter vinelandii, A. chroococcum* and several species of *Pseudomonas* (Remminghorst & Rehm, 2006) Recent advancements in regulation of alginate biosynthesis in bacteria along with relative ease of bacteria modification may permit production of alginate with tailor-made properties for wide range of medical applications (Sabra et al., 2001).

Alginate is an anionic and hydrophilic polysaccharide. It consists of blocks of (1–4)-linked β-D-mannuronic acid (M) and α-L-guluronic acid (G) monomers. Characteristically, the blocks are composed of three different forms of polymer segments: consecutive G residues, consecutive M residues and alternating MG residues which differ in composition and sequence affecting molecular weight and physical properties. Molecular weight of alginate ranges from 10 to 1000 kDa. Alginates obtained from different sources vary in M and G contents and length of each block. Currently, more than 200 different types of alginates are being manufactured (Tonnesen & Karlsen, 2002; d' Ayala et al., 2008). Figure 2.15 shows the chemical structure of alginate.
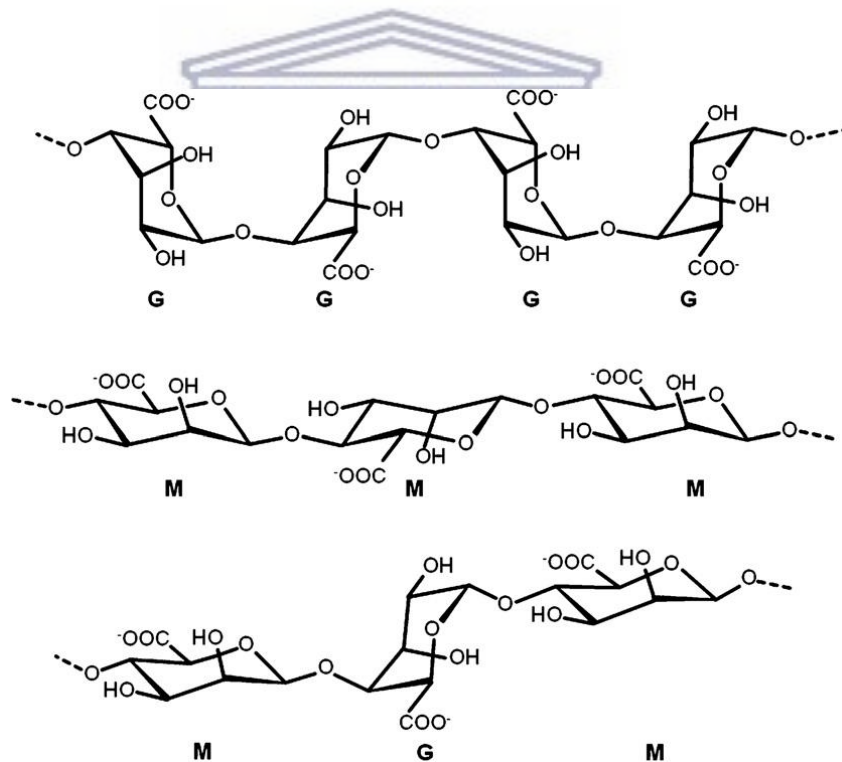
Fig: 2.15. Chemical structure of alginate, G block, M bock and alternating M & G blocks

(Adapted from Lee & Mooney, 2012)

44

Alginate has established enormous utility and potential for biomedical applications especially in the areas of wound dressings, (Pereira et al., 2013; Thu et al., 2012) drug delivery, (Liu et al., 2016; Jain & Bar-Shalmon, 2014) *in vitro* cell culturing (Andersen et al., 2015; Brito et al., 2014) and tissue engineering (Saltz & Kandalam, 2016; Sun & Tan, 2013; Draget & Taylor, 2011). For biomedical application the alginate is mainly used in the form of a hydrogels which are three-dimensionally cross-linked networks based on hydrophilic polymers with high water content, however, alginate gels have a drawback of limited mechanical stiffness (Augst et al., 2006; Lee et al., 2004).

Alginate alone has not been used widely for the development of GTR/GBR membranes however; it has extensively been blended with other polymers to produce GTR/GBR scaffolds. Ishikawa et al. (1999) designed a self setting alginate based GTR/GBR membrane which can be prepared and placed on bone defect during surgery. Ueyama et al., (2002) evaluated the biocompatibility and GBR potential of this self setting alginate membrane and concluded that the alginate membrane successfully works as a GBR membrane. In addition there was no inflammatory response surrounding the membrane. Jian-qi et al., (2002) compared the calcium alginate films (CAF) with collagen membranes (CM) for GBR in rabbits and reported that CAF induced more dense bone formation compared to CM due to its ability to collect osteoinductive factors early.

Alginate-based biomaterials demonstrate a promising future for repair and regeneration applications. However, current alginate is still unable to meet all the desired parameters such as biodegradation, bioactivities and mechanical properties, therefore, efforts should be made to develop more alginate based material with novel chemical, physical and biological properties (Sam & Pillai, 2014).

GELATIN: Gelatin is a natural polymer that is derived from collagen by acidic or basic hydrolysis and its chemical composition closely resembles natural collagen. The most common source of gelatin is from mammals mainly bovine and pork (Young et al., 2005; Patil et al., 2000). Gelatin has received great attention as an appropriate biomaterial for tissue engineering and GTR/GBR due to its abundant availability, low cost, easy handling, good biocompatibility, low immunogenicity, plasticity, adhesiveness, promotion of cell adhesion and growth. However, gelatin possesses weak mechanical properties and rapid degradation profile which makes it a poor candidate for GTR/GBR membranes (Zhan & Ping, 2012; Sisson et al., 2009; Wang et al., 2016).

In order to improve mechanical properties of gelatin cross-linking is performed either by physical or chemical method. Physical cross-linking methods include dehydrothermal treatment (DHT), plasma treatment and ultraviolet (UV) treatment while chemical cross-linking is achieved by using bifunctional reagents such as glutaraldehyde (GA) and 1-ethyl-3-(3-dimethylamino propyl) carbodiimide hydrochloride (EDC) (Ulubayram et al., 2002). Physical treatment usually results in a low degree of cross-linking because the reaction occurs superficially only at the surface of the materials. On the other hand, chemical treatment provides a higher level of cross-linking but sometimes changes the material chemical structure (Apostolov et al., 2000; Ratanavaraporn et al., 2010).

Cross linking of gelatin with genipin which is a natural occurring cross-linking agent has also been reported in literature (Bigi et al., 2002). Genipin can be obtained from an iridoid glucoside, geniposide, abundantly present in gardenia fruits. It is far less cytotoxic compared to GTA and gelatin films cross-linked with genipin exhibit properties very closed to GTA cross-linked films (Sung et al., 2001; Kawadkar et al., 2013).

46

Although the tensile properties of the gelatin fibrous membrane can be greatly improved by cross-linking showing high elastic characteristics in moist state however, an exceptionally lower Young's modulus has been observed (Bigi et al., 2002). Therefore, gelatin is rarely used alone for GTR/GBR membrane. Zhang et al., (2009) successfully synthesized nanofibrous GTR membrane by electrospinning of gelatin aqueous solution by elevating the spinning temperature. In order to improve the stability and mechanical properties in moist state, the gelatin nanofibrous membrane was chemically cross-linked by 1- ethyl-3-dimethyl-aminopropyl carbodiimide hydrochloride and N-hydroxyl succinimide. Tensile test revealed that the hydrated membrane becomes malleable and provides predetermined mechanical properties and *in vitro* culturing of periodontal ligament cells exhibited excellent cell attachment, growth, and proliferation. Noritake et al., (2011) fabricated GBR membrane by combining β-TCP particles with dissolved gelatin hydrogel and cross-linking molecules with glutaraldehyde. The results showed that membrane exhibited biocompatibility and stimulated statistically significant bone formation compared to uncovered controls.

SILK FIBROIN: Silk fibroin (SF) a natural protein based polymer that is spun into fibers by some lepidoptera larvae such as silkworms, spiders, scorpions, mites and flies. The most widely characterized silks are from the domesticated silkworm, *Bombyx mori*, and from spiders (*Nephila clavipes* and *Araneus diadematus*) (Mottaghitalab et al., 2015). SF has gained increased consideration in the recent years for its prospective use in biomedical applications due to its high biocompatibility, low immunogenicity, excellent mechanical properties, structural integrity, limited bacterial adhesion, and controllable biodegradability (Jao et al., 2016).

47

Biodegradation is a serious obstacle for the application of silk based biomaterials for tissue engineering. SF is difficult to degrade because of its special crystallization and orientation, as well as dense structure and is defined by United States Pharmacopeia as non-degradable biomaterial (Cao & Wang, 2009). However, literature suggests that SF is degradable but at a very slow rate (Horan et al., 2005). Being a protein SF is vulnerable to biological degradation by proteolytic enzymes and upon incubation with proteolytic enzymes, silk films display an obvious decrease of sample weight and degree of polymerization which is dependent on the type of enzyme. The final waste of SF is analogous amino acids which are simply absorbed *in vivo* (Arai et al., 2004). Degradation of SF by proteolytic enzymes typically occurs within a year in which it loses the majority of its tensile strength and fails to be recognized at implanted site within two years or even longer. In conclusion, silk degrades very slowly in vivo and absorption rate depends upon the type of SF, (virgin silk or extracted black braided fibroin), processing technique and diameter of SF fibers, health and physiological status of patient, implantation site and mechanical environment (Lia et al., 2003; Wang et al., 2008; Altman et al., 2003).

SF has extensively been used for biomedical applications in different forms such as films, gels, membranes, sponges and scaffolds. Applications of SF comprise burn wound dressings, drug delivery matrices, and 3D scaffolds for bone, cartilage, ligament, and vasculature regeneration (Murphy & Kaplan, 2009; Omenetto & Kaplan, 2010; Veparia & Kaplan, 2007).
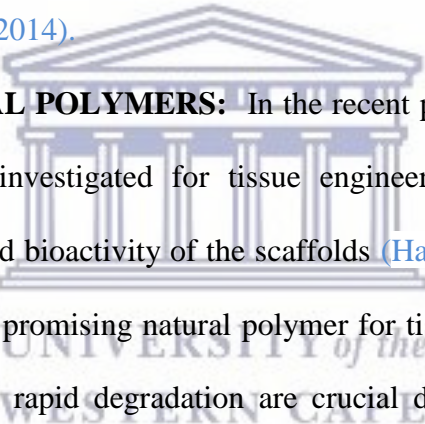
SF has also been investigated as GTR/GBR material. Kim et al., (2005) evaluated the biocompatibility and biological efficacy of SF membrane in a rabbit calvarial model and reported a complete union of bone across defect in 8 week and complete bone healing at

12 week. Kim et al., (2014) compared the efficacy of SF membrane with collagen membrane (Bio-Gide®) and concluded that SF membrane successfully enhanced the comparable bone volume in calvarial defects. Similarly, Ha et al., (2014) compared the silkworm-cocoon derived SF membrane with commercially available collagen and PTEF membranes and observed a higher bone fill in SF membrane group. Lu et al., (2015) investigated the GBR potential of an electrospun nanofibrous SF membrane in rat calvarial defects and compared it with a collagen membrane (Bio-Gide®), the results showed superior outcomes with SF membrane. Yoo et al., (2016) in their study observed various cellular responses (i.e., cell attachment, viability, and proliferation) of osteoblast-like MG63 cells on an SF membrane and found cell proliferation was significantly higher on SF membrane compared to controls.

BLENDS OF POLYMERS: No single polymer can meet all the criteria required for a perfect GTR/GBR membrane such as biocompatibility, adequate degradation, satisfactory mechanical and physical properties, and ample strength to avoid collapse and structure that mimics the extracellular matrix, therefore, it is still a challenge to develop a GTR/GBR membrane which meets the ideal properties. The solution to this dilemma may be the blinding of two or more different polymers to overcome their respective short comings and show more positively synergistic effects (Wang et al., 2016).

BLENDS OF SYNTHETIC POLYMERS: blends of different synthetic polymers have been investigated to overcome the limitation associated with individual polymer, such as poly (L-lactic acid) (PLLA) and poly (e-caprolactone) (PCL), shows almost opposite properties. PLLA is brittle with superior degradation profile and better tensile strength, while PCL is flexile with low degradation and better toughness. The varying

49

combinations of these polymers make them more useful for GTR/GBR applications (Chen et al., 2013; Ajami-Henriquez et al., 2008). Similarly, Poly Lactic-co-Glycolic Acid (PLGA) possesses excellent cytocompatibility while its mechanical strength is very week which makes it difficult to maintain the shape of PLGA membranes. Therefore, PLGA has been blended with other polymers such as PCL to improve the mechanical properties of PLGA and retain the superior cell affinity (Tsuji & Ishizaka, 2001; Ning et al., 2014) GTR/GBR scaffolds based of synthetic copolymers has also been recently developed by electrospinning with promising results which suggests that synthetic polymer composites may have brilliant future in GTR/GBR (Ershuai et al., 2016; Li et al., 2015; Goonoo et al., 2014).

BLENDS OF NATURAL POLYMERS: In the recent past blends of natural polymers have extensively been investigated for tissue engineering in order to improve the mechanical properties and bioactivity of the scaffolds (Harikumar et al., 2014). Collagen is known to be the most promising natural polymer for tissue engineering however, low mechanical strength and rapid degradation are crucial drawbacks associated with this biomaterial. In order to overcome these limitations collagen has been blended with other natural polymers such as chitosan, gelatin and silk fibroin (Zhou et al., 2010; Gorczyca et al., 2014).

Similarly, chitosan has gained immense popularity as a potential GTR/GBR biomaterial; however, its bioactivity is inferior to protein polymers and its mechanical properties are also poor. Many researchers have blended chitosan with other polymer to improve its mechanical properties and bioactivity (Chen et al., 2006; Yan et al., 2005; Gobin et al., 2005). Although alginate and gelatin are rarely used alone for GTR/GBR scaffolds owing

50

to their very poor mechanical properties and unpredictable degradation, however, these materials have widely been blended with other natural polymers for tissue engineering (Eslaminejad et al., 2007; Yang et al., 2009; Hongbin et al., 2008; Jetbumpenkul et al., 2012).

The results of such studies suggest that blends of natural polymers are promising future candidates for GTR/GBR applications because such blends possess adequate mechanical and structural properties and better bioactivity compared to individual polymer (Wang et al., 2016).

BLENDS OF NATURAL AND SYNTHETIC POLYMERS: Natural polymers always show better bioactivity and biocompatibility compared to synthetic polymers. When blended with synthetic polymers, the resultant copolymers may exhibit the advantages of both natural and synthetic polymers (Bottino & Thomas, 2015).

Gelatin when used alone for the synthesis of GTR/GBR membrane shows poor mechanical properties and unpredictable degradation profile while blending of Gelatin with poly(ε-caprolactone) (PCL) shows better biocompatibility and has been successfully used for the development of GTR/GBR membranes with improved mechanical, physical, and chemical properties. In addition biodegradation time can also be optimized to meet the requirements of GTR/GBR (Xue et al., 2014; Ji et al., 2013).

Many studies have reported chitosan and collagen based hybrid system developed by blending with synthetic polymers. GTR/GBR membranes based on such hybrid systems have shown higher potential of adhesion, proliferation and differentiation of osteoblasts on membranes surface both in vitro and in vivo. Superior mechanical properties and

biodegradation have also been reported for such hybrid systems (Liao et al., 2004; Liao et al., 2005; Jiang et al., 2006; Liao et al., 2010; Chen et al., 2013).

2.5.2. INCORPORATION OF BIOACTIVE INORGANIC FILLERS

In the recent past, substantial attention has been devoted to the structure of bone extracellular matrix (ECM) in order develop ideal biomaterials for GTR/GBR scaffolds. In order to design a GTR/GBR scaffold that structurally resembles the ECM, incorporation of inorganic fillers such as Hydoxyapatite (HA), β-tricalcium phosphate (β-TCP), bioactive glass (BG) and glass-ceramic in synthetic and/or natural polymers has extensively been investigated (Wang et al., 2016). Such composite membranes are considered to have the ability to conserve the structural and biological functions of damaged hard tissue in a more proficient and biomimetic way and exhibit suitable properties, such as bioactivity, osteoconduction, osteoinduction and biocompatibility for applications in the field of GTR/GBR (Gentile et al., 2011).

TRICALCIUM PHOSPHATE (TCP): TCP $[Ca_3(PO4)_2]$ is a porous calcium phosphate compound which exists either in alpha (α) or beta (β) crystalline forms. Both forms are produced in the same way, though they exhibit different resorption properties. α-TCP has a monoclinic structure and consists of columns of cations while β-TCP has rhombohederal structure. β form is more stable compared to α form (Sukumar et al., 2008; Yamada et al., 2010).

β-TCP contains almost similar proportions of calcium and phosphate to cancellous bone however, its compressive strength reaches only 1/20 of cortical bone (Barrere et al., 2006; Reynolds et al., 2010). β-TCP shows higher solubility thermodynamically, therefore, β-TCP ceramics are considered to degrade more rapidly than HA (Kamitakahara et al.,

52

2008). Several studies have reported that β-TCP favors the attachment, differentiation and proliferation of osteoblasts and mesenchymal cells and enhance bone formation (Kamitakahara et al., 2008; Haimi et al., 2009). Many investigator have incorporated β-TCP in both synthetic and natural polymer to synthesize scaffold for bone tissue engineering (Yanoso-Scholl et al., 2010; Bian et al., 2012; Lei et al., 2007; Ignatius et al., 2001).

BIOACTIVE GLASS (BAG): Bioactive-glass (BAG) is well known for its beneficial biological response due to its osteoconductive and osteostimulatory ability, and exceptional biocompatibility for use in human body (Profeta & Prucher, 2015). BAG was invented by Larry Hench and his co-workers at the University of Florida in late 1960's (Profeta & Prucher, 2015; Sarin & Rekhi, 2016). BAG has extensively been used in peiodontal surgery and implant dentistry for alveolar ridge preservation or reconstruction, maxillary sinus grafting, treatment of periodontal defects and surface coating for dental implants (Profeta & Prucher, 2015; Shue et al., 2012). One important factor that differentiates BAG from other bioactive ceramics or glass-ceramic is the option to design BAG with tailored property for a particular clinical application (Sarin & Rekhi, 2016). The base components of BAG are usually Silicon dioxide (SiO_2), Sodium Oxide (Na_2O), Calcium Oxide (CaO) and Phosphorus Pentoxide (P_2O_5). The BAGs can be produced with routine methods of the glass industry, however, it is crucial to confirm the purity of the raw materials, in order to avoid the contamination and the loss of volatile elements, like Na_2O, or P_2O_5 (Sarin & Rekhi, 2016; Jones et al., 2016).

BAG and polymers based composite membranes have extensively been investigated by many researchers for GTR/GBR with promising results (Puumanen et al., 2005; Tirri et

al., 2008; Mota et al., 2012; Li et al., 2015; Rodrigues et al., 2016). However, some studies reported that the addition of BAG particles do not enhance metabolic activity and cell proliferation and incorporation of BAG particles may even lead to retard the *in vitro* proliferative capacity in some cases due to reduced local pH upon ion release from BAG particles (Day et al., 2004; Misra et al., 2008; Caridade et al., 2012).

HYDROXYAPATITE (HA): HA $\{Ca_{10}(PO_4)_6(OH)_2\}$ has expansively been used in biomedical and dental applications due to its resemblance to core mineral components of hard tissues of human body such as bone, dental enamel and dentin. HA is the most stable calcium phosphate salt at normal temperatures and pH between 4 and 12 (Sadat-Shojai, 2009; Koutsopoulos, 2002). Calcium phosphate (CP)-based ceramic materials are group of compounds having Ca/P molar ratio in the range of 0.5–2. HA with a Ca/P ratio of I.67 is considered one of the most versatile bioceramic due to outstanding biocompatibility, osteoconductivity, osteointegeration and affinity to biopolymers (Fathi et al., 2008). It has been well recognized that HA can encourage new bone formation through osteoconduction mechanism without inducing any local or systemic toxicity, inflammation or foreign body response (Jaramillo et al., 2010; Sing, 2012; Rujitanapanich et al., 2014; Hoque et al., 2014).

Currently, HA is considered the material of choice for numerous biomedical applications such as repair of bony and periodontal defects, alveolar ridge augmentation, tissue engineering systems, drug delivery instrument and bioactive coating on metallic osseous implants (Trombelli et al., 2010; Strietzel et al., 2007; Krisanapiboon et al., 2006; Knabe et al., 2004). However, major limitations associated with HA are its inherent brittleness,

54

poor mechanical properties, long resorption time and difficulty for processing (Rujitanapanich et al., 2014; Wei & Ma, 2004).

HA can either be synthesized from natural organic based materials such as coral, seashell, eggshell, body fluids and bovine bone or by some synthetic chemical methods (Gergely et al., 2010; Agarwal et al., 2011). Several methods have been reported in literature to produce HA with different morphology, stoichiometry and level of crystallinity. Control of stoichiometry, crystal size, shape and agglomeration characteristics is very crucial in determining dissolution, bioactivity and mechanical properties of HA. Generally, HA produced from natural organic sources is non-stoichiometric due to the presence of trace amounts of ions which may be present in the natural organic source while synthetic HA is stoichiometric material (Rujitanapanich et al., 2014; Fathi et al., 2008; Kamalanathan et al., 2014). Figure 2.16 shows different synthetic routes for the production of HA.
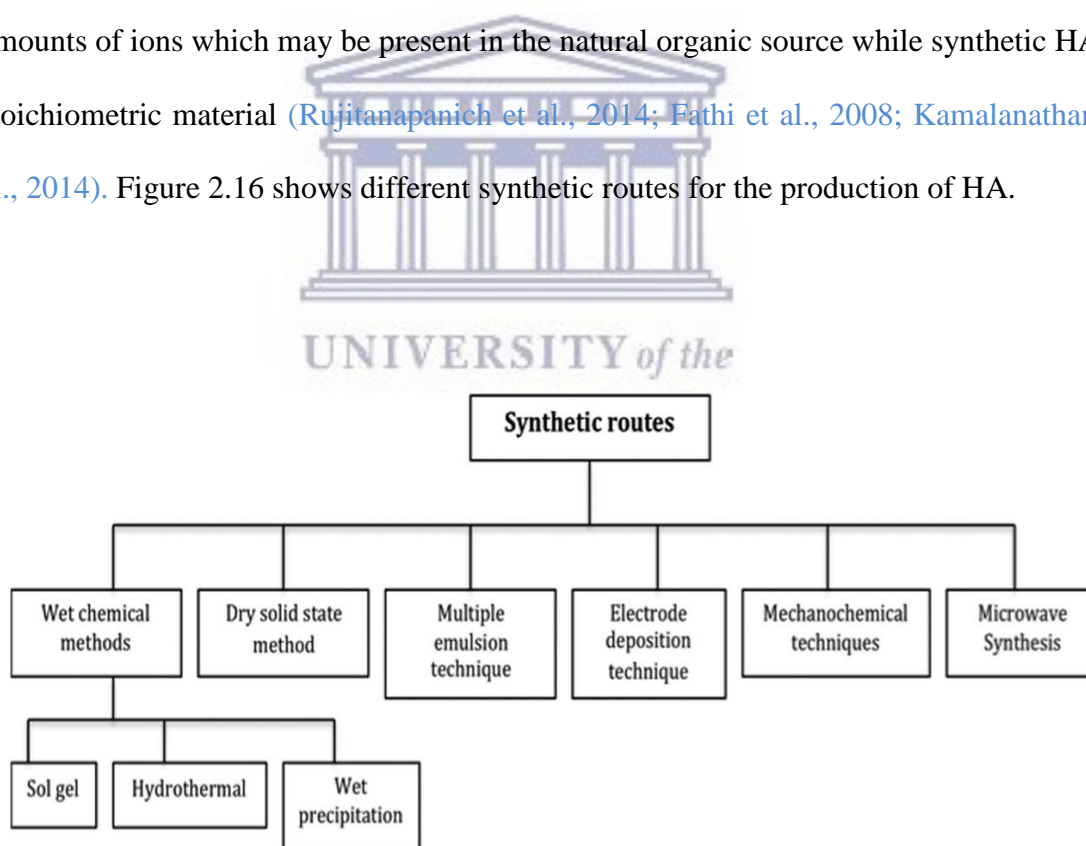
Fig: 2.16. Different synthetic routes for the production of HA with different morphologies, crystallinities, and stoichiometries (adapted from Ratnayake et al., 2016)

55

Although both types are considered equally bioactive, however, the key problem associated with biomaterials synthesized from inorganic components is high cost. Majority of the conventional chemical methods involves synthesis of HA without any trace of useful ions such as strontium (Sr), Sodium (Na^+), Potassium (K^+) zinc (Zn^{2+}), magnesium (Mg^{2+}), silicon (Si^{2+}), Barium (Ba^{2+}), fluoride (F^-) and carbonate (CO_3^{2-}) (Akram et al., 2014; Balázsi et al., 2007). These trace elements play a critical role in the life cycle of hard tissue, thus, scientists are investigating various methods to incorporate such beneficial ions into the structure of synthetic HA to improve osteoconductive properties (Akram et al., 2014).

The structure of HA crystals are incredibly similar to bone apatite and other hard tissues in mammals and conducive to a variety of ionic substitution (Rujitanapanich et al., 2014; Ratnayake et al., 2016). Figure 2.17 shows the structure of HA crystals.
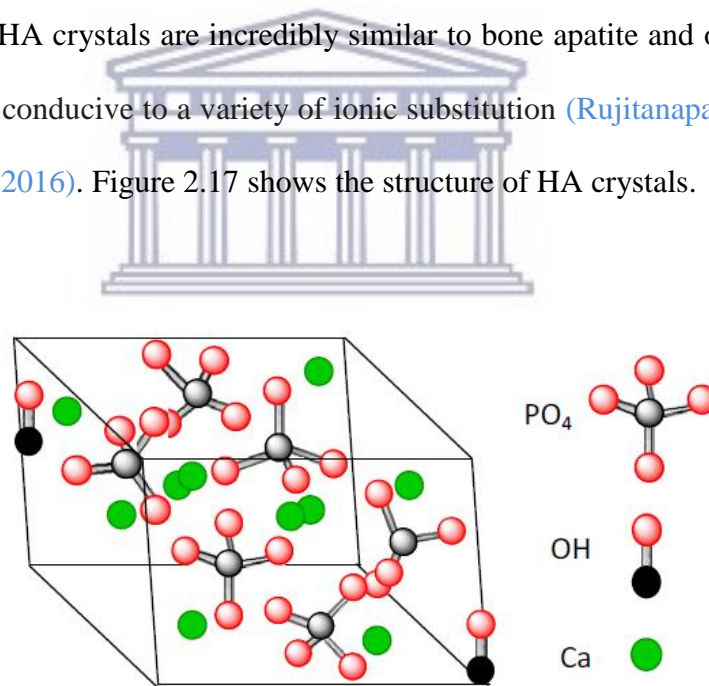
Fig: 2.17. Structure of HA crystals (Adapted from Rujitanapanich et al., 2014)

In order to match the calcium deficient and carbonate-containing nature of HA in bone, both cationic and anionic substituents have been incorporated into synthetic HA such as zinc, magnesium, strontium, silicon, fluoride, and carbonate (Boanini et al., 2010). Such

56

substitutions not only amend the microstructure, stability and crystallinity of HA structure but also have a considerable effect on bone cell colonization which in turn can significantly influence bone regeneration process. These substituted HAs are now commercially available (Ratnayake et al., 2016). Figure 2.18 shows the types of ionic substitutions in HA strucuture.
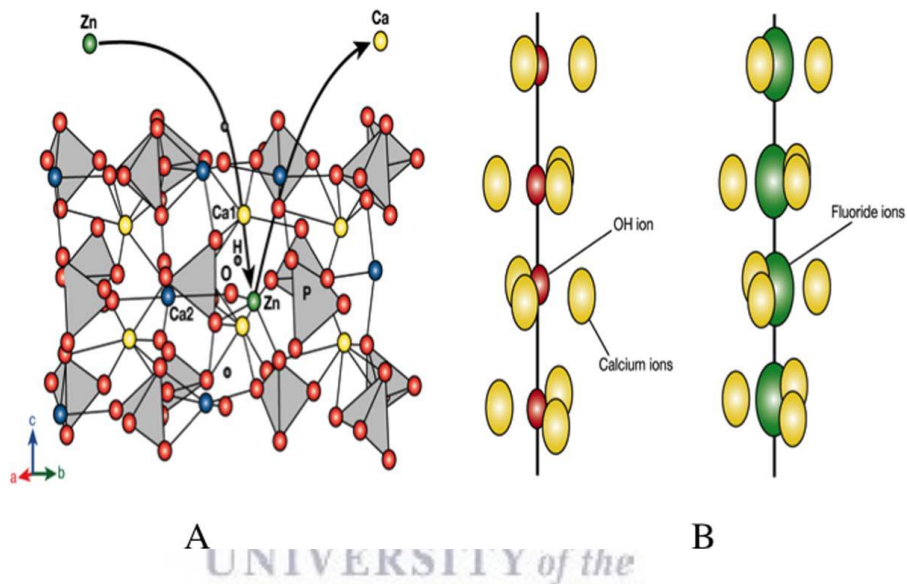
Fig: 2.18. Types of ionic substitutions in the HA structure: A: Cationic substitution, when calcium ion in HA is partially replaced with ions such as Mg21, Zn21, or Ag1. A decrease in the "a" axis and an increase "c" axis is observed. B: Anionic substitutions (I) Type A, a smaller hydroxyl ion is replaced by a large ion (mainly halide ions). (Adapted from Ratnayake et al., 2016)

SILICON SUBSTITUTED HA (Si-HA): The link between silicon and bone formation has been investigated since 1970s. Carlisle, (1970) was the 1st to report that 0.5 wt % silicon was present in active bone growth sites of mice and rats and abnormal skeletal growth was observed when diet was deficient in silicon. In a similar study, Schwarz and Milne, (1972) observed that silicon deficiency led to skull deformities in a rat model and resulted in nodular poorly defined mineral crystals, indicative of a primitive type of bone. A relationship between the level of dietary silicon and bone mineralization has also been

57

demonstrated and increase in silicon intake was reported to be associated with accelerated bone turnover (Hott & Nielson, 1993; Poellot, 2004). Various recent studies discovered that Si-substituted HA has superior bioactivity both *in vitro* and *in vivo*. Thus making Si-substituted HA an attractive and innovative material for enhancing bone growth (Thian et al., 2005; Patel et al., 2002; Hing et al., 2006; Balamurugana et al., 2008).

Several methods for the synthesis of Si-substituted HAs have been reported in literature such as sol-gel procedure (Ruys, 1993), hydrothermal method (Tang et al., 2005) and solid state reaction (Boyer et al., 1997). Silicon substitution means that silicon is substituted into the apatite crystal lattice and is not merely added. Silicon or silicates are believed to substitute for phosphorus or phosphates. The sum of silicon which can be substituted ranges from 0.1 to 5% by weight. Such small percentage is sufficient to yield bioactive improvement (Vallet-Regí & Arcos, 2005; Gibson et al., 2002).

In the review article on Si-substitution in calcium phosphate (CaP) bioceramics, Pietak et al., (2007) concluded that Si-substituted CaP materials have improved biological activity due to a number of factors acting synergistically. Si promotes biomimetic precipitation by increasing the solubility of the material through the creation of crystalline defects with substitution for PO_4^{3-} and associated charge compensation mechanism, by generating a more electronegative surface with the exchange of SiO_4^{4-} for PO_4^{3-} and by creating a nano-crystalline material. In addition the release of Si to the extracellular media has a direct effect on the differentiation and proliferation and collagen synthesis of osteoblasts. However, Bohner, (2009) in his critical review on Si-substituted calcium phosphates reported that despite the claims made in several articles, at present it is not clear if and how Si substitution positively influences the biological response of Si-substituted CaP.

58

Many investigators have incorporated HA particles into both natural and synthetic polymers to synthesize composite GTR/GBR scaffolds (Tripathi & Basu, 2012; Kharaziha et al., 2013; Yang et al., 2009; Xianmiao et al., 2009; Liao et al., 2015). While, till to date, Si-Subsituted HA has not been used by any researcher for the synthesis of GTR/GBR scaffold. Addition of inorganic nanostructures in biodegradable polymers could be an important option to increase and modulate mechanical, electrical and degradation properties. However, the interface adhesion between nanoparticles and polymer matrix is the major factor affecting the properties of resultant composite. Therefore, the mechanical properties of composite are controlled by the characteristics of the matrix, properties and distribution of inorganic filler and interfacial bonding (Armentano et al., 2010; Li et al., 2008). Due to the brittleness of the HA and to the lack of interaction with polymer, the HA nanoparticles may cause harmful effects on the mechanical properties of composite scaffold when added in high concentrations. Coupling agents are normally used to overpass the lack of interaction with polymer and HA. Therefore, the incorporation of HA in a polymeric matrix has to overcome processing and dispersion challenges (Armentano et al., 2010).

2.5.3. ADDITION OF GROWTH FACTORS

Growth factors are vital signaling molecules that modulate the cellular activity and offer stimulus for cell differentiation. These molecules bind to the specific transmembrane domains on target cells that consequently activate intracellular signal-transduction pathways hence causing differentiation and proliferation (Wang et al., 2016). They influence the tissue regeneration by promoting angiogenesis, chemotaxis and cell proliferation. GTR/GBR membranes can act as local delivery system for growth factors

59

thus to enhance the differentiation of osteogenic progenitor cells in the isolated space beneath the GTR/GBR membrane (Sam & Pillai, 2014; Bottino et al., 2012). In the recent past, scaffolds with different growth factors such as Platelet Derived Growth Factors (PDGF), Bone Morphogenetic Proteins (BMPs), Enamel Matrix Derivatives (EMDs), Fibroblast Growth Factors (FGFs) and Insulin like Growth Factors (IGFs) have been extensively investigated to enhance bone regeneration (Wang et al., 2016; Janicki & Schmidmaier, 2011).

PLATELET DERIVED GROWTH FACTORS (PDGF): PGDF is considered as the major wound healing hormone. Since its discovery in the late 1980's by Lynch and coworkers, its capability to stimulate periodontal and peri-implant regeneration have been investigated comprehensively (Kaigler et al., 2011). The chief source of PDGF is cytokine-laden granules (α-granules) of aggregated platelets however; it is also produced by activated macrophages and fibroblasts. PDGF exerts its biological effects by binding to α and β receptors on the surfaces of the mesenchymal origin cells (Phipps et al., 2012; Chong et al., 2006). PDGF is composed of disulfide bounded polypeptide chains A and B. Recently, C and D chain have also been discovered. PGDF exists either as homodimer (AA, BB, CC, DD) or a hetrodimer (AB). However, only three isoforms AA, BB and AB have been evaluated in periodontal therapy up till now. PDGF-BB is the most efficient on PDL cell mitogenesis and matrix biosynthesis (Mani et al., 2014; Raja et al., 2009).

Several investigators incorporated PDGF in GTR/GBR scaffolds. Phipps et al., (2012) produced a bone-mimetic electrospun scaffold composed of PCL, collagen type 1 and HA. PGDF-BB was passively absorbed into scaffold. The results of the study suggested that such scaffolds offer favorable environment for the attachment and proliferation of

60

mesenchymal cells and also deliver growth/chemotactic factors just like native ECM. Raghavendran et al., (2016) in their study tested the osteogenic potential of electruspun scaffold composed of poly(L-Lactide) (PLLA)/bovine collagen (Col)/nano-HA and PLLA/Col. PDGF-BB was incorporated into the eltrospun scaffolds. The results indicated that PDGF-BB significantly improved the osteogenic potential of PLLA/Col/HA and PLLA/HA composite scaffolds.

BONE MORPHOGENETIC PROTEINS (BMPs): Bone morphogenetic proteins (BMPs) are secreted signaling molecules which belong to the TGF-β superfamily and their function was 1st described by Urist, in 1965. It was reported that when implanted in ectopic sites in rodents, demineralized bone extracts have the ability to induce denovo bone formation (Ducy & Karsenty, 2000). However, the protein responsible for bone formation remained unrevealed till late 1980s when Wang and colleagues reported the isolation of BMP activity from extracts of bovine bone as a single gel band followed by sequencing the peptides obtained from trypsin digestion of the band (Wang et al. 1988, Katagiri & Watabe, 2016).

To date more than 20 different types of BMPs have been isolated and characterized, quite a few of which have been shown to influence bone formation. They stimulate angiogenesis, migration, proliferation, and differentiation of stem cells from the surrounding mesenchymal tissues into cartilage- and bone-forming cells in an area of injury. In addition they play a central role in morphogenesis and patterning of various organs, including the skeleton (Ducy & Karsenty, 2000; Huang et al., 2008). Figure 2.19 illustrates the mechanism of action of BMPs in bone repair.

61
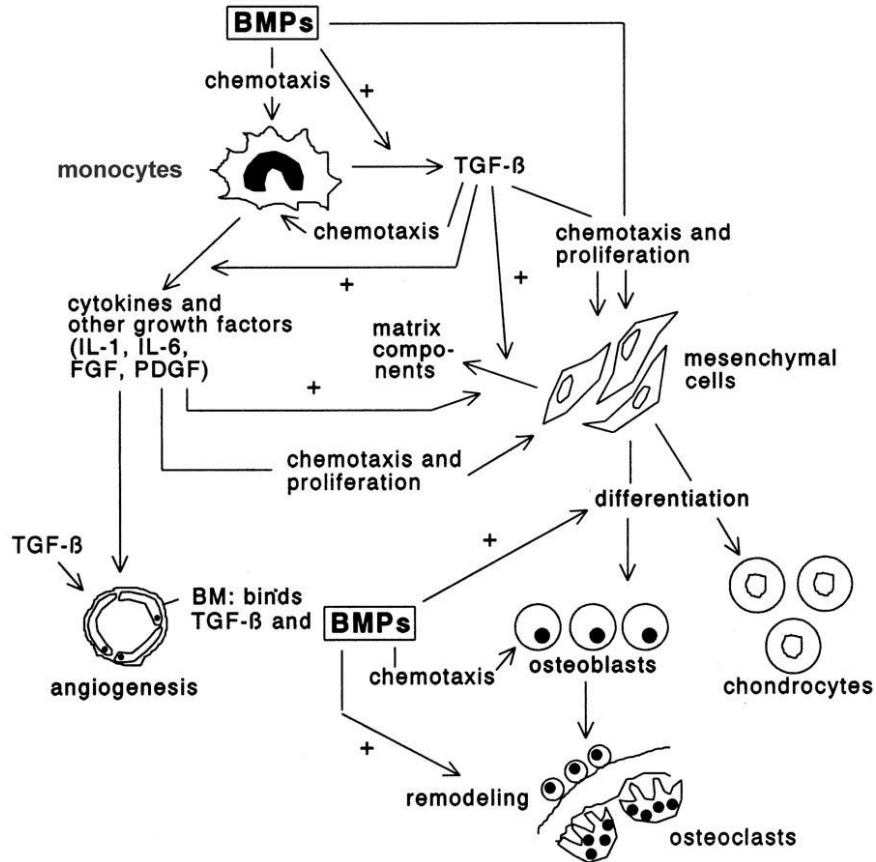
Fig: 2.19. Mechanisms of action of BMPs in bone repair: A typical sequence of events can be observed in endochondral bone formation induced by BMPs: recruitment and proliferation of monocytes and mesenchymal cells, differentiation into chondrocytes, calcification of the cartilage matrix, vascular invasion with associated osteoblast differentiation and bone formation, and remodeling of the newly formed bone. + = stimulating effect, BM = basement membrane, BMPs = bone morphogenetic proteins, TGF-β = transforming growth factor-β, IL-1 = interleukin-1, IL-6 = interleukin-6, FGF = fibroblast growth factor, and PDGF = platelet-derived growth factor (Adapted from Termaat et al., 2005)

Only a subset of BMPs has the unique property of inducing de novo bone formation, or osteoinduction, by themselves BMP-2 through 7 and BMP-9 have been shown to have this property meaning that these osteoinductive BMPs have the capacity to provide the primordial signal for the differentiation of mesenchymal stem cells into osteoblasts (Termaat et al., 2005; Cheng et al., 2003).

BMPs have extensively been investigated in periodontal regeneration. Several *in vitro* studies have reported that multipotent cells, either from pre- or postnatal animals or from animal and human bone marrow, showed responsiveness to various BMPs (Cheng et al.,

2003; Dorman et al., 2012; Shen et al., 2010). Similarly, many investigators have reported that BMPs stimulate *in vivo* bone formation in various animal models (Wikesjö et al., 2003; Wikesjö et al., 2004; Huang et al., 2005). BMPs have also been tested as coating material for dental implants and for repair of peri-implants defects (Wikesjö et al., 2008; Tatakis et al., 2002).

In human clinical trials recombinant human (rh) BMP-2 incorporated in an absorbable collagen was used for maxillary floor sinus augmentation (Boyne et al., 1997) and for the treatment of localized osseous defects and prevention of alveolar ridge after tooth extraction (Howell et al., 1997). Although no serious adverse effects were observed in the patients, however facial edema, oral erythema and rhinitis were reported (Boyne et al., 1997). Recombinant human (rh) BMP-2 was also tested in combination with xenograft for guided bone regeneration around dental implants and It was concluded that the combination of the xenogenic bone suhstitute mineral with rbBMP-2 can enhance the maturation process of bone regeneration and can increase the graft to bone contact in humans (Jung et al., 2003). In contrast, detrimental effects were reported by Kao et al., (2012) when adding it into bovine-derived deproteinized bone.

Delivering rhBMP to the surgical site, maintaining it in place, and preserving its appropriate folding are crucial issues. Commercially available BMPs are commonly associated with absorbable bovine collagen sponge. However, a considerable drawback is the significant proteolysis of the rhBMP and its collagen scaffold during the initial days after surgery, due to the inflammatory response caused by the surgical procedures, leading to its elimination by the body (Carreira et al., 2014; Rao et al., 2013). The retention of the BMPs in a delivery system may be performed by various methodologies

63

by means of adsorption, entrapment or immobilization, or by covalent binding. The easiest way to deliver the growth factor is adsorbing rhBMPs to the surface of the implant (Begam et al., 2017). There are three major categories of carrier materials like ceramics, synthetic polymer and natural polymer and/or composite carrier systems (Bessa et al., 2008).

Among synthetic polymers PCL, PEG and PLGA are widely used for BMPs delivery and are also combined with other osteinductive materials such as HA, TCP with very encouraging results in bone regeneration (Zhang et al., 2010; Kaito et al., 2005; Schofer et al., 2011; Fu et al., 2008). Natural polymers tested as promising source material for the synthesis of carrier systems for BMPs include chitosan, aliginate, silk fibroin and gelatin (Bessa et al., 2008). Several studies have reported the use of chitosan for delivering BMPs, particularly in composites with other synthetic or natural polymers and bone ceramics such as HA and TCP (Yilgor et al., 2009; Niu et al., 2009; Soran et al., 2012; He et al., 2014). Similarly, alginate has been used in the form of hydrogels (Suzuki et al. 2000) or as 3 dimensional scaffolds with other natural or synthetic polymer (Florczyk et al., 2013; Kolambkar et al., 2011). Due to its week mechanical properties alginate is rarely used alone for the synthesis of 3 dimensional scaffolds (Augst et al., 2006). Similarly, gelatin is not often used alone as a carrier system for BMPs however, gelatin sponges and electrospun fibers has been reported in literature as potential carrier systems for BMPs (Yamamoto et al., 2015; Lin et al., 2016). Composite electrospun scaffold of gelatin, PCL and BCP was tested *in vitro* and *in vivo* by Kim et al., (2014) with very encouraging results.

In the future, 3D porous scaffolds capable of releasing a concentration gradient of growth factors may become a useful tool for clinical use, overcoming the burst effect of BMPs release and providing a more natural flow of signaling molecules (Carreira et al., 2014).

ENAMEL MATRIX DERIVATIVES (EMD): Enamel Matrix Derivate (EMD) is composed of different enamel related proteins, being mainly amelogenin (90%). It also contains proteins such as enamelin, tufflin, and ameloblastin, among others. Enamel matrix proteins are secreted by Hertwig's epithelial root sheath, with cementogenesis being its main function (Suárez-López Del Amo et al., 2015). Although these proteins have shown favorable outcomes in periodontal regeneration, resulting in new bone formation, PDL, and cement, the exact mechanism of action remains unclear (Lyngstadaas et al., 2009). Of particular importance in periodontology are the commercially available products (Emdogain, Institut Straumann AG, Basel, Switzerland and Emdogain® Gel Biora AB, Malmö, Sweden). This product is extracted from developing porcine tooth buds (Venezia et al., 2004).

In a recent systematic review on periodontal regeneration with EMD Koop et al., (2012) reported that for intrabony defects, the meta-analysis showed a statistically significant additional improvement in CAL (1.30 mm), PD (0.92 mm), and radiographic bone levels (RAD 1.04) in favor of the use of EMD compared with a control 1 year after therapy. However, Plachokova et al., (2008) in their study on the regenerative properties of EMD absorbed on a carrier used unloaded poly(D,L-lactic-coglycolic acid)/calcium phosphate implants, and poly(D,L-lactic-coglycolic acid)/calcium phosphate implants loaded with different concentrations (0.25, 0.50 or 0.80 mg per implant) of enamel matrix derivative (EMD), and inserted them into cranial defects of 24 rats. The implantation time was 4

65

wk. New bone formation was most abundant in unloaded implants followed by 0.50-mg EMD composites. It was concluded Emdogain is not osteoinductive and is not able to enhance bone healing in combination with an osteoconductive material.

2.5.4. 3-DIMENTIONAL SCAFFOLDS

One of the main issues in tissue engineering is the fabrication of scaffolds that closely mimic the biomechanical properties of the tissues to be regenerated (Smith & Ma, 2004). It is demonstrated that tissue specific 3D architecture and functions can be recreated or maintained *in vitro* in a scaffold engineered with ECM like biomaterial. The chemistry of scaffold is also observed to be important for the phenotype regulation (Liang et al., 2007).

The engineering properties desired in a non-immunogenic ECM like scaffold include:

- Water retention capacity
- Tenacity for holding cells in stretched position
- Porosity to allow cells to grow and arrange in 3D
- Biodegradability to create space for nascent cells
- Connectivity to allow free flow of oxygen and nutrients in and around the growing cell mass. (Dutta & Dutta 2009)

In the native tissues, the structural ECM proteins (50–500 nm diameter fibers) are 1 to 2 orders of magnitude smaller than the cell itself; this allows the cell to be in direct contact with many ECM fibers, thereby defining its three dimensional orientation. This property may be a crucial factor in determining the success or failure of a tissue engineering scaffold (Barnes et al., 2007).

Scientists in tissue engineering have turned to nanotechnology, specifically nanofibers, as the solution to the development of tissue engineering scaffolds (Ma et al., 2005). At

66

present, only a few processing techniques can successfully produce fibers, and subsequent scaffolds, on the nanoscale. Conventional polymer processing techniques have difficulty in producing fibers smaller than 10 μm in diameter, which are several orders of magnitude larger than the native ECM (50–500 nm). For this reason, there has been a concerted effort to develop methods of producing nanofibers to more adequately simulate the ECM geometry (Barnes et al., 2007; Ma et al., 2005).

Three distinct techniques have proven successful in routinely creating nanofibrous tissue engineering structures: selfassembly, phase separation and electrospinning (Smith & Ma, 2004). Table 2.3 shows the comparison of nanofiber producing techniques.

PROCESS	LAB/ INDUSTRIAL APPLICATION	EASE OF PROCESSING	ADVANTAGES	DISADVANTAGES
Self assembly	Lab	Difficult	Achieve fiber diameter on lowest ECM scale (4-8 nm)	Only short fibers can be created(≤ 1µm) Low yield Matrix directly fabricated Limited to a few polymers
Phase separation	Lab	Easy	Tailorable mechanical properties, pore size and interconnectivity Batch to batch consistency	Low yield Matrix directly fabricated Limited to a few polymers
Electrospinning	Lab/ Industry	Easy	Cost effective Long continuous nanofibers Production of aligned nanofibers Tailorable mechanical properties, size, shape Plethora of polymers may be used	Large nanometer to micron scale fibers Use of organic solvents No control over 3D pore structure

Table: 2.3.Comparison of nanofiber producing techniques (adapted from Barens et al., 2007)

2.6. ELECTROSPINNING

Since the invention of electrospinning in the early 20th century, there has been enormous activity in this area during the last two decades with more than 1500 annual reports and 15,000 publications being written on the subject. This technology has also been considered as highly useful for fabricating scaffolds for culture of tissue cells and the treatment of damaged and diseased tissues, including blood vessels, muscles, skins, tendons, ligaments, cartilage, nerves, and bones (Shin et al., 2012).

The process of electrospraying was first observed in 1897 by Rayleigh and described in detail by Zeleny, (1914). The term 'electrostatic spinning' was used by Formhals in the 1940s, who published a number of patents related to the set-up needed to produce polymeric filament by means of electrostatic forces. The term 'electrospinning' was subsequently coined by Reneker and co-workers in the mid-1990s. Since that time little about the process has changed (Bhardwaj & Kundu, 2010). In its simplest form, electrospinning essentially consists of the creation of an electric field between a grounded target and a positively charged capillary filled with a polymer solution. When the electrostatic charge becomes larger than the surface tension of the polymer solution at the capillary tip, a polymer jet is created. This fine polymer jet travels from the charged capillary to the grounded mandrel and allows for the production of continuous micro- to nanoscale polymer fibers, which can be collected in various orientations to create unique structures in terms of composition and mechanical properties (Barnes et al., 2007; Ingavle & Leach, 2014). At a laboratory level, a typical electrospinning unit consists of three major components, a high voltage power supplier (up to 30 kV), injection pump holding a syringe (polymers reservoir) with pipette or needle of small diameter and a conducting

68

collector (Teo & Ramakrishna, 2006; Valizadeh & Mussa-Farkhani, 2014). Figure 2.20

shows a typical electrospinning unit.
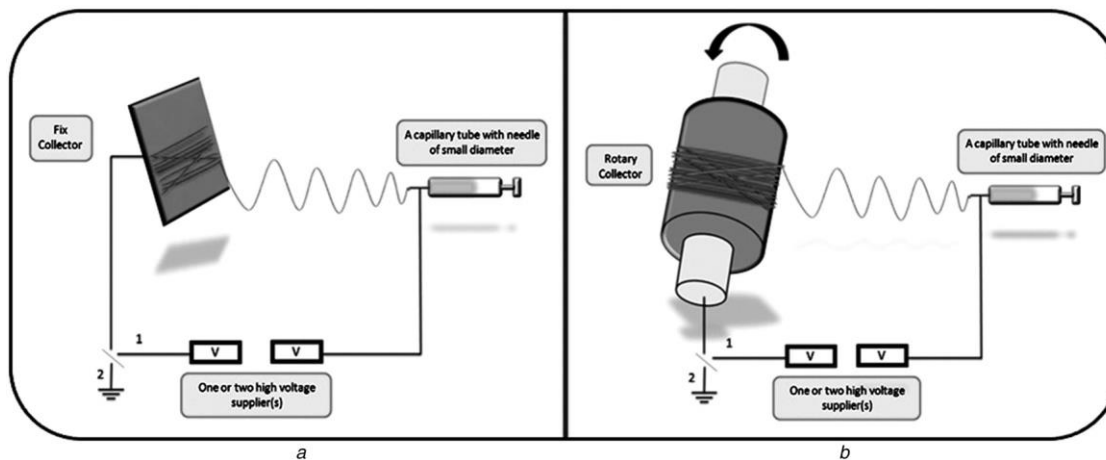
Fig: 2.20. A typical electrospinning unit with one or two high voltage power suppliers and fix or rotating collector (Adapted from Valizadeh & Mussa-Farkhani, 2014)

In conventional electrospinning, during the electrospinning process, polymer solutions

are transferred to syringe and placed in injection pump. The drop of polymer solution is

held at a needle tip by surface tension and form a cone known as the Taylor cone. There

may be one, two or mutifold nozzles in an electrospinning unit that produce various types

and morphologies of resultant scaffolds (Yarin et al., 2001; Valizadeh & Mussa-Farkhani,

2014).

One promising nozzle design is the core–shell nozzle. In most cases, the design

originates from the need to incorporate drugs inside of the nanofibers. Drugs sheathed

inside will be initially protected from environmental factors, such as the solvents used for

electrospinning. Furthermore, the encapsulated drugs will be released past the outer shell

69

layer in a more sustainable pattern (shin et al., 2012). In addition to drug carriers, the core–shell strategy can be used in another way. By setting synthetic polymer as the core material and natural polymer such as collagen as the shell material, nanofibers with strong mechanical strength and good biocompatible surface can be obtained (Ma et al., 2005). Figure 2.21 illustrates Core–shell nozzle design used to encapsulate drugs within the nanofiber.
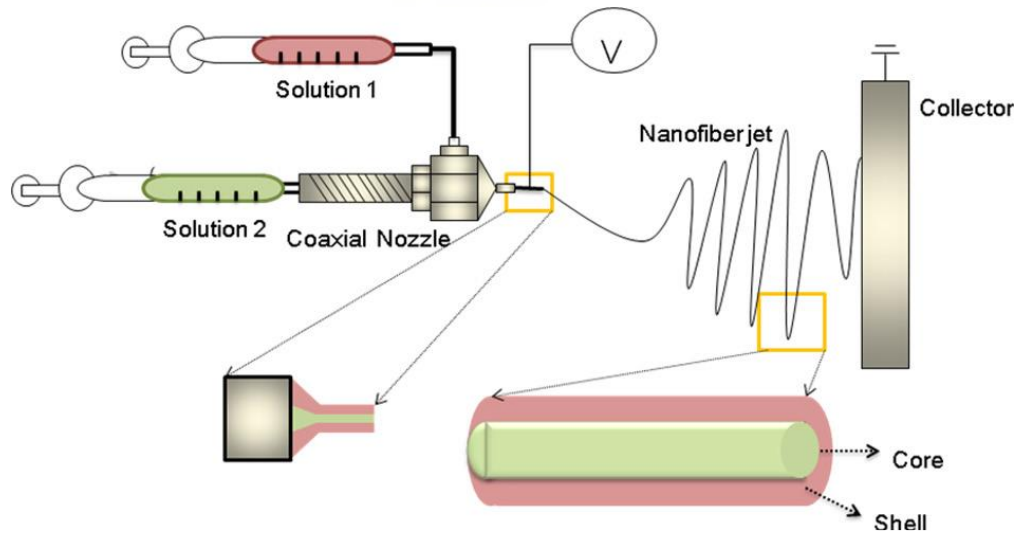
Fig: 2.21. Core–shell nozzle design used to encapsulate drugs within the nanofiber (adapted from Shin et al., 2012)

High-voltage supplier produce electric field that causes uniaxial stretching of a viscoelastic jet derived from the polymer solution. The electrospinning device might have one or two high voltage suppliers because in some cases, initiation of jet of polymer

requires high electric fields to overcome the surface tension of polymer (Sill & Recum, 2008; Valizadeh & Mussa-Farkhani, 2014).

Collector capture synthetic nanofibres on its surface and it could fix or rotate. In fix condition, collector does not move and thereby synthetic nanofibres orientations are random while aligned fibers can be produced by using a rotating collector (Reneker & Yarin, 2008). The presence of the disoriented fibers collected on the rotating mandrel may be the result of residual charge accumulation on the deposited fibers, which interferes with the alignment of incoming fibers (Teo & Ramakrishna, 2006).

The adjustment of several electrospinning parameters allows for further control and refinement of scaffold characteristics. Altering the concentration/viscosity of the polymer solution affects fiber diameter: the higher the concentration, the larger the diameter of the fibers (Sukigara et al., 2003). Varying the geometry of the grounded target will change the size and shape of the electrospun scaffold. Scaffold thickness is dependent on the volume of polymer solution to be electrospun; greater volumes equate to thicker specimens (Pham et al., 2006). Fiber alignment is controlled by rotation of the grounded target. A high rotational speed will draw the fibers into a highly aligned formation parallel to the direction of rotation, while low rotational speeds allow the fibers to collect randomly on the grounded target (Barnes et al., 2007; Villarreal-Gómez et al., 2016). Table 2.4 shows the Effects of processing parameters on fiber morphology.

PROCESS PARAMETERS	EFFECT OF FIBER MORPHOLOGY	REFRENCES
Viscosity	Low viscosities yielded defects in the form of beads and junctions; High viscosities increased fiber diameter and made fiber jet formation difficult	Sukigara et al. 2003, Zhao et al. 2005,
Conductivity/solution charge density	Increasing the conductivity aided in the production of uniform charge density bead-free fibers Higher conductivities yielded smaller fibers in general	Pham et al. 2006, Jun et al. 2003
Surface tension	No conclusive link established between surface tension and fiber morphology	Zhang et al. 2005 Zuo et al. 2005
Polymer molecular weight	Increasing molecular weight reduced the number of beads and droplets	Chen & Ma 2004, Gupta et al. 2005
Polymer concentration	Increase in fiber diameter with increase of concentration	Kim et al. 2005, Jun et al. 2003
Flow rate	Lower flow rates yielded fibers with smaller diameters High flow rates produced fibers that were not dry upon reaching the collector	Sill & Recum 2008 Zuo et al. 2005
Field strength/voltage	At too high voltage, beading was observed Correlation between voltage and fiber diameter was ambiguous	Jun et al. 2003, Valizadeh & Mussa-Farkhani 2014
Distance between tip and collector	A minimum distance was required to obtain dried fibers At distances either too close or too far, beading was observed	Zhang et al. 2005 Ki et al. 2005
Needle tip design	Using a coaxial, 2-capillary spinneret, hollow fibers were produced Multiple needle tips were employed to increase throughput	shin et al. 2012, Pham et al. 2006,
Collector composition and geometry	Smoother fibers resulted from metal collectors; more porous fiber structure was obtained using porous collectors Aligned fibers were obtained using a conductive frame, rotating drum, or a wheel-like bobbin collector	Wang et al. 2005, Li et al. 2004, Reneker & Yarin 2008
Ambient parameters	Increased temperature caused a decrease in solution viscosity, resulting in smaller fibers Increasing humidity resulted in the appearance of circular pores on the fibers	Casper et al. 2004, Li & Xia 2004

Table: 2.4. Effects of processing parameters on fiber morphology

72

The electrospinning of degradable polymers, either with a synthetic or natural origin, was considered to generate suitable bone cell matrices largely due to their ease of processing including solution preparation (Jin et al., 2012). Furthermore, the flexibility and shape-availability of polymeric materials gives them great potential in the bone regeneration area. However, due to the innate hydrophobic nature, the initial cell adhesion behavior to the synthetic polymers is limited Blending with natural polymers is another way of improving the cell compatibility (Jang et al., 2009). As natural polymer sources, collagen has long been studied for the electrospinning into nanofibers. Type I collagen is the major organic component of bone ECM, and has attracted considerable attention for use as a bone cell supporting matrix (Matthews et al., 2002). Although electrospun collagen mimics the nanofibrous morphology of native ECM, there is some debate as to whether the native structure and biological characteristics are preserved (Zeugolis et al., 2008). Compared to other natural polymers, chitosan is considered relatively difficult to electrospin mainly due to the limited solvents and high viscosity at low concentrations (Jang et al., 2009). However, Chitosan nanofibers were succesfully electrospun by Geng et al., (2005) from aqueous chitosan solution using concentrated acetic acid solution as a solvent. A uniform nanofibrous mat of average fiber diameter of 130 nm was obtained. Similarly, Shin et al., (2005) synthesized chitosan nanofiber membrane for guided bone regeneration. Chitosan nanofiber membranes that were grafted into rat subcutaneous tissue maintained their shape and space for bone regeneration for as long as 6 weeks. No inflammation could be seen on the membrane surface or in the surrounding tissues.

Combining degradable polymers with bioactive inorganic materials during the course of electrospinning is considered a fascinating and reasonable way of generating nanofibers

73

with the appropriate properties targeted for bone regeneration (Jin et al., 2012). The inorganic phase may act to improve the biological properties of polymeric nanofibers, such as cell compatibility and bone forming process, involving the osteogenic differentiation and calcification of bone matrix (Jang et al., 2009; Shin et al., 2012). Current electrospinning of composite fibers has focused mainly on incorporating bioactive inorganic nanoparticles evenly within a polymeric matrix without breaking down the fibrous morphology. This has been possible to a large extent through the introduction of ultrafine particles or control of the level of homogenization (Jang et al., 2009).

Due to their importance in regulating bone cell behavior and tissue formation, the development of effective strategies to deliver osteogenic cues (*e.g.*, bone morphogenetic proteins (BMPs) and other signaling molecules) in a sustained manner from a biodegradable scaffold remains an area of intense interest (Srouji et al., 2011; Ingavle & Leach, 2014). Because of their ultrathin fiber diameter and large surface area-to-volume ratio, translating to better control of release kinetics, electrospun scaffolds have gained increasing popularity in delivering biomolecules for bone tissue engineering (Jang et al., 2009; Ingavle & Leach, 2014).

A key goal in tissue engineering is the development of materials that effectively mimic the structure and function of the natural tissue ECM and capable of supporting cell attachment and proliferation. Over the last two decades, synthetic and natural polymers have been used to produce electrospun fibers on the dimentional scale of ECM, along with bioactive molecules, to drive cell behavior and promote tissue generation (Jin et al., 2012). Unlike more conventional manufacture methods that create matrices with

74

nonphysiological pores sizes or dimensions, electrospinning results in fibrous matrices with dimensions similar to ECM. By altering parameters of the electrospinning technique, scaffolds with different compositions, improved mechanical properties, varying degree of degradation or functional moieties can be reproducibly fabricated (Bhardwaj & Kundu, 2010; Ingavle & Leach, 2014).

REFRENCES:

- Agnihotri, S.A., Mallikarjuna, N.N., Aminabhavi, T.M. (2004). Recent advances on chitosan-based micro- and nanoparticles in drug delivery. *Journal of Controlled Release,* 100: 5-28.

- Agrawal, K., Singh, G., Puri, D., Prakash, S. (2011). Synthesis and characterization of hydroxyapatite powder by sol-get method for biomedical applications. *Journal of Minerals & Materials Chararterization & Engineering*, 10(8): 727-734.

- Aimetti, M., Mariani, G.M., Ferrarotti, F., Ercoli E., Audagna M., Bignardi C., Romano, F. (2015). Osseous resective surgery with and without fibre retention technique in the treatment of shallow intrabony defects: a split-mouth randomized clinical trial. *Journal of Clinical Periodontology,* 42: 182–189.

- Ajami-Henriquez, D., Rodríguez, M., Sabino, M., Castillo, R.V., Müller, A.J., Boschetti-de-Fierro, A., Abetz, C., Abetz, V., Dubois, P. (2008). Evaluation of cell affinity on poly(L-lactide) and poly(epsilon-caprolactone) blends and on PLLA-b-PCL diblock copolymer surfaces. *Journal of Biomedical Materials Research A*, 87(2):405-417.

- Akram, M., Ahmed, R., Shakir, I., Ibrahim, W.A.W., Hussain, R. (2014). Extracting hydroxyapatite and its precursors from natural resources. *Journal of Materials science,* 49(4):1461-1475.

- Albandar, J.M., Tinoco, E.M.B. (2002). Global epidemiology of periodontal diseases in children and young persons. *Periodontology 2000*, 29: 153-176.

- Albandar, J.M., Susin, C., Hughes, F.J. (2018). Manifestation of systemic diseases and conditions that affect the periodontal attachment apparatus: Case definition and diagnostic considerations. *Journal of Clinical Periodontology,* 45(Supply20): S171-S189.

- Almazrooa, S.A., Noonan, V., Woo, S.B. (2014). Resorbable collagen membranes: histopathologic features. *Oral Surg Oral Med Oral Pathol Oral Radiol*, 118(2): 236-240.

- Altman, G.H., Diaz, F., Jakuba, C., Calabro, T., Horan, R.L., Chen, J., Lu, H., Richmond, J., Kaplan, D.L. (2003). Silk-based biomaterials. *Biomaterials,* 24: 401–416.

- Andersen, T., Auk-Emblem, P., Dornish, M. (2015). 3D cell culture in alginate hydrogels. *Microarrays*, 4(2):133-161.

- Aoki, A., Sasaki, K.M., Watanabe, H., Ishikawa, I. (2004). Lasers in nonsurgical periodontal therapy. *Periodontology 2000,* 36:59-97.

- Apostolov, A.A., Boneva, D., Vassileva, E., Mark, J.E., Fakirov, S. (2000). Mechanical properties of native and cross linked gelatins in a bending deformation. *Journal of Applied Polymer Science*, 76:2041–2048.

- Aranaz, I., Mengíbar, M., Harris, R., Paños, I., Miralles, B., Acosta, N., Galed, G., Heras, Á. (2009). Functional Characterization of Chitin and Chitosan. *Current Chemical Biology*, 23: 203-230.

- Arai, T., Freddi, G., Innocenti, R., Tsukada, M. (2004). Biodegradation of Bombyx mori Silk Fibroin Fibers and Films. *Journal of Applied Polymer Science*, 91: 2383–2390.

77

- Armentano, I., Dottori, M., Fortunati, E., Mattioli, S., Kenny, J.M. (2010). Biodegradable polymer matrix nanocomposites for tissue engineering: A review. *Polymer Degradation and Stability,* 95: 2126-2146.

- Armitage, G.C. (1999). Development of a classification system for periodontal diseases and conditions. *Annals of Periodontology,* 4:1-6.

- Armitage, G.C. (2013). Bidirectional relationship between pregnancy and periodontal disease. *Periodontology 2000,* 61:160-176.

- Armitage, G.C., Cullinan, M.P. (2010) Comparison of clinical features of chronic periodontitis and aggressive periodontitis. *Periodontology 2000,* 58: 12-27.

- Assenza, B., Piattell, M., Scarano, A., Lezzi, G., Petrone, G., Piattelli, A. (2001). Localized ridge augmentation using titanium micromesh. *Journal of Oral Implantology,* 27: 287-292.

- Augst, A.D, Kong, H.J, Mooney, D.J. (2006). Alginate hydrogels as biomaterials. *Macromolecular Bioscience,* 6:623–633.

- Aurer, A., Jorgić-Srdjak, K. (2005). Membranes for periodontal regeneration. *Acta Stomatologica Croatica,* 39 (1): 107-112.

- Balamurugana, A., Rebeloa, A.H.S., Lemosa, A.F., Rochab, J.H.G., Venturaa, J.M.G., Ferreiraa, J.M.F. (2008) Suitability evaluation of sol–gel derived Si-substituted hydroxyapatite for dental and maxillofacial applications through in vitro osteoblasts response. *Dental Materials,* 24: 1374-1380
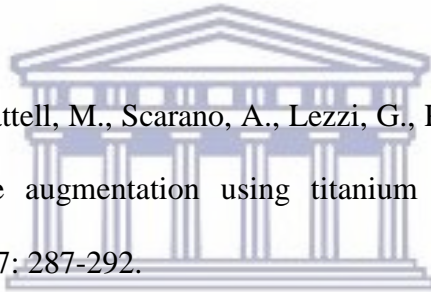
- Balázsi, C., Wéber, F., Kövér, Z., Németh, C. (2007). Preparation of calcium–phosphate bioceramics from natural resources. *Journal of the European Ceramic Society,* 27(2):1601-1606.

- Baldrick, P. (2010). The safety of chitosan as a pharmaceutical excipient. *Regulatory Toxicology and Pharmacology,* 56:290-299.

- Barber, H.D., Lignelli, J., Smith, B.M., Bartee, B.K. (2007). Using a dense PTFE membrane without primary closure to achieve bone and tissue regeneration. *Journal of Oral and Maxillofacial surgery,* 65(4):748-752.

- Barnes, C.P., Sell, S.A., Boland, E.D., Simpson, D.G., Bowlin, G.L. (2007). Nanofiber technology: Designing the next generation of tissue engineering scaffolds. *Advanced Drug Delivery Reviews,* 59:1413–1433.

- Barrere, F., van Blitterswijk, C.A., de Groot, K. (2006) Bone regeneration: molecular and cellular interactions with calcium phosphate ceramics. *International Journal of Nanomedicine,* 1(3): 317-332.

- Bartee, B.K. (1995). The use of high-density polytetrafluoroethylene membrane to treat osseous defects: clinical reports. *Implant Dentistry,* 4:21-26.

- Batista, E.L. Jr., Batista, F.C., Novaes, A.B. Jr. (2001). Management of soft tissue ridge deformities with acellular dermal matrix. Clinical approach and outcome after 6 months of treatment. *Journal of Periodontology*, 72: 265-273.

- Bavariya, A.J., Andrew-Norowski, P.Jr. Mark-Anderson, K., Adatrow, P.C., Garcia-Godoy, F., Stein, S.H., Bumgardner, J.D. (2014). Evaluation of biocompatibility and degradation of chitosan nanofiber membrane crosslinked

79

with gingipin. *Journal of Biomedical Materials Research Part B: Applied Biomaterials,* 102(5): 1084-1092.

- Bayerlein, T., Mundt, T., Mack, F., Bienengräber, V., Proff, P., Gedrange, T. (2006). Bone graft substitutes in periodontal and peri-implant bone regeneration. *Folia Morphologica,* 65(1): 66-69.

- Begam, H., Nandi, S.K., Kundu, B., Chanda, A. (2017). Strategies for delivering bone morphogenetic protein for bone healing. *Materials Science and Engineering C,* 70(1):856-869.

- Benhabiles, M.S., Salah, R., Lounici, H., Drouiche, N., Goosen, M.F.A., Mameri, N. (2012). Antibacterial activity of chitin, chitosan and its oligomers prepared from shrimp shell waste. *Food Hydrocolloids* 29: 48-56.

- Bernkop-Schnürch, A., Dünnhaupt, S. (2012). Chitosan-based drug delivery systems. *European Journal of Pharmaceutics and Biopharmaceutics,* 81:463-469.

- Bessa, P.C., Casal, M., Reis, R.L. (2008). Bone morphogenetic proteins in tissue engineering: the road from laboratory to clinic, part II (BMP delivery). *Journal of Tissue Engineering and Regenerative Medicine,* 2: 81-96.

- Bhardwaj, N., Kundu, S.C. (2010). Electrospinning: A fascinating fiber fabrication technique. *Biotechnology Advances*, 28:325-347.

- Bhattarai, N., Gunn, J., Zhang, M. (2010). Chitosan-based hydrogels for controlled, localized drug delivery. *Advanced Drug Delivery Reviews,* 62: 83–99.

- Bian, W., Li, D., Lian, Q., Li, X., Zhang, W. Wang, K., Jin, Z. (2012). Fabrication of a bio-inspired beta-Tricalcium phosphate/collagen scaffold based

80

on ceramic stereolithography and gel casting for osteochondral tissue engineering. *Rapid Prototyping Journal,* 18(1):68-80.

- Bigi, A., Cojazzi, G., Panzavolta, S., Roveri, N., Rubini, K. (2002). Stabilization of gelatin films by crosslinking with genipin. *Biomaterials*, 23(24):4827-4832.

- Bogle, G., Garrett, S., Stoller, N. H., Swanbom, D. D., Fulfs, J. C., Rodgers, P. W., Whitman, S. L., Dunn, R. L., Southard, G. L., Polson, A. M. (1997). Periodontal regeneration in naturally occurring class II furcation defects in beagle dogs after guided tissue regeneration with bioabsorbable barriers. *Journal of Periodontology*, 68: 536-544.

- Bohner, M. (2009). Silicon-substituted calcium phosphates- A critical view. *Biomaterials*, 30:6403-6406.

- Boanini, E., Gazzano, M., Bigi, A. (2010). Ionic substitutions in calcium phosphates synthesized at low temperature. *Acta Biomaterialia*, 6(6): 1882-1894.

- Borges, G.J., Novaes, A.B.Jr., Crisi, M.F., Palioto, D.B., Taba, M.Jr. de Souza, S.L. (2009). Acellular dermal matrix as a barrier in guided bone regeneration: a clinical, radiographic and histomorphometric study in dogs. *Clinical Oral Implant Research*, 20: 1105–1115.

- Bosshardt, D.D., Sculean, A. (2009). Does periodontal tissue regeneration really work? *Periodontology 2000*, 51:208-219.

- Bottino, M.C., Thomas, V. (2015). Membranes for periodontal regeneration - A materials perspective. *Frontiers of Oral Biology,* 17: 90-100.

- Bottino, M.C., Thomas, V., Schmidt, G., Vohra, Y.K., Chu, T.G., Kowolik, M.J., Janowski, G.M. (2012). Recent advances in the development of GTR/GBR

membranes for periodontal regeneration—A materials perspective. *Dental Materials,* 28: 703–721.

- Boyer, L., Carpena, J., Lacout, J. (1997). Synthesis of phosphate–silicate apatites at atmospheric pressure. *Solid State Ionics,* 95:121–129.

- Boyne, P.J., Marx, R.E., Nevins, M., Triplett, G., Lazaro, E., Lilly, L.C., Alder, M., Nummikoski, P. (1997). A feasibility study evaluating rhbmp-2/absorbable collagen sponge for maxillary sinus floor augmentation. *The International Journal of Periodontics and Restorative Dentistry,* 17:10-25.

- Brito, I.R., Lima, I.M., Xu, M., Shea, L.D., Woodruff, T.K., Figueiredo, J.R. (2014). Three-dimensional systems for in vitro follicular culture. Overview of alginate-based matrices. *Reproduction, Fertility and Development,* 26(7): 915-930.

- Brunel, G., Piantoni, P., Elharar, F., Benque´, E., Marin, P., Zahedi, S. (1996). Regeneration of rat calvarial defects using bioabsorbable membrane technique: influence of collagen cross-linking. *Journal of Periodontolology*, 67:1342–1348.

- Bunyaratavej, P., Wang, H.L. (2001). Collagen membranes: A review. *Journal of Periodontology*, 72:215-229.

- Camargo, P.M., Melnick, P.R., Pirih, F.Q.M., Lagos, R., Takei, H.H. (2001). Treatment of drug induced gingival enlargement: aesthetic and functional considerations. *Periodontology 2000*, 27:131-138.

- Canullo, L., Malagnino VA. (2008). Vertical ridge augmentation around implants by e-PTEF titanium-reinforced membrane and bovine bone matrix. A

24 to 54 month study of 10 consecutive cases. *International Journal of Oral Maxillofacial Implants* 23:858-866.

- Cao, Y., Wang, B. (2009). Biodegradation of Silk Biomaterials. *International Journal of Molecular Sciences,* 10: 1514-1524.

- Carbonell, J.M., Martı´n, I.S., Santos, A., Pujol, A., Sanz-Moliner, J.D., Nart, J. (2014). High-density polytetrafluoroethylene membranes in guided bone and tissue regeneration procedures: a literature review. *International Journal of Oral Maxillofacial Surgery,* 43: 75–84.

- Caridade, S.G., Merino, E.G., Gabriela V Martins, G.V., Luz, G.M., Alves, N.M., Mano, J.F. (2012). Membranes of poly(d,l-lactic acid)/Bioglass® with asymmetric bioactivity for biomedical applications. *Journal of Bioactive and Compatible Polymers,* 0(0):1-12.

- Carlisle E.M. (1970). Silicon: A possible factor in bone calcification. *Science,* 167:279–280.

- Carnevale, G., Kaldahl, W.B. (2000). Osseous resective surgery. *Periodontology 2000*, 22:59-87.

- Carreira, A.C., Lojudice, F.H., Halcsik, E., Navarro, R.D., Sogayar, M.C., Granjeiro, J.M. (2014). Bone Morphogenetic Proteins: Facts, Challenges, and Future Perspectives. *Journal of Dental Research*, 93(4):335-345.

- Casper, C.L., Stephens, J.S., Tassi, N.G., Chase, D.B., Rabolt, J.F. (2004) Controlling surface morphology of electrospun polystyrene fibers: effect of humidity and molecular weight in the electrospinning process. *Macromolecules*, 37:573-578.

- Caton, J.G., Armitage, G., Berglundh, T., Chapple, I.L.C., Jepsen, S., Kornman, K.S., Mealey, B.L., Papapanou, P.N., Sanz, M., Tonetti, M.S. (2018). A new classification scheme for periodontal and peri-implant diseases and conditions-Introduction and key changes from the 1999 classification. Journal of Clinical Periodontology, 45(supply 20): S1-S8.

- Chen, F.M., Jin. Y. (2010). Periodontal tissue engineering and regeneration: current approaches and expanding opportunities. *Tissue Engineering Part B*: *Reviews,* 16(2):219-255.

- Chen, L., Bai, L., Liao, G., Peng, E., Wu, B., Wang, Y., Zeng, X., Xie, X. (2013). Electrospun Poly(L-lactide)/Poly(ε-caprolactone) blend nanofibrous scaffold: Characterization and biocompatibility with human adipose-derived stem cells. *PLoS One,* 8(8): e71265.

- Chen, T.W., Chang, S.J., Niu, G.C., Hsu, Y.T., Kuo, S.M. (2006). Alginate-coated chitosan membrane for guided tissue regeneration. *Journal of Applied Polymer Science,* 102(5): 4528-4534.

- Chen, S., Hao, Y., Cui, W., Chang, J., Zhou, Y. (2013). Biodegradable electrospun PLLA/chitosan membrane as guided tissue regeneration membrane for treating periodontitis. *Journal of Materials Science,* 48: 6567–6577.

- Chen, V.J., Ma, P.X. (2004). Nano-fibrous poly (L -lactic acid) scaffolds with interconnected spherical macropores. *Biomaterials*, 25:2065-2073.

- Cheng, H., Jiang, W., Phillips, F.M., Haydon, R.C., Peng, Y., Zhou, L., Luu, H.H., An, N., Breyer, B., Vanichakarn, P., Szatkowski, J.P., Park, J.Y., He, T.C.

84

(2003). Osteogenic activity of the fourteen types of human bone morphogenetic proteins (BMPs). *The Journal of Bone & Joint Surgery*, 85-A(8):1544-1552.

- Chong, C.H., Carnes, D.L., Moritz, A.J., Oates, T., Ryu, O.H., Simmer, J., Cochran, D.L. (2006). Human periodontal fibroblast response to enamel matrix derivative, amelogenin and platelet-derived growth factor-bb. *Journal of Periodontology*, 77:1242-1252.

- Christgau, M., Bader, N., Felden, A., Gradl, J. (2002). Guided tissue regeneration in intrabony defects using an experimental bioresorbable polydioxanon (PDS) membrane. A 24-month split-mouth study. *Journal of Clinical Periodontology,* 29: 710-723.

- Claffey, N., Polyzois, I. Ziaka, P. (2004). An overview of non-surgical and surgical therapy. *Periodontology 2000*, 36: 35-44.

- Committee on Research, Science and Therapy of the American Academy of Periodontology. (2001). Tissue banking of bone allografts used in periodontal regeneration. *Journal of Periodontology,* 72:834–838.

- Cortellini, P., Tonetti, M.S. (2000). Focus on itrabony defects: guided tissue regeneration. *Periodontology 2000,* 22: 104-132.

- Cortellini, P., Prato, G.P., Tonettif, M.S. (1993). Periodontal regeneration of human infrabony defects. II. Re-entry procedures and bone measures. *Journal of Periodontology,* 64:261-268.

- Cortellini, P., Prato, G.P., Tonettí', M.S. (1995). Periodontal regeneration of human intrabony defects with titanium reinforced membranes. A controlled clinical trial. *Journal of Periodontology,* 66:797-803.

85

- Cortellini, P., Prato, G.P., Tonettï, M.S. (1996). Periodontal regeneration of human intrabony defects with bioresorbable membranes. A controlled clinical trial. *Journal of Periodontology*, 67:217-223.

- Costa-Pinto, A.R., Reis, R.L., Neves, N.M. (2011). Scaffolds Based Bone Tissue Engineering: The Role of Chitosan. *Tissue Engineering: Part B,* 17(5): 331-347.

- d'Ayala, G.G., Malinconico, M., Laurienzo, P. (2008). Marine Derived Polysaccharides for Biomedical Applications: Chemical Modification Approaches. *Molecules,* 13:2069-2106.

- Dahlin, C., Sennerby, L., Lekholm, U., Linde, A., Nyman, S. (1989). Generation of new bone around titanium implants using a membrane technique: an experimental study in rabbits. *International Journal of Oral Maxillofacial Implants,* 4(1):19-25.

- Dash, M., Chiellini, F., Ottenbrite. R.M., Chiellini, E. (2011). Chitosan- A versatile semi-synthetic polymer in biomedical applications. *Progress in Polymer Science,* 36: 981–1014.

- Day, R.M., Boccaccini, A.R., Shurey, S., Roether, J.A., Forbes, A., Hench, L.L., Gabe, S.M. (2004). Assessment of polyglycolic acid mesh and bioactive glass for soft-tissue engineering scaffolds. *Biomaterials,* 25(27): 5857–5866.

- de Andrade, P.F., de Souza, S.L., de, Oliveira Macedo, G., Novaes, A.B. Jr., de Moraes Grisi, M.F., Taba, M. Jr., Palioto, D.B. (2007). Acellular Dermal Matrix as a membrane for guided tissue regeneration in the treatment of class II

86

furcation lesions: A histometric and clinical Study in Dogs. *Journal of Periodontology,* 78:1288-1299.

- Dimitriou, R., Mataliotakis, G. I., Calori, G. M., Giannoudis, P.V. (2012). The role of barrier membranes for guided bone regeneration and restoration of large bone defects: current experimental and clinical evidence. *BM Medicine,* 10(81): 1-24

- Dorman, L.J., Tucci, M., Benghuzzi, H. (2012). In vitro effects of bmp-2, bmp-7, and bmp-13 on proliferation and differentation of mouse mesenchymal stem cells. *Biomedical Sciences Instrumentation,* 48:81-87.

- Draget, K.I, Taylor, C. (2011). Chemical, physical and biological properties of alginates and their biomedical implications. *Food Hydrocolloids,* 25: 251–256.

- Drisko, C.H. (2001). Nonsurgical periodontal therapy. *Periodontology 2000*, 25:77-88.

- Ducy, P., Karsenty, G. (2000). The family of bone morphogenetic proteins. *Kidney International,* 57: 2207–2214.

- Dutta, P.K., Dutta, J., Tripathi, V.S. (2004). Chitin and chitosan: Chemistry, properties and applications. *Journal of Scientific & Industrial Research*, 63: 20-31.

- Dutta, R.C., Dutta, A.K. (2009). Cell-interactive 3D-scaffold; advances and applications. *Biotechnology Advances,* 27: 334–339.

- Eickhilz, P., Pretzl, B., Holle, R., Kim, T. (2006). Long term results of guided tissue regeneration therapy with non-resorbable and bioresorbable barriers. III. Class II furcations after 10 years. *Journal of Periodontology*, 77:88-94.

87

- Ershuai, Z., Chuanshun, Z., Jun, Y., Hong, S., Xiaomin, Z., Suhua, L., Wang Yonglan, W., Lu, S., Fanglian, Y. (2016). Electrospun PDLLA/PLGA composite membranes for potential application in guided tissue regeneration. *Materials Science and Engineering C,* 58:278–285.

- Eslaminejad, M.B., Mirzadeh, H., Mohamadi, Y., Nickmahzar, A. (2007). Bone differentiation of marrow-derived mesenchymal stem cells using β-tricalcium phosphate–alginate–gelatin hybrid scaffolds. *Journal of Tissue Engineering and Regenerative Medicine,* 1(6): 417-424.

- Falk, H., Laurrel, L., Ravald, N., Teiwik, A., Persson, R. (1997). Guided tissue regeneration therapy of 203 consecutively treated intrabony defects using a bioresorbable matrix barrier. Clinical and radiographic findings. *Journal of Periodontology*, 68: 571-81.

- Fathi, M.H., Mortazavi, V., Esfahani, S.I.R. (2008). Bioactivity evaluation of synthetic nanocrystalline hydroxyapatite. *Jouranl of Dental Research*, 5(2):81-87.

- Ferreira, A.M., Gentile, P., Chiono, V., Gianluca Ciardelli, G. (2012). Collagen for bone tissue regeneration. *Acta Biomaterialia,* 8: 3191–3200.

- Figuero, E., Carrillo-de-Albornoz, A., Martin, C., Tobias, A., Herrera, D. (2013). Effect of Pregnancy on gingival inflammation in systemically healthy women: A systematic review. *Journal of Clinical Periodontology*, 40:457-473.

- Fine, D.H., Patil, A.G., Loos, B.G. (2018). Classification and diagnosis of aggressive periodontitis. *Journal of Clinical Periodontology,* 45(Supply20): S95-S111.

- Fleischer, N., De Waal, H., Bloom, A. (1998). Regeneration of lost attachment apparatus in the dog using Vicryl absorbable mesh (Polyglactin 910). *International Journal of Periodontics and Restorative Dentistry,* 8(2): 44-55.

- Florczyk, S.J., Leung, M., Li, Z., Huang, J.I., Hopper, R.A., Zhang, M. (2013). Evaluation of three-dimensional porous chitosan–alginate scaffolds in rat calvarial defects for bone regeneration applications. Jourmal of Biomedical Materials Research Part A, 101(10):2474-2483.

- Fritoli, A., Goncalves, C., Faveri, M., Figueiredo, L.C., Pérez-Chaparro, P.J., Fermiano, D., Feres, M. (2015). The effect of systemic antibiotics administered during the active phase of non-surgical periodontal therapy or after the healing phase: a systematic review. *Journal of Applied Oral Sciences*, 23(3): 249-254.

- Fu, Y.C., Nie, H., Ho, M.L., Wang, C.K., Wang, C.H. (2008). Optimized bone regeneration based on sustained release from three-dimensional fibrous PLGA/Hap composite scaffolds loaded with BMP-2. *Biotechnology and Bioengineering*, 99(4):996-1006.

- Geng, X., Kwon, O.H., Jang, J. (2005). Electrospinning of chitosan dissolved in concentrated acetic acid solution. *Biomaterials,* 26:5427–5432.

- Gentile, P., Chiono, V., Tonda-Turo, C., Ferreira, A.M., Ciardelli, G. (2011). Polymeric membranes for guided bone regeneration. *Biotechnology Journal*, 6: 1187–1197.

- Gentile, P., Chiono, V., Carmagnola, I., Hatton, P.V. (2014). An overview of Poly(lactic-*co*-glycolic) Acid (PLGA)-based biomaterials for bone tissue engineering. *International Journal of Molecular Sciences*, 15: 3640-3659.

89

- Gergely, G., Wéber, F., Lukács, I., Illés, L., Tóth, A.L., Horváth, Z.E., Judit Mihály, J., Balázsi, C. (2010). Nano-hydroxyapatite preparation from biogenic raw materials. *Central European Journal of Chemistry,* 8(2):375–381.

- Ghanaati, S. (2012). Non-cross-linked porcine-based collagen I–III membranes do not require high vascularization rates for their integration within the implantation bed: A paradigm shift. *Acta Biomaterialia,* 8(8): 3061-3072.

- Giannoudis, P.V., Dinopoulos, H., Tsiridis, E. (2005). Bone substitutes: an update. *Injury,* 36s: 20-27.

- Gibson, I., R., Best, S., M., Bonfield, W. (2002). Effect of Silicon substitution on the sintering and microstructure of hydroxyapatite. *Jouranal of the American Ceramic society,* 85(11):2771-2777.

- Gobin, A.S, Froude, V.E., Mathur, A.B. Structural and mechanical characteristics of silk fibroin and chitosan blend scaffolds for tissue regeneration. *Journal of Biomaterial research Part A.* 74(3): 465-473.

- Goonoo, N., Bhaw-Luximon, A., Rodriguez, I.A., Daniel Wesner, D., Schönherr, H., Gary L. Bowlinb, G.L., Jhurry, D. (2014) Poly(ester-ether)s: II. Properties of electrospun nanofibres from polydioxanone and poly(methyl dioxanone) blends and human fibroblast cellular proliferation. *Biomaterials Science,* 2:339-351.

- Gorczyca, G., Tylingo, R., Szweda, P., Augustin, E., Sadowska, M., Sławomir Milewski, S., (2014). Preparation and characterization of genipin cross-linked porous chitosan–collagen–gelatin scaffolds using chitosan–CO_2 solution. *Carbohydrate Polymers,* 102:901–911.

- Gottlow, J., Nyman, S., Karring, T., Lindhe, J. (1984). New attachment formation as the result of controlled tissue regeneration. *Journal of Clinical Periodontology,* 11(8):494–503.

- Gottlow, J., Nyman, S., Lindhe, J., Karring, T., Wennström, J. (1986). New attachment formation in the human periodontium by guided tissue regeneration. Case reports. *Journal of Clinical Periodontology,* 13(6):604–616.

- Gottlow, J. (1993). Guided tissue regeneration using bioresorbable and non-resorbable devices: Initial healing and long-term results. *Journal of periodontology,* 64(11):1157-1165.

- Gottlow, J., Laurell, L., Lundgreen, D., Mathisen, T., Nyman, S., Rylander, H., Bogentoft, C. (1994). Periodontal tissue response to a new bioresorbable guided tissue regeneration device: a longitudinal study in monkeys. *International Journal of Periodontics Restorative Dentistry,* 14: 436-49.

- Greenstein, G. (2000). Nonsurgical periodontal therapy in 2000: A literature review. *JADA*, 131:1580-1592.

- Griffin, T.J., Cheung, W.S., Hirayama, H. (2004). Hard and soft tissue augmentation in implant therapy using acellular dermal matrix. *International Journal of Periodontics and Restorative Dentistry*, 24:352-361.

- Gupta, P., Elkins, C., Long, T.E., Wilkes, G.L. (2005). Electrospinning of linear homopolymers of poly(methylmethacrylate): exploring relationships between fiber formation, viscosity, molecular weight and concentration in a good solvent. *Polymer*, 46:4799-4810.

- Ha, Y.Y., Park, Y.W., Kweon, H.Y., Jo, Y.Y., Kim, S.G. (2014). Comparison of the physical properties and *in vivo* bioactivities of Silkworm-Cocoon-derived silk membrane, Collagen Membrane, and Polytetrafluoroethylene Membrane for guided bone regeneration. *Macromolecular Research*, 22(9): 1018-1023.

- Haimi, S., Suuriniemi, N., Haaparanta, A.M., Ella, V., Lindroos, B., Huhtala, H., Raty, S., Kuokkanen, H., Sandor, G.K., Kellomaki, M., Miettinen, S., Suuronen, R. (2009). Growth and osteogenic differentiation of adipose stem cells on PLA/bioactive glass and PLA/beta-TCP scaffolds. *Tissue Engineering Part A,* 15:1473–1480.

- Haipeng, G., Yinghui, Z., Jianchun, L., Yandao, G., Nanming, Z., Xiufang, Z. (2000). Studies on nerve cell affinity of chitosan-derived materials. *Jouurnal of Biomedical Materials Research*, 52(2):285–95.

- Harikumar, K., Nandakumar, K., Devadas, C., Mathew, S. (2014). Collagen-Chitosan barrier membrane, a novel, indigenous, and economic material for management of periodontal infrabony defects - A case-Control Study. *Universal research Journal of dentistry,* 4(2): 87-92.

- He, X., Liu, Y., Yuan, X., Lu, L. (2014). Enhanced healing of rat calvarial defects with MSCs loaded on BMP-2 releasing Chitosan/Alginate/Hydroxyapatite scaffolds. *PLoS ONE,* 9(8):e104061.

- Herrera, D., Retamal-Valdes, B., Alonso, B., Feres, M. (2018). Acute periodontal lesions (Periodontal abscesses and necrotizing periodontal diseases) and endo-periodontal lesions. *Journal of Clinical Periodontology*, 45(Supply20): S78-S94.

- Hing, K.A., Revell, P.A., Smith, N., Buckland, T. (2006). Effect of silicon level on rate, quality and progression of bone healing within silicate-substituted porous hydroxyapatite scaffolds. *Biomaterials*, 27: 5014–5026

- Hitti, R.A, Kerns, D.G. (2011). Guided Bone Regeneration in the Oral Cavity: A Review. *The Open Pathology Journal,* 5: 33-45.

- Ho, M.H., Hsieh, C.C., Hsiao, S.W., Thien, D.V.H. (2010) Fabrication of asymmetric chitosan GTR membranes for the treatment of periodontal disease. *Carbohydrate Polymers,* 79:955–963.

- Holmstrup, P. (1999). Non-plaque induced gingival lesions. *Annals of Periodontology,* 4:20-29.

- Holmstrup, P., Plemons, J., Meyle, J. (2018). Non-plaque-induced gingival diseases. *Journal of Clinical Periodontology*, 45(Supply20): S28-S43.

- Hong, H., Wei, J., Liu, C. (2007). Development of asymmetric gradational-changed porous chitosan membrane for guided periodontal tissue regeneration. *Composites: Part B,* 38:311–316.

- Hongbin, F., Haifeng, L., Yue, W., Lok, T.S., Goh, Hong, G.J.C. (2008). Development of a Silk Cable-Reinforced Gelatin/Silk Fibroin Hybrid Scaffold for Ligament Tissue Engineering. *Cell Transplantation,* 17(12):1389-1401.

- Hoogeveen, E. J., Gielkens, P. F., Schortinghuis, J., Ruben, J. L., Huysmans, M.-C.D.N.J.M., Stegenga, B. (2009). Vivosorb as a barrier membrane in rat mandibular defects. An evaluation with transversal microradiography. *International Journal of Oral Maxillofacial Surgery,* 38: 870–875.

93

- Hoque, M.E., Sakinah, N., Chuan, Y.L., Ansari, M.N.M. (2014) Synthesis and characterization of hydroxyapatite bioceramic. *International Journal of Science Engineering and Technology* 3(5):458–462.

- Horan, R. L., Antle, K., Collette, A.L., Wang, Y., Huang, J., Moreau, J.E., Volloch, V. Kaplan, D.L., Altman, G.H. (2005). *In vitro* degradation of silk fibroin. *Biomaterials*, 26: 3385-3393.

- Hott, M. (1993). Short term effects of organic silicon on trabecular bone in mature ovariectomized rats. *Calcified Tissue International*, 53:174–179.

- Hou, L.T., Yan, J.J., Tsai, A.Y.M., Lao, C.S., Lin, S.J., Liu, C.M. (2004). Polymer-assisted regeneration therapy with Atrisorbs barriers in human periodontal intrabony defects. *Journal of Clinical Periodontology*, 31: 68–74.

- Howell, T.H., Fiorellini, J., Jones, A., Alder, M., Nummikoski, P., Lazaro, M., Lilly, L., Cochran, D. (1997). A feasibility study evaluating rhBMP-2/absorbable collagen sponge device for local alveolar ridge preservation or augmentation. *The International Journal of Periodontics and Restorative Dentistry,* 17:125–139.

- Huang, Y., Polimeni, G., Qahash, M., Wikesjö, U.M.E. (2008).   Bone morphogenetic proteins and osseointegration: current knowledge – future possibilities. *Periodontology 2000*, 47:206–223.

- Huang, K.K, Shen, C., Chiang, C.Y., Hsieh, Y.D., Fu, E. (2005). Effects of bone morphogenetic protein-6 on periodontal wound healing in a fenestration defect of rats. *Journal of Periodontal Research*, 40:1–10.

- Hürzeler, M.B., Quiñones, C.R., Caffesse, R.G., Peter Schűpbach, P., Morrison, E.C. (1997). Guided periodontal tissue regeneration in interproximal intrabony defects following treatment with a synthetic bioabsorbable barrier. *Journal of Periodontology,* 68: 489-497.

- Ignatius, A.A., Ohnmacht, M., Claes, L.E., Kreidler, J., Palm, F. (2001). A Composite Polymer/Tricalcium Phosphate Membrane for Guided Bone Regeneration in Maxillofacial Surgery. *Journal of Biomedical Materials Research*, 58(5):564-569.

- Ingavle, G.C., Leach, J.K. (2014). Advancements in electrospinning of polymeric nanofibrous scaffolds for tissue engineering. *Tissue engineering part B Review,* 20(4):277-293.

- Ishikawa, I., Baehni, P. (2004). Non-surgical periodontal therapy- where do we stand. *Periodontology 2000*, 36: 9-13.

- Ishikawa, K., Ueyama, Y., Mano, T., Koyama, T., Suzuki, K., Matsumura, T. (1999). Self-setting barrier membrane for guided tissue regeneration method: Initial evaluation of alginate membrane made with sodium alginate and calcium chloride aqueous solutions. *Journal of Biomedical Materials Research,* 47: 111–115.

- Jain, D., Bar-Shalmon, D. (2014). Alginate drug delivery systems: applications in context of pharmaceutical and biomedical research. *Drug Development and industrial Pharmacy,* 40(12): 1576-1584.

95

- Jang, J.H., Castano, O., Kim, H.W. (2009). Electrospun materials as potential platforms for bone tissue engineering. *Advanced Drug Delivery Reviews,* 61:1065–1083.

- Janicki, P., Schmidmaier, G. (2011). What should be the characteristics of the ideal bone graft substitute? Combining scaffolds with growth factors and/or stem cells. *Injury*, 42(2): 77-81.

- Jao, D., Mou, X., Hu, X. (2016). Tissue engineering: A Silk Road. *Journal of Functional Biomaterials*, 7(3): 22-39.

- Jaramillo, C.D., Rivera, J.A., Echavarría, A., O'byme, J., Congote, D., Restrepo, L.F. (2010). Osteoconductive and osseointegration properties of a commercial hydroxyapatite compared to a synthetic product. *Rev Colomb Cienc Pecu,* 23:471–483.

- Jayakumar, R., Prabaharan, M., Sudheesh, P.T., Kumar, P.T., Nair, S.V., Tamura, H. (2011). Biomaterials based on chitin and chitosan in wound dressing applications. *Biotechnology Advances*, 29(3): 322-337.

- Jepsen, K., Jepsen, S. (2016). Antibiotics/antimicrobials: systemic and local administration in the therapy of mild to moderately advanced periodontitis. *Periodontology 2000*, 71(1): 82-112.

- Jetbumpenkul, P., Amornsudthiwat, P., Kanokpanont, S., Damrongsakkul, S. (2012). Balanced electrostatic blending approach – An alternative to chemical crosslinking of Thai silk fibroin/gelatin scaffold. *International Journal of Biological Macromolecules*, 50: 7–13.

96

- Ji, W., Yang, F., Ma, J., Bouma, M.J., Boerman, O.C., Chen, Z., van den Beucken, J.J.J.P., Jansen, J.A. (2013). Incorporation of stromal cell-derived factor-1 in PCL/gelatin electrospun membranes for guided bone regeneration. *Biomaterials,* 34: 735–745.

- Jiang, T., Abdel-Fattah, W.I., Laurencin, C.T. (2006). *In vitro* evaluation of chitosan/poly(lactic acid-glycolic acid) sintered microsphere scaffolds for bone tissue engineering. *Biomaterials,* 27:4894–4903.

- Jian-qi, H., Hong, H., Lieping, S., Genghua, G. (2002).Comparison of Calcium Alginate film with Collagen membrane for guided bone regeneration in mandibular defects in rabbits. *Journal of Oral Maxillofacial Surgery,* 60:1449-1454.

- Jin, L., Wang, T., Zhu, M.L., Leach, M.K., Naim, Y.I., Corey, J.M., Feng, Z.Q., Jiang, Q. (2012). Electrospun fibers and tissue engineering. *Journal of Biomedical Nanotechnology,* 8:1-9.

- Jones, J.R., Brauer, D.S., Hupa, L., Greenspan, D.C. (2016). Bioglass and bioactive glasses and their impact on healthcare. *International Journal of Applied Glass Science,* 1-12.

- Jun, Z., Hou, H., Schaper, A., Wendorff, J.H., Greiner, A. (2003). Poly-L-Lactide nanofibers by electrospinning – influence of solution viscosity and electrical conductivity on fiber diameter and fiber morphology. *e-Polymers*, 9:1-9.

- Jung, R.E., Glauser, R. Schdrer, P., Hammerle, C.H.F., Sailer, H.F., Weber, F.E. (2003). Effect of rhBMP-2 on guided bone regeneration in humans. A

97

randomized, controlled clinical and histomorphometric study. *Clinical Oral Implant Research,* 14(5):556-568

- Kaigler, D., Avila, G., Wisner-Lynch, L., Nevins, M.L., Nevins, M., Rasperini, G., Lynch, S.E., Giannobile, W.V. (2011). Platelet-Derived Growth Factor Applications in Periodontal and Peri-Implant Bone Regeneration. *Expert Opinion Biological Therapy,* 11(3): 375–385.

- Kaito, T., Myoui, A., Takaoka, K., Saito, N., Nishikawa, M., Tamai, N., Ohgushi, H., Yoshikawa, H. (2005). Potentiation of the activity of bone morphogenetic protein-2 in bone regeneration by a PLA-PEG/hydroxyapatite composite, *Biomaterials,* 26:73–79.

- Kamalanathan, P., Ramesh, S., Bang, L.T., Niakan, A., Tan, C.Y., Purbolaksono, J., Chandran, H., Teng, W.D. (2014). Synthesis and sintering of hydroxyapatite derived from eggshells as a calcium precursor. *Ceramic International,* 40(10):16349–16359.

- Kamitakahara, M., Ohtsuki, C., Miyazaki, T. (2008). Review paper: behavior of ceramic biomaterials derived from tricalcium phosphate in physiological condition. *Journal of Biomaterials Applications*, 23: 197–212.

- Kao, D.W.K., Kubota, A., Nevins, M., Fiorellini, J.P. (2012). The negative effect of combining rhBMP-2 and Bio-Oss on bone formation for maxillary sinus augmentation. *The International Journal of Periodontics & Restorative Dentistry*, 32(1): 61–67.

- Karring, T., Nyman, S., Gottlow, J., Laurell, L. (1993). Development of the biological concept of guided tissue regeneration - animal and human studies. *Periodontology 2000,* 1:26-35.

- Katagiri, T, Watabe, T. (2016). Bone morphogenetic proteins. *Cold Spring Harbor Prospective in Biology,* 8(6):a021899.

- Kawadkar, J., Jain, R., Kishore, R., Pathak, A., Chauhan, M.K. (2013). Formulation and evaluation of flurbiprofen-loaded genipin cross-linked gelatin microspheres for intra-articular delivery. *Journal of drug targeting,* 21(2):200-210.

- Kean, T., Thanou, M. (2009). Biodegradation, biodistribution and toxicity of chitosan. *Advanced drug Delivery Reviews,* 62: 3–11.

- Keestra, J.A., Grosjean, I., Coucke, W., Quirynen, M., Teughels, W. (2015). Non-surgical periodontal therapy with systemic antibiotics in patients with untreated chronic periodontitis: A systematic review. *Journal of Periodontal Research*, 50(3): 294-314.

- Kharaziha, M., Fathi, M.H., Edris, H. (2013). Development of novel aligned nanofibrous composite membrane for guided bone regeneration. *Journal of the Mechanical Behavior of Biomedical Materials,* 24:9-20.

- Ki, C.S., Baek, D.H., Gang, K.D., Lee, K.H., Um, I.C., Park, Y.H. (2005). Characterization of gelatin nanofiber prepared from gelatin-formic acid solution. *Polymer*, 46:5094-5102.

99

- Kim, I.Y., Seo, S.J., Moon, H.S., Yoo, M.K., Park, I.Y., Kim, B.C., Cho, C.S. (2008). Chitosan and its derivatives for tissue engineering applications. *Biotechnology Advances,* 26: 1-21.

- Kim, K.H., Jeong, L., Park, H.N., Shin, S.Y., Park, W.H., Lee, S.C., Kim, T.I., Park, Y.J., Seol, Y.J., Lee, Y.M., Ku, Y., Rhyu, I.C., Han, S.B., Chung, C.P. (2005). Biological efficacy of silk fibroin nanofiber membranes for guided bone regeneration. *Journal of Biotechnology,* 120, 327–339.

- Kim, J.Y., Yang. B.E., Ahn, J.H., Park, S.O., Shim, H.W. (2014). Comparable efficacy of silk fibroin with the collagen membranes for guided bone regeneration in rat calvarial defects. *Journal of Advanced Prosthodontics,* 6(6):539-46.

- Kim, B.R., Nguyen, T.B. L, Min, Y.K., Lee, B.T. (2014) *In vitro* and *in vivo* studies of BMP-2 loaded PCL-Gelatin-BCP electrospun scaffolds. *Tissue Engineering. Part A*, 20(23-24):3279–3289.

- Kim, B., Park, H., Lee, S.H., Sigmund, W.M. (2005). Poly (acrylic acid) nanofibers by electrospinning. *Materials Letters*, 59:829–32.

- Kinane, D.F. (2001). Causation and pathogenesis of periodontal disease. *Periodontology 2000*, 25: 8-20.

- Knabe, C., Howlett, C.R., Klar, F., Zreiqat, H. (2004). The effect of different titanium and hydroxyapatite-coated dental implant surfaces on phenotypic expression of human bone-derived cells. *Journal of Biomedical Materials Research,* 71(A): 98 –107.

- Kolambkar, Y.M., Dupont, K.M., Boerckel, J.D., Huebsch, N., Mooney, D.J., Dietmar W. Hutmacher, D.W., Guldberg, R.E. (2011). An alginate-based hybrid system for growth factor delivery in the functional repair of large bone defects. *Biomaterials* 32: 65-74.

- Kong, M., Chen, X.G., Xing, K., Park, H.J. (2010). Antimicrobial properties of chitosan and mode of action: A state of the art review. *International Journal of Food Microbiology,* 144: 51–63.

- Koop, R., Merheb, J., Quirynen, M. (2012). Periodontal regeneration with enamel matrix derivatives in reconstructive periodontal therapy. A systematic review. *Journal of Periodontolgy,* 83:707-720.

- Koutsopoulos, S. (2002). Synthesis and characterization of hydroxyapatite crystals: a review study on the analytical methods. *Journal of Biomedical Materials Research*, 62(4):600–612.

- Krisanapiboon, A., Buranapanitkit, B., Oungbho, K. (2006). Biocompatibility of hydroxyapatite composite as a local drug delivery system. *Journal of Orthopaedic Surgery*, 14(3):315-318.

- Kumirska, J., Czerwicka, M., Kaczyński, Z., Bychowska, A., Krzysztof Brzozowski, K., Thöming, J., Piotr Stepnowski, P. (2010). Application of spectroscopic methods for structural analysis of chitin and chitosan. *Marine Drugs,* 8: 1567-1636.

- Kuo, S.M., Chang, S.J., Chen, T.W., Kuan, T.C. (2006). Guided tissue regeneration for using a chitosan membrane: An experimental study in rats. *Journal of Biomedical Materials Research,* 76(2):408-415.

101

- Lang, N. P., Hammerle, C. H., Bragger, U., Lehmann, B., Nyman, R. S. (1994). Guided tissue regeneration in jaw bone defects prior to implant placement. *Clinical Oral Implants Research*, 5: 77–92.

- Langer, R., Vacanti, J.P. (1993). Tissue Engineering. *Science,* 260: 920-926.

- Lee, J.Y., Kim, Y.K., Yun, P.Y., Oh, J.S., Kim, S.G. (2010). Guided bone regeneration using two types of non-resorbable barrier membranes. *Journal of Korean Association of Oral Maxillofacial Surgery,* 36:275-279.

- Lee, K.Y., Mooney, D.J., (2012). Alginate: Properties and biomedical applications. *Progress in Polymer Science* 37:106– 126.

- Lee, K.Y., Bouhadir, K.H., Mooney, D.J. (2004). Controlled degradation of hydrogels using multifunctional cross-linking molecules. *Biomaterials,* 25:2461-2466.

- Lei, Y., Rai, B., Ho, K.H., Teoh, S.H. (2007). *In vitro* degradation of novel bioactive polycaprolactone-20% tricalcium phosphate composite scaffolds for *bone* engineering. *Materials Science and Engineering C,* 27:293-298.

- Levine, R.A., Manji, A., Faucher, J., Present, S. (2014). Use of Titanium Mesh in Implant Site Development for Restorative-Driven Implant Placement: Case Report. Part 1—Restorative Protocol for Single-Tooth Esthetic Zone Sites. *Compendium,* 35 (4): 264-273.

- Li, X.F., Feng, X.Q., Yang, S., Fu, G.Q., Wang, T.P., Su, Z.X. (2010). Chitosan kills Escherichia coli through damage to be of cell membrane mechanism. *Carbohydrate Polymers* 79: 493-499.

102

- Li, H., Qiao, T., Song, P., Guo, H., Song, X., Zhang, B. (2015). Star-shaped PCL/PLLA blended fiber membrane via electrospinning. *Journal of Biomaterials Science Polymer Edition,* 26(7):420-32.

- Li, J., Lu, X.L., Zheng, Y.F. (2008). Effect of surface modified hydroxyapatite on the tensile property improvement of HA/PLA composite. *Applied Surface Science,* 255:494-497.

- Li, W., Ding, Y., Yu, S., Yao, Q., Boccaccini, A.R. (2015). Multifunctional chitosan-45S5 bioactive glass-PHBV microsphere composite membranes for guided tissue/bone regeneration. *ACS Applied Materials & Interfaces*, 7(37): 20845–20854.

- Li, D., Xia, Y. (2004). Electrospinning of nanofibers: reinventing the wheel. *Advanced Materials*, 16: 1151-1570.

- Li, D., Wang, Y., Xia, Y. (2004). Electrospinning nanofibers as uniaxially aligned arrays and layer by layer stacked films. *Advanced Materials*, 16:361-366.

- Lia, M., Ogisob, M., Minourab, N. (2003). Enzymatic degradation behavior of porous silk fibroin sheets. *Biomaterials,* 24: 357–365.

- Liang, D., Hsiao, B.S., Chu, B. (2007). Functional electrospun nanofibrous scaffolds for biomedical applications. *Advanced Drug Delivery Reviews,* 59(14): 1392-1412.

- Liao, S.S., Cui, F.Z., Zhang, W., Feng, Q.L. (2004). Hierarchically Biomimetic Bone Scaffold Materials: Nano-HA/Collagen/PLA Composite. *Journal of Biomedical Materials Research.* 69(B): 158–165.

- Liao, S., Wang, W., Uo, M., Ohkawa, S., Aksaka, T., Tamura, K., Cui, F., Watari, F. (2005). A Three-layered nano-carbonated Hydroxyapatite /Collagen/ PLGA composite membrane for guided tissue regeneration, *Biomaterials,* 26: 7564-7571.

- Liao, S., Wang, W., Yokoyama, A., Zhu, Y., Watari, F., Ramakrishna, S., Chan, C.K. (2010). *In vitro* and *in vivo* behaviors of the three layered nanocarbonated hydroxyapatite/collagen/ PLGA composite. *Journal of Bioactive and compatible polymers,* 25:154-168.

- Liao, H., Shi, K., Peng, J., Qu, Y., Liao, J., Qian, Z. (2015). Preparation and properties of nano-hydroxyapatite/ Gelatin/ Poly(vinylalcohol) composite membrane. *Journal of Nanoscience and Tecnology,* 15(6):4188-4192.

- Lin, H.Y., Chen, S.H., Chang, S.H., Huang, S.T. (2015). Trilayered chitosan scaffold as a potential skin substitute. *Journal of Biomaterials Science, Polymer Edition,* 26(3):855-867.

- Lin, W.H., Yu, J., Chen, G., Tsai, W.B. (2016). Fabrication of multi-biofunctional gelatin based electrospun fibrous scaffolds for enhancement of osteogenesis of mesenchymal stem cells. *Colloids and Surfaces B: Biointerfaces,* 138: 26–31.

- Lindhe, J., Kinane, D., Ramney, R., Listgarten, M., Lamster, A., Loe, H., Charles, A., Schoor, R., Chung, C.P., Seymour, G., Flemmig, T., Someman, M. (1999). Consensus report: Chronic Periodontitis. *Annal of periodontology,* 4(1): 38.

- Lisa, J., Heitz-Mayfield, A., Lang, N.P. (2013). Surgical and non-surgical periodontal therapy. Learnt and unlearnt concepts. *Periodontology 2000*, 62: 218-231.

- Liu, H., Du, Y., Wang, X., Sun, L. (2004). Chitosan kills bacteria through cell membrane damage. *International Journal of Food Microbiology,* 95(2): 147-155.

- Liu, G., Zhou, H., Wu, H., Chen, R., Guo, S. (2016). Preparation of alginate hydrogels through solution extrusion and the release behavior of different drugs. *Journal of biomaterials science. Polymer edition*, 7:1-16.

- Lu, S., Wang, P., Zhang, F., Zhou, X., Zuo, B., You, X., Gao, Y. Liu, H., Tang, H. (2015). A novel silk fibroin nanofibrous membrane for guided bone regeneration: a study in rat calvarial defects. *Amercian Journal of Translational Research,* 7(11): 2244-2253.

- Lynch, S.E., Williams, R.C., Polson, A.M., Howell, T.H., Reddy, M.S., Zappa, U.E., Antoniades, H.N. (1989). A combination of platelet-derived and insulin-like growth factors enhances periodontal regeneration. *Journal of Clinical Periodontology*, 16(8):545–548.

- Lyngstadaas, S.P., Wohlfahrt, J.C., Brookes, S.J., Paine, M.L., Snead, M.L., Reseland, J.E. (2009). Enamel matrix proteins; old molecules for new applications. *Orthodontics and Craniofacial Research,* 12(3): 243–253.

- Ma, Z., Kotaki, M., Inai, R., Ramakrishna, S. (2005). Potential of nanofiber matrix as tissue-engineering scaffolds. *Tissue Engineering,* 11:101-109.

- Majeti N.V. Kumar, R. (2000). A review of chitin and chitosan applications. *Reactive & Functional Polymers,* 46: 1–27.

105

- Mani, R., Mahantesha, S., Nandini, T.K., Lavanya, R. (2014). Growth factors in periodontal regeneration. *Journal of Advanced Oral Research,* 5(2):1-5.

- Marouf, H.A., El-Guindi, H.M. (2000). Efficacy of high-density versus semipermeable PTFE membranes in an elderly experimental model. *Oral Surg Oral Med Oral Pathol Oral Radiol Endod,* 89:164-170.

- Matthews, J.A., Wnek, G.E., Simpson, D.G., Bowlin, G.L. (2002). Electrospinning of collagen nanofibers. *Biomacromolecules*, 3 (2):232–238.

- McAllister, B.S., Haghighat, K. (2007). Bone augmentation techniques. *Journal of Periodontology,* 78:377-396.

- Meisel, P., Kocher, T. (2005). Photodynamic therapy for periodontal diseases: state of the art. *Journal of Photochemistry and Photobiology B: Biology,* 79: 159–170.

- Melcher, A.H. (1976). On the repair potential of periodontal tissues. *Journal of Periodontology,* 47:256-260.

- Merli, M., Migani, M., Esposito, M. (2007). Vertical ridge augmentation with autogenous bone grafts: Resorbable barriers supported by ostheosynthesis plates versus titanium-reinforced barriers. A preliminary report of a blinded randomized controlled clinical trial. *International Journal of Oral Maxillofacial Implants,* 22: 373-382.

- Miron, R.J., Fujioka-Kobayashi, M., Buser, D., Zhang, Y., Bosshardt, D.D., Sculean, A. (2017). Combination of collagen barrier membrane with Enamel Matrix Derivative-liquid improves osteoblast adhesion and

differentiation. *The International Journal of Oral & Maxillofacial Implants*, 32(1):196-203.

- Misra, S.K., Mohn, D., Brunner, T.J., Stark, W.J., Philip, S.E., Roy, I., Salih, V., Knowles, J.C., Boccaccini, A.R. (2008). Comparison of nanoscale and microscale bioactive glass on the properties of P (3HB)/Bioglass® composites. *Biomaterials,* 29(12): 1750–1761.

- Mota, J., Yu, N., Caridade, S.G., Luz, G.M., Gomes, M.E., Reis, R.L.,John A. Jansen, J.A., X. Walboomers, X.F., Mano, J.F. (2012). Chitosan/bioactive glass nanoparticle composite membranes for periodontal regeneration. *Acta Biomaterialia,* 8: (2012) 4173–4180.

- Mottaghitalab, F., Hosseinkhani, H., Shokrgozar, M.A., Mao, C, Yang, M., Farokhi, M. (2015). Silk as a potential candidate for bone tissue engineering. *Journal of Control Release*, 10 (215):112-128.

- Murphy, A.R., Kaplan D.L. (2009). Biomedical applications of chemically-modified silk fibroin. *Journal of Material Chemistry*, 19(36): 6443–6450.

- Nasr, H.F., Aichelmann-Reidy, M.E., Yukna, R.A. (1999). Bone and bone substitutes. *Periodontology 2000,* 19:74–86.

- Nassar, H., Kantarci, A., Van-Dyke, T.E. (2007). Diabetic periodontitis: a model for activated innate immunity and impaired resolution of inflammation. *Periodontology 2000,* 43:233-44.

- Nielson, F., Poellot, R. (2004). Dietary Si affects bone turnover and differentiation in overiectomized and sham operated growing rats. *The Journal of Trace Elements in Experimental Medicine,* 17:137–149.

- Ning, Z., Jiang, N., Gan, Z. (2014). Four-armed PCL-b-PDLA diblock copolymer: 1. Synthesis, crystallization and degradation. *Polymer Degradation and Stability,* 107: 120-128.

- Niu, X., Feng, Q., Wang, M., Guo, X., Zheng, Q. (2009). *In vitro* degradation and release behavior of porous poly(lactic acid) scaffolds containing chitosan microspheres as a carrier for BMP-2-derived synthetic peptide. *Polymer Degradation and stability,* 94(2):176-182.

- Noritake, K., Kuroda, S., Nyan, M., Ohya, K., Tabata, Y., Kasugai, S. (2011). Development of a new barrier membrane for guided bone regeneration: An *in vitro* and *in vivo* study. *Journal of Oral Tissue Engineering*, 9: 53–63.

- Núñez, J., Caffesse, R., Vignoletti, F., Guerra2, F., Roman, F.S., Sanz, M. (2009). Clinical and histological evaluation of an acellular dermal matrix allograft in combination with the coronally advanced flap in the treatment of miller class I recession defects: an experimental study in the mini-pig. *Journal of Clinical Periodontology,* 36: 523–531.

- Nyman, S., Gottlow, J., Karring, T., Lindhe, J. (1982). The regenerative potential of the periodontal ligament. An experimental study in the monkey. *Journal of Clinical Periodontology,* 9(3): 257–265.

- Nyman, S., Lindhe, J., Karring, T., Rylander, H. (1982). New attachment following surgical treatment of human periodontal disease. *Journal of Clinical Periodontology,* 9: 290–296.

- Omenetto, F.G., Kaplan, D.L. (2010). New opportunities for an ancient material. *Science,* 329: 528-531.

- Ong, S.Y., Wu, J., Moochhala, S.M., Tan, M.H., Lu, J. (2008). Development of a chitosan-based wound dressing with improved hemostatic and antimicrobial properties. *Biomaterials,* 29(32):4323-4332.

- Owens, K.W., Yukna, R.A. (2001). Collagen membrane resorption in dogs: A comparative study. *Implant Dentistry,* 10(1): 49-58.

- Parrish, L.C., Miyamoto, T., Fong, N., Mattson, J.S., Cerutis, D.R. (2009). Non-bioabsorbable vs. bioabsorbable membrane: assessment of their clinical efficacy in guided tissue regeneration technique. A systematic review. *Journal of Oral Science*, 51(3): 383-400.

- Park, I.K., Yang, J., Jeong, H.J., Bom, H.S., Harada, I., Akaike, T., Kim, S.I., Cho, C.S. (2003). Galactosylated chitosan as a synthetic extracellular matrix for hepatocytes attachment. *Biomaterials*, 24: 2331–2337.

- Patel, N., Best, S., Gibson, I.R., Hing, K., Damien, E., Bonfield, W. A. (2002). Comparative study on the *in vivo* behaviour of hydroxyapatite and silicon substituted hydroxyapatite granules. Journal *of Materials Science Materials in Medicine,* 13:1199–1206.

- Patino, M.G., Neiders, M.E., Andreana, S., Noble, B., Robert E., Cohen, R.E. (2002). Collagen as an implantable material in medicine and dentistry. *Journal of Oral Implantology,* 28(5):220-225.

- Patil, R.D., Mark, J.E., Apostolov, A., Vassileva, E., Fakirov, S., 2000. Crystallization of water in some crosslinked gelatins. *European Polymer Journal,* 36 (5):1055–1061.

- Pereira, R, Carvalho, A., Vaz, D.C., Gil, M.H., Mendes, A., Bártolo, P. (2013). Development of novel alginate based hydrogel films for wound healing applications. *International Journal of Biological Macromolecules,* 52: 221-230.

- Petelin, M., Perkič, K., Seme, K., Gašpirc, B. (2015). Effect of repeated adjunctive antimicrobial photodynamic therapy on subgingival periodontal pathogens in the treatment of chronic periodontitis. *Lasers in Medical Science,* 30:1647–1656.

- Pham Q.P., Sharma, U., Mikos A.G. (2006). Electrospinning of Polymeric Nanofibers for Tissue Engineering Applications: A Review. *Tissue Engineering*, 12(5):1197-1211.

- Phipps, M.C., Xu, Y., Bellis, S.L. (2012). Delivery of platelet-derived growth factor as a chemotactic factor for mesenchymal stem cells by bone-mimetic electrospun scaffolds. *PLoS One*, 7(7):e40831.

- Pietak, A.M., Reid, J.W., Stott, M.J., Sayer, M. (2007). Silicon substitution in calcium phosphate. Review. *Biomaterials*, 28:4023-4032.

- Pinchuk, L. (1994). A review of biostability and carcinogenicity of polyurethanes in medicine and the new generation of 'biostable' polyurethanes. *Journal of Biomaterial Science Polymer Education,* 6: 225-267.

- Plachokova, A.S., Dolder, J.V., Jansen, J.A. The bone-regenerative properties of Emdogain adsorbed onto poly (D,L-lactic-coglycolic acid)/calcium phosphate composites in an ectopic and an orthotopic rat model. *Journal of Periodontal Research*, 43:55-63.

110

- Pontoriero, R., Lindhe, J. (1998). Guided tissue regeneration in the treatment of degree III furcation defeets in maxillarv molars. *Journal of Clinical Periodontology,* 22: 810-812.

- Pontoriero, R., Lindhe, J., Nyman, S., Karring, R., Rosenberg, E., Sanavi, F. (1988). Guided tissue regeneration in degree II furcation involved mandibular molars. A clinical study. *Journal of Clinical Periodontology,* 15: 247–254.

- Position paper. (2001). Guidelines for periodontal therapy. *Journal of periodontology,* 72: 1624-1628.

- Position paper. (2005). Periodontal regeneration. *Journal of Periodontology,* 76:1601-1622.

- Pretzl, B., Kim, T., Holle, R., Eickholz, P. (2008). Long-term results of guided tissue regeneration therapy with non-resorbable and bioabsorbable barriers. IV. A case series of infrabony defects After 10 Years. *Journal of Periodontology*, 79:1491-1499.

- Profeta, A.C., Prucher, G.M. (2015). Bioactive-glass in periodontal surgery and implant dentistry. *Dental Materials Journal,* 34(5): 559–571.

- Proussaefs, P., Lozada, J. (2006). Use of titanium mesh for staged localized alveolar ridge augmentation: clinical and histologic-histomorphometric evaluation. *Journal of Oral Implantology,* 32:237–47.

- Puumanen, K., Kellomäki, M., Ritsilä, V., Böhling, T., Törmälä, P., Waris, T., Ashammakhi, N. (2005). A Novel Bioabsorbable Composite Membrane of Polyactive® 70/30 and Bioactive Glass Number 13-93 in Repair of Experimental

111

Maxillary Alveolar Cleft Defects. *Journal of Biomedical Material Research, Part B Applied Biomaterials,* 75B (1):25-33.

- Raja, S., Byakod, G., Pudakalkatti, P. (2009). Growth factors in periodontal regeneration. *International Journal of Dental Hygiene*, 7(2):82-89.

- Rakhmatia, Y.D., Ayukawa, Y., Furuhashi A, Koyano, K. (2013). Current barrier membranes: Titanium mesh and other membranes for guided bone regeneration in dental applications. *Journal of Prosthodontic Research,* 57 3–14.

- Ramseier, C.A., Rasperini, G., Batia, S., Giannobile, W. (2012). Advanced reconstructive technologies for periodontal tissue repair. *Periodontology 2000,* 59:185-202.

- Rao, S.M., Ugale, G.M., Warad, S.B. (2013). Bone Morphogenetic Proteins: Periodontal Regeneration. *North American Journal of Medical Sciences*, 5(3):161-168.

- Ratner, B.D., Gladhill, K.W., Horbett, T.A. (1988). Analysis of *in vitro* enzymatic and oxidative degradation of polyurethanes. *Journal of Biomedical Materials Research*, 22: 509-527.

- Ratanavaraporn, J., Rangkupan, R.H., Jeeratawatchai, H., Kanokpanont, S., Damrongsakkul, S.P. (2010). Influences of physical and chemical cross-linking techniques on electrospun type A and B gelatin fiber mats. *International Journal of Biological Macromolecules,* 47: 431-438.

- Ratnayake, J.T.B., Mucalo, M., DiaS, G.J. (2016). Substituted hydroxyapatite for bone regeneration. A review of current trends. *Journal of Biomedical Materials Research Part B,* 00B: 000-000.

- Remminghorst, U., Rehm, B.H.A. (2006). Bacterial alginates: from biosynthesis to applications. *Biotechnology Letters*, 28:1701–1712.

- Reneker, D.H., Yarin, A.L. (2008). Electrospinning jets and polymer nanofibers. *Polymer*, 49:2387-2425.

- Reynolds, M.A., Aichelmann-Reidy, M.E., Branch-Mays, G.L. (2010). Regeneration of periodontal tissue: bone replacement grafts. *Dental Clinics of North America,* 54:55-71.

- Reynolds, M.A., Kao, R.T., Nares, S., Camargo, P.M., Caton. J.G., Clem, D.S., Fiorellini, J.P., Geisinger, M.L., Mills, M.P., Nevins, M.L., Rosen, P.S. (2015). Periodontal regeneration-intrabony Defects: Practical applications from the AAP Regeneration Workshop. *Clinical Advances in Periodontics,* 5(1): 21-29.

- Reynolds, M.A., Aichelmann-Reidy, M.E., Branch-Mays, G.L. (2010). Regeneration of periodontal tissue: bone replacement grafts. *Dental Clinics of North America* 54:55-71.

- Rinaudo M. (2008). Main properties and current applications of some polysaccharides as biomaterials. *Polymer International*, 57:397-430.

- Roccuzzo, M., Ramieri, G., Spada, M.C., Bianchi, S.D., Berrone, S. (2004). Vertical alveolar ridge augmentation by means of a titanium mesh and autogenous bone grafts. *Clinical Oral Implants Research, 15*:73-81.

- Rodrigues, J.R., Alves, N.M., João F. Mano, J.F. (2016). Biomimetic polysaccharide/bioactive glass nanoparticles multilayer membranes for guided tissue regeneration. *RSC Advances*, 6: 75988-75999.

113

- Rujitanapanich, S., Kumpapan, P., Wanjanoi, P. (2014). Synthesis of hydroxyapatite from oyster shell via precipitation. *Energy Procedia,* 56: 112-117.

- Ruys A. (1993). Silicon doped hydroxyapatite. *Journal of Australian Ceramic Society*, 29: 71–80.

- Sabra, W., Zeng, A.P., Deckwer, W.D. (2001). Bacterial alginate: physiology, product quality and process aspects. *Applied Microbiology Biotechnology*, 56:315–325.

- Sadat-Shojai, M. (2009). Preparation of hydroxyapatite nanoparticles: Comparison between hydrothermal and solvo-treatment processes and colloidal stability of produced nanoparticles in a dilute experimental dental adhesive. *Journal of Iranian Chemical Society,* 6(2):386-392.

- Saltz, A., Kandalam, U. (2016). Mesenchymal stem cells and alginate microcarriers for craniofacial bone tissue engineering: A review. *Journal of Biomedical Materials Research Part A,* 104(5): 1276-1284.

- Sam, G., Pillai, B.R.M. (2014). Evolution of barrier membranes in periodontal regeneration-"Are the third generation membranes really here?" *Journal of Clinical and Diagnostic Research,* 8(12):14-17.

- Sanz, M., Giovannoli, J.L. (2000). Focus on furcation defects: guided tissue regeneration. *Periodontology 2000,* 22:169–189.

- Sarin, S., Rekhi, A. (2016). Bioactive glass: A potential next generation biomaterial. *SRM Journal of Research in Dental Sciences,* 7(1):27-32.

114

- Scantlebury, T., Ambruster, J. (2012). The Development of Guided regeneration: Making the impossible possible and the unpredictable predictable. *Journal of Evidence Based Dental Practice,* S1: 110-117.

- Schofer, M.D., Roessler, P.P., Schaefer, J., Theisen, C., Schlimme, S., Heverhagen, J.T., Voelker, M., Dersch, R., Agarwal, S., Fuchs-Winkelmann, S., Paletta1, J.R.J. (2011). Electrospun PLLA nanofiber scaffolds and their use in combination with BMP-2 for reconstruction of bone defects. *PLoS ONE,* 6(9):e25462.

- Schwarz, K., Milne D.B. (1972). Growth-promoting effects of silicon in rats. *Nature,* 239:333–334.

- Sculean, A., Jepsen, S. (2004). Biomaterials for the reconstructive treatment of periodontal intrabony defects. Part 1. Bone grafts and bone substitutes. *Perio,* 1(1): 5-15.

- Sculean, A., Nikolidakis, D., Schwarz, F. (2008). Regeneration of periodontal tissue. Combination of barrier membrane and graft materials- biological foundations and preclinical evidence: a systematic review. *Journal of clinical periodontolgy,* 35 (8 supply): 106-116.

- Seymour, R.A. (2006). Effect of medications on the periodontal tissues in health and disease. *Periodontology 2000,* 40: 120-129.

- Sgolastra, F., Petrucci, A., Severino, M., Graziani, F., Gatto, R., Monaco, A. (2013). Adjunctive photodynamic therapy to non-surgical treatment of chronic periodontitis: a systematic review and meta-analysis. *Journal of Clinical Periodontology*, 40:514–526.

- Shen, B., Wei, A., Whittaker, S., Williams, L.A., Tao, H., Ma, D.D.F., Ashish D. Diwan, A.D. (2010). The role of BMP-7 in chondrogenic and osteogenic differentiation of human bone marrow multipotent mesenchymal stromal cells *in vitro. Journal of Cellular Biochemistry,* 109(2):406-416.

- Shin, S.H., Purevdorj, O., Castano, O., Planell, J.A., Kim, H.W. (2012). A short review: Recent advances in electrospinning for bone tissue regeneration. *Journal of Tissue Engineering,* 3(1) 2041731412443530.

- Shin, S.Y., Park, H.N., Kim, K.H., Lee, M.H., Choi, Y.S., Park, Y.J., Lee, Y.M., Rhyu, I.C., Han, S.B., Lee, S.J., Chung, C.P. (2005). Biological evaluation of chitosan nanofiber membrane for guided bone regeneration. *Journal of Periodontology,* 76:1778–1784.

- Shue, L., Yufeng, Z., Mony, U. (2012). Biomaterials for periodontal regeneration. A review of ceramics and polymers. *Biomaterials,* 2(4): 271–277.

- Sill, T.J., Recum, H.A.V. (2008). Electrospinning: application in drug delivery and tissue engineering. *Biomaterials*, 29:1989-2006.

- Simion, M., Fontana, F., Rasperini, G., Maiorana, C. (2007). Vertical ridge augmentation by expanded-polytetrafluoroethylene membrane and a combination of intraoral autogenous bone graft and deproteinized anorganic bovine bone (Bio Oss). *Clinical Oral Implant Research,* 18:620–629.

- Singh, A. (2012). Hydroxyapatite, a biomaterial: its chemical synthesis, characterization and study of biocompatibility prepared from shell of garden snail, Helix aspersa. *Bulletin of Material Science,* 35(6):1031–1038.

116

- Sisson, K., Zhang, C., Farach-Carson, M.C., Chase, D.B., Rabolt, J.F. (2009). Evaluation of cross-linking methods for electrospun gelatin on cell growth and viability. *Biomacromolecules*, 10(7):1675–1680.

- Smith, L.A, Ma, P.X. (2004). Nano-fibrous scaffolds for tissue engineering. *Colloids and surfaces B: Biointerfaces,* 39(3): 124-131.

- Soheilifar, S., Soheilifar, S., Bidgoli, M., Torkzaban, P. (2014). Barrier Membrane, a Device for Regeneration: Properties and Applications. *Avicenna Journal of Dental Research*, 6(2): 1-5.

- Son, W.K., Youk, J.H., Lee, T.S., Park, W.H. (2004). The effects of solution properties and polyelectrolyte on electrospinning of ultrafine poly (ethylene oxide) fibers. *Polymer*, 45:2959-2966.

- Soran, Z., Aydin, R.S.T., Gümüşderelioğlu, M. (2012). Chitosan scaffolds with BMP-6 loaded alginate microspheres for periodontal tissue engineering. *Journal of Microencapsulation,* 29(8): 770-780.

- Srouji, S., Ben-David, D., Lotan, R., Livne, E., Avrahami, R., Zussman, E. (2011). Slow-release human recombinant bone morphogenetic protein-2 embedded within electrospun scaffolds for regeneration of bone defect: *In vitro* and *in vivo* evaluation. *Tissue Engineering Part A,* 17:269-277.

- Stoecklin-Wasmer, C., Rutjes, A.W.S., da Costa, B.R., Salvi, G.E., Jüni, P., Sculean, A. (2013). Absorbable Collagen Membranes for Periodontal Regeneration: A Systematic Review. *Journal of Dental Research,* 92(9):773-781.

- Strietzel, F.P., Reichart, P.A., Graf, H.L. (2007). Lateral alveolar ridge augmentation using a synthetic nano-crystalline hydroxyapatite bone substitution material (Ostim®). *Clinical Oral Implants Research,* 18:743–51.

- Suárez-López Del Amo, F., Monje, A., Padial-Molina, M., Tang, Z., Wang, H.L. (2015). Biologic agents for periodontal regeneration and implant site development. *BioMed Research International*, Article ID 957518: 1-10.

- Suh, J.K.F., Matthew, H.W.T. (2000). Application of chitosan-based polysaccharide biomaterials in cartilage tissue engineering: a review. *Biomaterials* 21: 2589-2598.

- Sukigara, S., Gandhi, M., Ayutsede, J., Micklus, M., Ko, F. (2003). Regeneration of Bombyx mori silk by electrospinning- part 1: processing parameters and geometric properties. *Polymer*, 44:5721-5727.

- Sun, J., Tan, H. (2013). Alginate-based biomaterials for regenerative medicine applications. *Materials,* 6:1285-1309.

- Sung, H.W, Liang, I.L., Chen, C.N., Huang, R.N., Liang, H.F. (2001). Stability of a biological tissue fixed with a naturally occurring crosslinking agent (genipin). *Journal of Biomedical Material Research*, 55:538–546

- Susin, C., wikesjö, U.M.E. (2013). Regenerative periodontal therapy: 30 years of lessons learned and unlearned. *Periodontology 2000*, 62:232-242.

- Suzuki, Y., Tanihara, M., Suzuki, K., Saitou, A., Sufan, W., Nishimura, Y. (2000). Alginate hydrogel linked with synthetic oligopeptide derived from BMP-2 allows ectopic osteoinduction *in vivo*. *Journal of Biomedical Materials Research,* 50:405–409.

118

- Taba, M. Jr., Jin, Q., Sugai, J.V., Giannobile, W.V. (2008). Current concepts in periodontal bioengineering. *Orthodontics and craniofacial research*, 8: 292-302.

- Takasaki, A.A., Aoki, A., Mizutani, K., Schwarz, F., Sculean, A., Wang, C.Y., Koshy, G., Romanos, G., Ishikawa, I., Izumi, Y. (2009). Application of antimicrobial photodynamic therapy in periodontal and peri-implant diseases. *Periodontology 2000*, 51:109-140.

- Tal, H., Kozlovsky, A., Artzi, Z., Carlos E., Nemcovsky, C.E., Moses, O. (2008). Cross-linked and non-cross-linked collagen barrier membranes disintegrate following surgical exposure to the oral environment: a histological study in the cat. *Clinical Oral Implant Research*, 19: 760–766.

- Tanaka, S., Avigadg, G., Eikenberry, E.F., Brodsky, B. (1988). Isolation and Partial Characterization of Collagen Chains Dimerized by Sugar-derived Cross-links. *The Journal of Biological Chemistry*, 263(33):17650-17657.

- Tang, X., Xiao, X., Liu, R. (2005). Structural characterization of silicon substituted hydroxyapatite synthesized by hydrothermal method. *Materials Letters,* 59:3841–3846.

- Tatakis, D.N., Kumar, P.S. (2005). Etiology and pathogenesis of periodontal disease. *Dental Clinics of North America,* 49: 491-516.

- Tatakis, D.N., Koh, A., Jin, L., Wozney, J.M., Rohrer, M.D., Wikesjö, U.M.E. (2002). Peri-implant bone regeneration using recombinant human bone morphogenetic protein-2 in a canine model: a dose-response study. *Journal of Periodontal Research,* 37(2):93-100.

- Teo, W.E., Ramakrishna, S. (2006). A review on electrospinning design and nanofibre assemblies. *Nanotechnology,* 17: R89–R106

- Termaat, M.f., Den Boer F.C., Bakker, F.C., Patka, P., Haarman, H.J.TH.M. (2005). Bone Morphogenetic Protein. Development and clinical efficacy in the treatment of fractures and bone defects. *The Journal of Bone & Joint Surgery*, 87-A (6): 1367-1378.

- Thian, E.S., Huang, J., Best, S.M., Barber, Z.H., Bonfield, W. (2005). Magnetron co-sputtered silicon-containing hydroxyapatite thin films—an *in vitro* study. *Biomaterials*, 26: 2947–2956.

- Thu, H.E., Zulfakar, M.H., Ng, S.F. (2012). Alginate based bilayer hydrocolloid films as potential slow-release modern wound dressing. *International Journal of Pharmaceutics*, 434: 375-383.

- Tinti, C., Benfenati, S.P. (2001). Treatment of Peri-implant Defects with the Vertical Ridge Augmentation Procedure: A Patient Report. *International Journal of Oral Maxillofacial Implants,* 16:572–577.

- Tirri, T., Rich, J., Wolke, J., Seppälä, J., Yli-Urpo, A., Närhi, T.O. (2008). Bioactive glass induced in vitro apatite formation on composite GBR membranes. *Journal of Materials Science: Materials in Medicine*, 19:2919-2923.

- Tonnesen, H.H, Karlsen, J. (2002). Alginate in drug delivery systems. *Drug development and industrial pharmacy*, 28:621–630.

- Tonetti, M.S., Greenwell, H., Korman, K.S. (2018). Staging and grading of periodontitis: framework and proposal of a new classification and case definition. *Journal of Clinical Periodontology*, 45(Supply20): S149-S161.

120

- Tripathi, G., Basu, B. (2012). A porous hydroxyapatite scaffold for bone tissue engineering: Physico-mechanical and biological evaluations. *Ceramics International,* 38:341-349.

- Trombelli, L., Farinal, R., Silva, C.O., Tatakis, D.N. (2018). Plaque induced gingivitis: Case definition and diagnostic considerations. *Journal of Clinical Periodontology,* 45(Supply20):S44-S67.

- Trombelli, L., Simonelli, A., Pramstraller, M., Wikesjo, U.M.E., Farina, R. (2010). Single flap approach with and without guided tissue regeneration and a hydroxyapatite biomaterial in the management of intraosseous periodontal defects. *Journal of Periodontology*, 81:1256–63.

- Tseng, H.J., Tsou, T.L., Wang, H.J., Hsu, S.H. (2013). Characterization of choitosan-gelatin scaffolds for dermal tissue engineering. *Journal of Tissue Engineering and Regenerative Medicine,* 7(1):20-31.

- Tsuji H, Ishizaka, T. (2001) Blends of aliphatic polyesters. VI. Lipase-catalyzed hydrolysis and visualized phase structure of biodegradable blends from poly(epsilon-caprolactone) and poly(L-lactide). *International Journal of Biological Macromolecules,* 29: 83–89.

- Ueyamaa, Y., Ishikawa, K., Manoc, T., Koyamac, T., Nagatsukad, H., Suzukib, K., Ryoke, K. (2002). Usefulness as guided bone regeneration membrane of the alginate membrane. *Biomaterials*, 23: 2027–2033.

- Ulubayram, K., Aksu, E., Gurhan, S.I., Serbetci, K., Hasirci, N. (2002). Cytotoxicity evaluation of gelatin sponges prepared with different cross-linking agents. *Journal of Biomaterial Science Polymer Edition*, 13(11):1203-1219.

121

- Urist, M.R. (1965). Bone: Formation by autoinduction. *Science (New York, NY),* 150:893-899.

- Valizadeh, A., Mussa-Farkhani, S., (2014). Electrospinning and electrospun nanofibres. *IET Nanobiotechnology*, 8(2):83-92.

- Vallet-Regí, M., Arcos, D. (2005). Silicon substituted hydroxyapatites. A method to upgrade calcium phosphate based implants. *Journal of Materials Chemistry*, 15: 1509-1516.

- Venezia, E., Goldstein, M., Boyan, B.D., Schwartz, Z. (2004). The use of enamel matrix derivative in the treatment of periodontal defects: A literature review and meta-analysis. *Critical Reviews in Oral Biology & Medicine,* 15(6):382-402

- Veparia, C., Kaplan, D.L. (2007). Silk as a biomaterial. *Progress in Polymer Science* 32: 991–1007.

- Villar, C.C., Cochran, D.L. (2010). Regeneration of periodontal tissue: Guided tissue regeneration. *Dental clinics of North America,* 54: 73-92.

- Villarreal-Gómez, L.J., Cornejo-Bravo, J.M., Vera-Graziano, R., Grande, D. (2016). Electrospinning as a powerful technique for biomedical applications: a critically selected survey. *Journal of Biomaterials Science, Polymer Edition,* 27(2):157-176

- Walker, C.B., Karpinia, K., Baehni, P. (2004). Chemotherapeutics: antibiotics and other antimicrobials. *Periodontology 2000*, 36: 146–165.

- Wang, H.L., Greenwell, H. (2001). Surgical periodontal therapy. *Periodontology 2000*, 25:89-99.

- Wang, J., Wang, L., Zhou, Z., Lai, H., Xu, P., Liao, L., Wei, J. (2016). Biodegradable Polymer Membranes Applied in Guided Bone/Tissue Regeneration: A Review. *Polymers,* 8 (4): 115-135.

- Wang, Y.Z., Rudym, D.D., Walsh, A., Abrahamsen, L., Kim, H.J., Kim, H.S., Kirker-Head, C., Kaplan, D.L. (2008). *In vivo* degradation of three-dimensional silk fibroin scaffolds. *Biomaterials,* 29: 3415-3428.

- Wang, E.A., Rosen, V., Cordes, P., Hewick, R.M., Kriz, M.J., Luxenberg, D.P., Sibley, B.S., Wozney, J.M. (1988). Purification and characterization of other distinct bone-inducing factors. *Proceedings of National Academy of Science*, 85: 9484–9488.

- Wang, X., Um, I.C., Fang, D., Okamoto, A., Hsiao, B.S., Chu, B. (2005). Formation of water-resistant hyaluronic acid nanofibers by blowing-assisted electro-spinning and non-toxic post treatments. *Polymer*, 46:4853-4867.

- Wei, G., Ma, P.X. (2004). Structure and properties of nano-hydroxyapatite/polymer composite scaffolds for bone tissue engineering. *Biomaterials,* 25: 4749–4757.

- Wikesjö, U.M.E., Xiropaidis, A.V., Thomson, R.C., Cook, A.D., Selvig, K.A., Hardwick, W.R. (2003). Periodontal repair in dogs: rhBMP-2 significantly enhances bone formation under provisions for guided tissue regeneration. *Journal of Clinical Periodontology*, 30(8):705-714.

- Wikesjö, U.M.E., Sorensen, R.G., Kinoshita, A., Li, X.J., Wozney, J.M. (2004). Periodontal repair in dogs: effect of recombinant human bone morphogenetic

protein-12 (rhBMP-12) on regeneration of alveolar bone and periodontal attachment. *Journal of Clinical Periodontology*, 31(8):662-670.

- Wikesjö, U.M.E., Qahash, M., Polimeni, G., Susin, C., Shanaman, R.H., Rohrer, M.D., Wozney, J.M., Hall, J. (2008). Alveolar ridge augmentation using implants coated with recombinant human bone morphogenetic protein-2: histologic observations. *Journal of Clinical Periodontology,* 35(11): 1001-1010.

- Xianmiao, C., Yubao, L., Yi, Z., Li, Z., Jidong, L., Huanan, W. (2009). Properties and in vitro biological evaluation of nano-hydroxyapatite/chitosan membranes for bone guided regeneration. *Materials Science and Engineering C* 29:29–35.

- Xu, C., Lei, C., Meng, L., Wang, C., Song, Y. (2012) Chitosan as a barrier membrane material in periodontal tissue Regeneration *Journal of Biomedical Materials Research Part B Applied Biomaterials*, 100(5):1435-1443.

- Xue, J., He, M., Liang, Y., Crawford, A., Coates, P., Chen, D., Shi, R., Zhang, L. (2014). Fabrication and evaluation of electrospun PCL-gelatin micro-/nanofiber membranes for anti-infective GTR implants. *Journal of Materials Chemistry B,* 2: 6867–6877.

- Yamada M, Minamikawa H, Ueno T, Sakurai K, Ogawa T (2010). N-acetyl cysteine improves affinity of beta-tricalcium phosphate granules for cultured osteoblast-like cells. *Journal of Biomaterials Applications,* 27(1):27-36.

- Yamamoto, M., Hokugo, A., Takahashi, Y., Nakano, T., Hiraoka, M., Tabata, Y. (2015). Combination of BMP-2-releasing gelatin/β-TCP sponges with

124

autologous bone marrow for bone regeneration of X-ray-irradiated rabbit ulnar defects, Biomaterials 56:18–25.

- Yan-Huang, Y., Onyeri, S., Siewe, M., Moshfeghian, A., Madihally, S.V. (2005). *In vitro* characterization of chitosan–gelatin scaffolds for tissue engineering. *Biomaterials*, 26(36): 7616-7627.

- Yang, C., Frei, H., Rossi, F.M., Burt, H.M. (2009). The differential *in vitro* and *in vivo* responses of bone marrow stromal cells on novel porous gelatin–alginate scaffolds. *Journal of Tissue Engineering and Regenerative Medicine,* 3(8): 601-614.

- Yang, F., Both, S.K., Yang, X., Walboomers, X.F., Jansen, J.A. (2009). Development of an electrospun nano-apatite/PCL composite membrane for GTR/GBR application. *Acta Biomaterialia,* 5: 3295–3304.

- Yanoso-Scholl, L., Jacobson, J.A., Bradica, G., Lerner, A.L., O'Keefe, R.J., Schwarz, E.M., Zuscik, M.J., Awad, H.A. (2010). Evaluation of dense polylactic acid/beta-tricalcium phosphate scaffolds for bone tissue engineering. *Journal of Biomedical Materials Research Part A,* 95(3):717-726.

- Yarin, A.L., Koombhongse, S., Reneker, D.H., (2001). Bending instability in electrospinning of nanofibers. *Journal of Applied Physics*, 89:3018-3026.

- Yeo, Y.J., Jeon, D.W., Kim, C.S., Choi, S.H., Cho, K.S., Lee, Y.K., Kim, C.K. (2005). Effects of Chitosan Nonwoven Membrane on Periodontal Healing of Surgically Created One-wall Intrabony Defects in Beagle Dogs. *Journal of biomedical materials research Part B Applied Biomaterials,* 72(1):86-93.

- Yilgor, P., Tuzlakoglu, K., Reis, R.L., Hasirci, N., Hasirci, V. (2009). Incorporation of a sequential BMP-2/BMP-7 delivery system into chitosan-based scaffolds for bone tissue engineering. *Biomaterials,* 30: 3551-3559.

- Yoo, C.K., Jeon, J.Y., Kim, Y.J., Kim, S.G., Hwang, K.G., (2016). Cell attachment and proliferation of osteoblast-like MG63 cells on silk fibroin membrane for guided bone regeneration. *Maxillofacial Plastic and Reconstructive Surgery*, 38(1):17-22.

- Young, S., Wong, M., Tabata, Y., Mikos, A.G. (2005). Gelatin as a delivery vehicle for the controlled release of bioactive molecules. *Journal of Controlled Release,* 109: 256– 274.

- Yuan, Y., Zhang, P., Yang, Y., Wang. X., Gu, X. (2004). The interaction of Schwann cells with chitosan membranes and fibers *in vitro*. *Biomaterials* 25:4273–8.

- Zeleny, J. (1914). The electrical discharge from liquid points, and a hydrostatic method of measuring the electric intensity at their surface. *Physical Review*, 3:69-91.

- Zeugolis, D.I., Khew, S.T., Yew, E.S.Y., Ekaputra, A.K., Tong, Y.W., Yung, L.L., Hutmacher, D.W., Sheppard, C., Raghunath, M. (2008). Electro-spinning of pure collagen nanofibres-just an expensive way to make gelatin? *Biomaterials*, 29:2293–2305.

- Zhan, J., Lan, P. (2012). The Review on Electrospun Gelatin Fiber Scaffold. *Journal of Research Updates in Polymer Science,* 1: 59-71.

- Zhang, Y., Zhang, X., Shi, B., Miron, R.J. (2013). Membranes for guided tissue and bone regeneration. *Annals of Oral & Maxillofacial Surgery,* 1(1):1-10.

- Zhang, S., Huang, Y., Yang, X., Mei, F., Ma, Q., Chen, G., Ryu, S., Deng, X. (2009). Gelatin nanofibrous membrane fabricated by electrospinning of aqueous gelatin solution for guided tissue regeneration. *Journal of Biomedical Materials Research Part A,* 90(3):671-679.

- Zhang, H., Migneco, F., Lin, C.Y., Hollister, S.J. (2010) Chemically-Conjugated Bone Morphogenetic Protein-2 on Three-Dimensional Polycaprolactone Scaffolds Stimulates Osteogenic Activity in Bone Marrow Stromal Cells. *Tissue engineering Part A,* 16(11): 3441-3448.

- Zhang, C., Yuan, X., Wu, L., Sheng, J. (2005). Study on morphology of electrospun poly(vinyl alcohol) mats. *European Polymer Journal*, 41:423-432.

- Zhao, Z.Z., Li, J.Q., Yuan, X.Y., Zhang, Y.Y., Sheng, J. (2005). Preparation and properties of electrospum poly(vinylidene fluoride) membranes. *Journal of Applied Polymer Science*, 97:466-474.

- Zhou, J., Cao, C., Ma, X., Lin, J. (2010). Electrospinning of silk fibroin and collagen for vascular tissue engineering. *International Journal of Biological Macromolecules,* 47(4): 514-519.

- Zhuang, Z.X., Lin, Z.Y., Cao, J.F. (2003). Biocompatibility of chitosan-arboxymethylchitosan as membrane for periodontal guided tissue regeneration. *Shanghai Kou Qiang Yi Xue*, 12:362–365.

- Zimmermann, G., Moghaddam, A. (2011). Allograft bone matrix versus synthetic bone graft substitutes. *Injury,* 42: 16-21.

- Zuo, W.W., Zhu, M.F., Yang, W., Yu, H., Chen, Y.M., Zhang, Y. (2005). Experimental study on relationship between jet instability and formation of beaded fibers during electrospinning. *Polymer Engineering and Science*, 45:704-709.

CHAPTER 3

AIMS & OBJECTIVES

3.1. AIMS

Although GTR/GBR procedures are extensively employed for periodontal regeneration however, the clinical outcomes remain unpredictable. There is thus a need to improve the clinical outcomes by developing new versions of barrier membranes which play a crucial role in isolating the periodontal defect and providing a favorable environment for periodontal regeneration to take place. Currently used GTR/GBR membranes are bio-inert and do not show any bioactivity. There is substantial research in the past two decades into the possible incorporation of growth factors in GTR/GBR scaffolds in order to improve the outcome of existing regenerative procedures.

Therefore, the aim of the present study is to develop and characterize a *biopolymer nano-apatite composite electrospun bioactive GTR/GBR scaffold* with ability to release growth factors at defect site.

3.2. OBJECTIVES

To extract Chitosan from a natural source

To syntheisizs a copolymer of chitosan and alginate by chemical bonding

To develop a 3D GTR/GBR scaffold that mimics Extracellular Matrix (ECM) by electrospinning using the chitosan-alginate copolymer and Si-HA.

To investigate the possibility of incorporation of growth factors in 3D scaffold

130

To investigate the mechanical properties of the nanofibour scaffold

 To investigate the swelling behavior of the 3D scaffold

To investigate the cytotoxity and cell proliferation behaviour on electrospun nanofibrous

scaffolds with and without growth factors

UNIVERSITY *of the*
WESTERN CAPE

CHAPTER 4

MATERIALS & METHODS
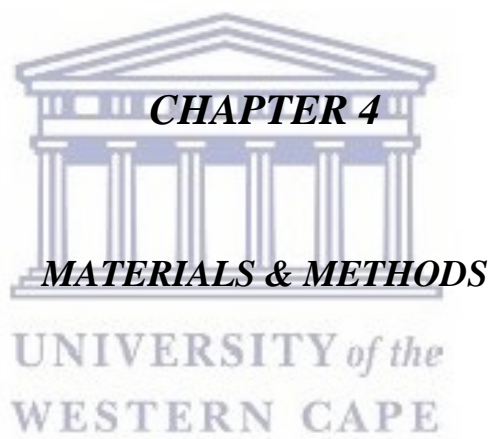
4.1. MATERIALS

Chitosan was extracted from shrimps (DD- 70-80%) and was purified. Hydroxyapatite (HA) and Silicon Subsituted Hydroxy apatite (Si-HA) was locally produced at IRCBM, with the help of Bone Repair and Regeneration Group following the protocol already established by them. Analytical grade calcium nitrate ($Ca(NO_3)_2.4H_2O$) (UniChem, Pakistan) and Diammonium hydrogen phosphate (($NH_4)_2HPO_4$) (AppliChem, Germany) were used as precursors. Cetyltrimethylammonium bromide (CTAB) was purchased from Sigma Aldrich, Spain.

Sodium alginate, Sodium hydroxide (NaOH), hydrochloric acid (HCl), Acetic acid and Formic acid (Anla Limited, UK), Potassium hydroxide (KOH), (Acros Organic USA), Methanol and Ethanol (Merk Germany), Ethyl dimethylaminopropylcarboiimide (EDC) and N hydroxy succinamide (NHS), (Merk Germany), N, N, N', N' – Tetramethylethylenediamine (TEMED), (Scharlau, Spain), Ammonium hydroxide (BDH, UK), Ammonia (Merck, Germany), Gelatin powder from bovine skin (Honeywell Fluka, Ireland), Phosphate Buffered saline (PBS) tablets (Merk, Germany) were used.

PBS solution was prepared by dissolving one tablet in 1L of deionized water which yielded 140mM NaCl, 10mM Phosphate Buffer, and 3mM KCl, pH 7.4 at 25°C.

BMPs used for coating were obtained from Millipore Temecula (California, USA). Mouse pre-osteoblast cell line MC3T3-E1 sub-clone 14, were purchased from ATCC cell bank, USA. 3-(4,5-dimethylthiazol-2-yl)-2, 5-diphenyl tetrazolium bromide (MTT) kit (Millipore Catalog no CT01/CT02) was bought from Merk, Germany. Deionized water prepared by PURELAB *Ultra*. (ELGA, UK).

133

4.2. SYNTHESIS

Synthesis of chitosan-alginate-HA and Si-HA based membrane and nanofibrous scaffolds involved the extraction of the chitin from natural source and deacetylation of chitin to produce chitosan. The chitosan extracted from shrimp exoskeleton was further purified.

Sodium alginate was bought from Anla limited (UK) and was further purified by precipitation. A copolymer of chitosan and alginate was created using cross-linking agents.

Hydroxyapatite (HA) and Silicon Subsituted Hydroxy apatite (Si-HA) was locally produced at IRCBM with the help of Bone Repair and Regeneration group following the protocol already established by them.

HA was dissolved in chitosan–alginate copolymer solution in different concentrations (20%, 40%, 60%, 80% wt/v) and membranes were produced by solvent casting method for initial characterization.

Copolymer solution with different concentrations of Si-HA was electrospum to produce nanofibers. These nanofibrous scaffolds were characterized.

Nanofibers were coated with bone morphogenetic protein 2 (BMP-2) by dipping method and cytoxity and cell proliferation behaviour was assessed.

The following flow chart explains the steps involved in the synthesis;

134

```
┌─────────────────────────────────────────────┐
│ Extraction of chitin from natural source &   │
│ deacetylation of chitin to develop chitosan  │
└─────────────────────────────────────────────┘
                     ⇩
┌─────────────────────────────────────────────┐
│ Precipitation of Alginic Acid from Sodium    │
│ Alginate for purification                    │
└─────────────────────────────────────────────┘
                     ⇩
┌─────────────────────────────────────────────┐
│ Synthesis of biopolymer based on chitosan and│
│ alginic acid by co-polymerization using cross-│
│ linking agent                                │
└─────────────────────────────────────────────┘
                     ⇩
┌─────────────────────────────────────────────┐
│ Synthesis of HA & Si-substituted HA          │
└─────────────────────────────────────────────┘
                     ⇩
┌─────────────────────────────────────────────┐
│ Preparation of Copolymer solution using acetic acid│
│ and formic in 70% and 30% ratio respectively │
└─────────────────────────────────────────────┘
                     ⇩
┌──────────────────┐      ┌─────────────────────────────────────┐
│ Membranes were   │      │ HA & Si-HA is then dissolved in copolymer│
│ produced by solvent│ ⇐  │ solution in different concentration  │
│ casting method for│      │ (ie. 20%, 40% & 60%, 80% by weight). │
│ initial          │      └─────────────────────────────────────┘
│ characterization │                 ⇩
└──────────────────┘      ┌─────────────────────────────────────┐
                          │ Copolymer- Gelatin-Si-HA solution based│
                          │ nanofibers were generated by electrospinning│
                          │ and characterized                    │
                          └─────────────────────────────────────┘
```

135

4.2.1. CHITOSAN EXTRACTION FROM SHRIMP'S EXOSKELETON

The shrimps were obtained from the coastal city Karachi, Pakistan. The shells and operculum were removed and the resultant exoskeleton was washed several times and completely dried in sun light. The dried exoskeletons were sorted out and crushed to make powder. The powder was dried in oven at 65°C (WiseVen Dry Oven, Daihan Scientific.co.Ltd, Korea) until a constant weight is achieved on two consecutive measures.

4.2.1.1. EXTRACTION OF CHITIN

A total of 20g shrimp powder (4% w/v) sample was placed in 500 mL Sodium hydroxide (NaOH) solution and stirred at 320 rmp over hot plate (Corning PC-420D, UK) and left for 1 hour at 90°C in order to dissolve proteins and unnecessary sugars and the solution was decanted. After decantation, washing by boiling NaOH (4%) for 1 hour was done for chitin preparation. The solution was decanted again, cooled for 30 minutes at room temperature and then dried in oven (WiseVen Dry Oven, Daihan Scientific.co.Ltd, Korea) at 60°C for 4 hours to obtain chitin powder.

Chitin powder obtained as a result of deproteination was demineralized by 1% HCl (use the solution 4 times the quantity of sample). The sample was soaked in 1% HCl for 24 hours at room temperature. This process was used to remove the minerals mostly calcium carbonate. The demineralized samples were then treated with 50mL of 2% NaOH solution for one hour to decompose the albumen into water soluble amino-acids. The remaining chitin then filtered (Whatman filter paper, Merck Germany) and washed with

136

deionized water prepared by PURELAB *Ultra*. (ELGA, UK). Figure 4.1 shows the chemical structure of chitin.
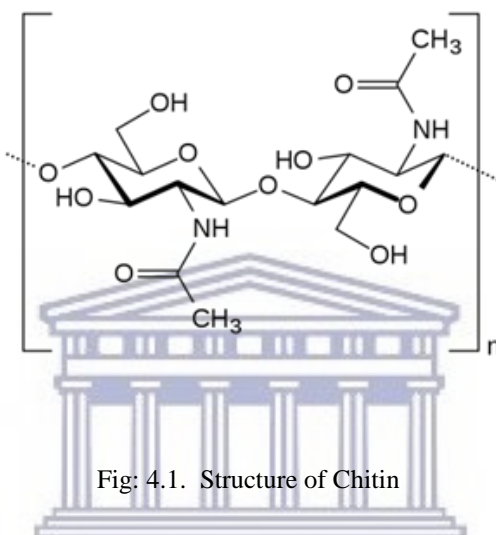
Fig: 4.1. Structure of Chitin

The chitin was further converted into chitosan by the process of deacetylation.

4.2.1.2. CHITOSAN PREPARATION

The sample was refluxed in 50% NaOH solution for 2 hours at 100°C on a hot plate (Corning PC-420D, UK) and then placed under hood at room temperature for 30 min to let it cool down. The sample was then washed continuously with 50% NaOH for at least 48 hours on vacuum pump and filtered (Whatman filter paper, Merck, Germany) in order to retain solid mass. Afterwards, the sample was left uncovered and oven dried at 110°C (WiseVen Dry Oven, Daihan Scientific.co.Ltd, Korea) for six hours. The color of the

137

resultant sample should be creamy white. Figure 4.2 illustrates the deacetylation of chitin into chitosan.
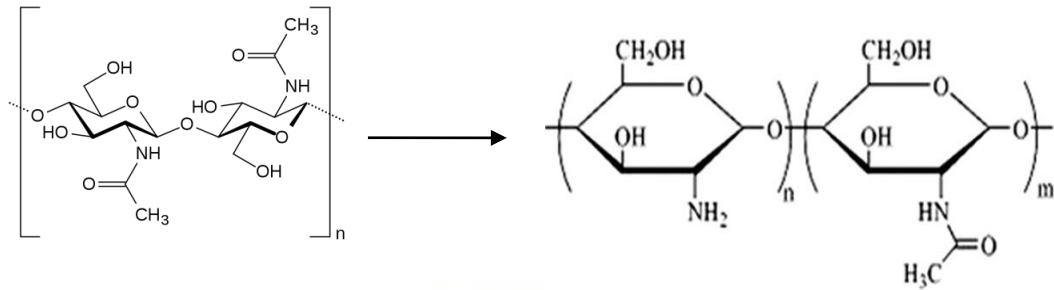
Chitin   ⟶   Deacytalation   ⟶   chitosan

Fig: 4.2. Preparation of chitosan from chitin
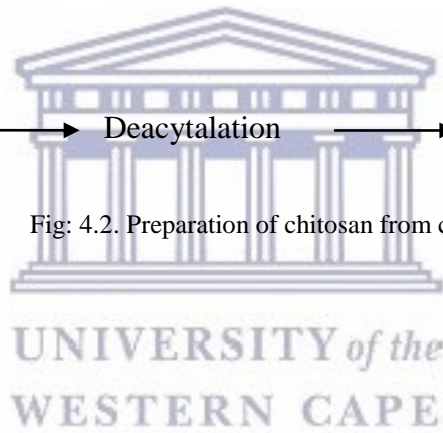
4.2.1.3 PURIFICATION OF CHITOSAN:

The chitosan was further purified to make it suitable for pharmaceutical use. The purification of chitosan consists of following different procedures.

- Removal of insolubles

- Re-precipitation with 1N NaOH

- Deproteinization

- Deacetylation

138

REMOVAL OF INSOLUBLES: For this purpose, 1 mg/mL (0.1% wt/v) solution of Chitosan was prepared in 1% acetic acid solution and stirred at 300 rmp (Corning PC-420D, UK) until homogeneous solution was obtained. Insoluble substances were removed by filtering (Whatman filter paper, Merck, Germany) the solution.

REPRECIPITATION WITH 1N NaOH: After filtration, the solution was re-precipitated with the slow addition of 1N NaOH solution until pH become 8.5. The chitosan obtained was further washed with distilled water by centrifuging at 8,000 to 10,000 xg (eppendorf, Centrifuge 5810 R, Germany). The resultant sample was freeze dried (Christ Alpha 1-2 LD plus freeze dryer, UK).

DEPROTEINIZATION: For deproteinization, 60g of chitosan (7.05% wt/v) was dissolved in 4% KOH solution with the total volume of 850 mL. The solution was stirred with magnetic stirrer (Corning PC-420D, UK) for 4 hours and then refluxed at 100^0C at 300 rpm for 2 hours. The solution was filtered and neutralized it by washing with deionized water (PURELAB *Ultra*, ELGA, UK) using vacuum filtration assembly. After neutralization, the sample was dried in oven at 40^oC (WiseVen Dry Oven, Daihan Scientific.co.Ltd, Korea).

DEACETYLATION: The dried chitosan was weighed, 50% NaOH was added to make volume upto 850 mL and then boiled at 100 ^{o}C on hot plate for two hours. The sample was placed under the hood and allowed to cool down for 2 hrs.

The cooled sample was stirred for 72 hours at 320 rpm and refluxed for four hours at 320 rpm at 230^oC on hot plate. The solution was filtered to neuterlize and dried at 37^oC for 72

139

hrs and weighed. Again placed it at 37°C for 1 hour to observe stability or consistency in weight (if fluctuation occurs, moisture is present).

(Puvvada et al., 2012; Rødde et al., 2008)

4.2.2. PURIFICATION OF ALGINIC ACID:

Purification of alginic acid was done by dissolving 10g sodium alginate (2.5% wt/v) in 400mL of 0.5M HCL solution. Alginic acid was precipitated and filtered (Whatman filter paper, Merck, Germany).

Precipitates were washed with deionized water and dried it in oven at 37°C overnight (WiseVen Dry Oven, Daihan Scientific.co.Ltd, Korea).

The dried alginic acid was dissolved in 400mL of 0.5M NaOH and stirred for 2 hours at 280 rpm (Corning PC-420D, UK) until a homogenous solution was made.

2M HCL was then added drop wise under magnetic stirring at 320 rpm (Corning PC-420D, UK) to achieve the pH 2, once the pH was maintained it was stirred for 24 hrs at 400 rpm. After 24 hours the solution was filtered and washed with ethanol and filtered out solvent overnight.

Next day, it was dried in vacuum oven at 40°C for 24 hours.

(Soares et al., 2004)

4.2.3. COPOLYMERIZATION OF CHITOSAN AND ALGINIC ACID:

Coupling of chitosan with Alginic Acid was performed by using ethyl dimethylaminopropylcarboiimide (EDC) and N hydroxy succinamide (NHS).

Briefly, copolymerization of chitosan and alginate was done by dissolving 0.500 g of Chitosan (4.4% wt/v) in 11.35 ml Tetramethylethylenediamine (TEMED)/HCl buffer solution with the molarity of 10mM and pH 4.7.

1.917g (4 equi) of EDC and 1.151g (4 equi) of NHS were dissolved in 5mL of TEMED/HCl buffer solution.
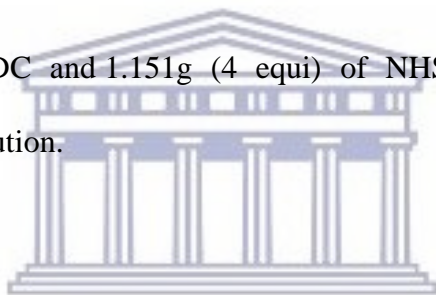
0.5225g Alginic acid was activated with the EDC/NHS buffer solution. The activated alginic acid solution was added into chitosan solution under magnetic stirring and allowed to react for about 72 hours at room temperature.

After the complete copolymerization of chitosan and alginate the resulting product was filtered and washed with excess of water for 4 days.

Complete drying of the product was done in freeze dryer at – 50 ˚C (Christ Alpha 1-2 LDplus freeze dryer, UK) and was stored in vacuum at room temperature before use.

141

Figure 4.3 illustrates the chemical reaction of copolymerization of Chitosan and Alginic acid.
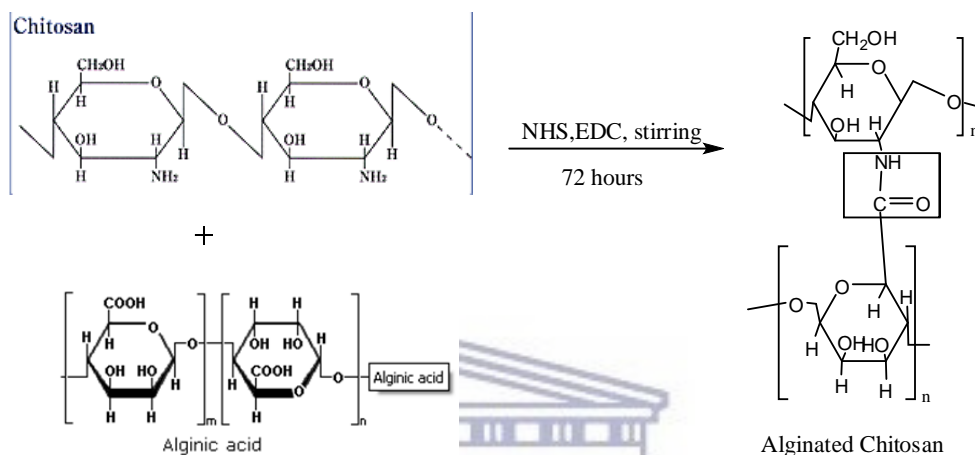
Fig: 4.3. Copolymerization of chitosan and Alginic acid (Adapted from Kulig et al., 2016)
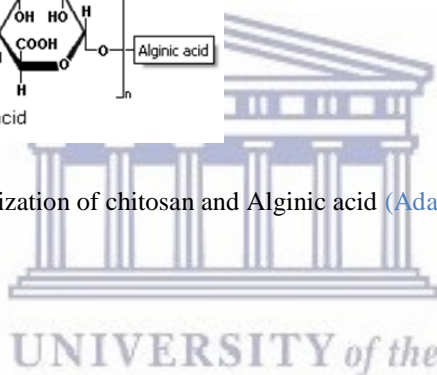
4.2.4. SYNTHESIS OF HYDROXYAPATITE (HA)

HA was synthesized with the help of Bone repair and regeneration group of IRCBM. Briefly, 1M $(Ca(NO_3)_2.4H_2O)$ and 0.6M $(NH_4)_2HPO_4)$ solutions were prepared in water and ethanol respectively with initial Ca/P molar ratio of 1.67. Cetyltrimethylammonium bromide (CTAB) was added as surfactant to phosphorous precursor and pH of both solutions was maintained at 10 by adding ammonium hydroxide. $(NH_4)_2HPO_4$ solution was added drop wise to $(Ca(NO_3)_2.4H_2O)$ solution at a dropping rate of $2mL.min^{-1}$. The reaction mixture was then stirred for 30min (pH maintained at 10) before refluxing in a domestic microwave oven (Samsung MW101P) at1000W for 3min. After microwave

142

irradiation the resulting reaction mixture was filtered, washed with distilled water and aged in drying oven at 80^0C for 22 hrs. The resulting powder was heat treated at 1000^oC for 1hr (ramp rate≈10^oC.min^{-1}) and cooled down to room temperature (ramp rate≈30^0C.min^{-1}).

4.2.5. SYNTHESIS OF SILICON SUBSTITUTED HA

Silicon substituted hydroxyapatite (Si-HA) was also synthesized with the help of Bone Repair and Regeneration Group of IRCBM. It was synthesized using a wet chemical synthesis method and contained ~ 0.7 wt% Si (of total weight).

4.2.6. MEMBRANE FORMATION OF COPOLYMER AND HA & Si-HA

The membranes of copolymer alone and copolymer with different concentrations of HA and Si-HA were prepared by solvent casting method.

To dissolve the copolymer, 10mL solution of acetic acid and formic acid with the ratio of 70:30 was prepared and 0.1g copolymer (1% wt/v) was added in it. The solution was stirred at 300 rpm for about 24 hours with magnetic stirrer. After the complete dissolution of copolymer the solution was poured into the molds and dried at 37^oC. When completely dried the films were separated from the molds.

In order to prepare copolymer membrane with different concentrations of HA and Si-HA 10mL solution of acetic acid and formic acid with the ratio of 70:30 was prepared and 0.1g (1% wt/v) copolymer was added and stirred at 300 rpm for about 24 hours. After the

143

complete dissolution of copolymer, 0.02, 0.04, 0.06, and 0.08g of HA and Si-HA was added in it to make 20%, 40%, 60% and 80% solutions respectively under magnetic stirring until the HA was completely dispersed. The resulting mixture was poured into the molds and dried it at 37°C. When completely dried films were removed from the molds, however, films with 80% HA were too brittle to be removed from the mold. Therefore, these films were not used for characterization.

Copolymer and copolymer with 20, 40 and 60% HA membranes were used for initial characterization such as Scanning Electron Microscopy (SEM) and Fourier Transform Infrared (FTIR) spectroscopy.

4.2.7. ELECTROSPINNING TO GENERATE NANO-FIBERS

A custom made electrospinning unit was used for electrospinning. Figure 4.4 shows the electrospnning unit used.

Fig: 4.4. Ccustom made electrospinning unit.

144
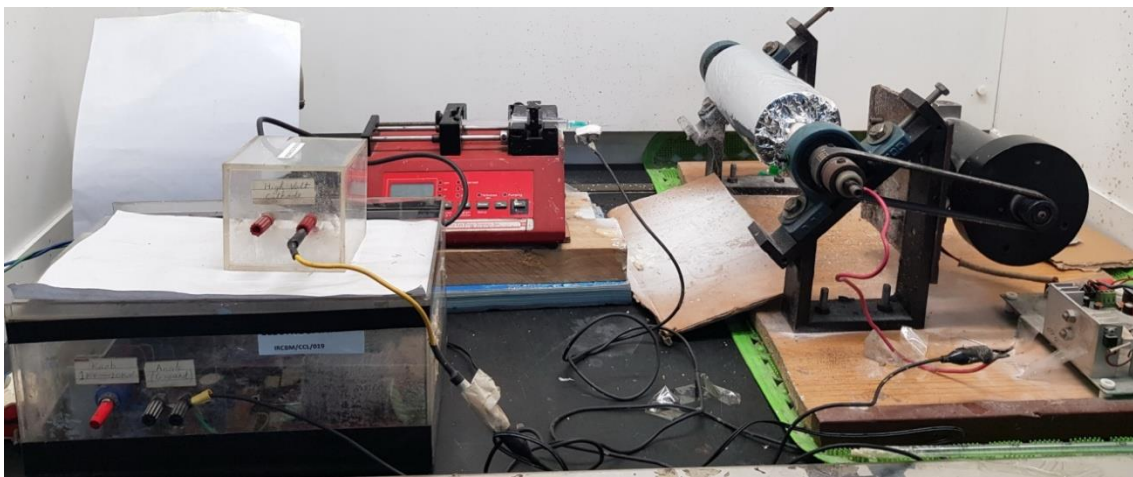
Repeated attempts were made over a span of one year to electrospun the Alginate-Chitosan copolymer and Si-HA solution. In order to make it electrospinning friendly gelatin was added into the solution. The methodology used is described below.

1% acetic acid solution was prepared by dissolving 1mL acetic acid in 99mL of deionized water. 3.5g (17.5% wt/v) gelatin was dissolved 20mL acetic acid solution and sonicated (Almasonic E 30 H, Cousins UK) for 30 minutes.

In another beaker 1.497g (7.4% wt/v) of copolymer was dissolved in acetic acid and formic acid solution with ratio of 70:30. When completely dissolved copolymer solution was added into gelatin solution under magnetic stirring and kept on stirring this mixture at 450 rpm and 37°C (Corning PC-420D, UK) for at least 30 minutes until a homogenous solution is obtained.
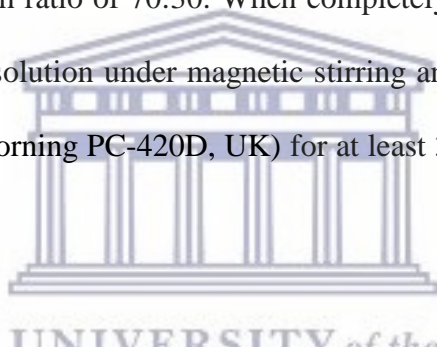
The resultant solution was filled in 5mL glass syringe (BD multifit syringe) fitted with a guage 20 stainless steel needle used as nozel and was mounted in the pumping system (New Era Pump System NE-300, USA). Electrospinning was done at a flow rate of 6µl/hr with the distance of 7cm at electric potential of 17KV. The nanofibers were collected at an aluminium sheet placed on a stationary collector.

In order to make 20, 40 and 60% Si-HA solutions for electrospinning 0.29g (wt/v 20%) 0.5988g (wt/v 40%) and 0.898g (wt/v 60%) of Si-HA was added into copolymer-gelatin solution.

145

The solution was stirred until complete dispersion of Si-HA into the copolymer and gelatin solution, electrospinning was performed using the same parameters.

The resultant nanofibrous scaffolds were dried at room temperature before further investigation.

4.3. CHARATERIZATION

Degree of Deacetylation (DD) of chitosan was determined by FTIR spectroscopy.

Copolymer and composite membranes and nanofibrous scaffolds were characterized using Scaning Electron Microscopy (ECM) for surface morphology and Energy dispersive X-ray (EDS) for elemental analysis.

Characteristic functional groups of copolymer and copolymer/Si-HA were identified using Fourier Transform Infrared Spectroscopy (FTIR)

In order to gauge the mechanical properties, tensile mechanical test was chosen to determine the maximum strength and elongation at break.

 The swelling behavious of the nanofibrous scaffols were also analysed.

Cytotoxicity and cell proliferation behavious of nanofibrous scaffold with and without growth factors (BMP-II) was assessd using MC3T3-E1 Mouse pre-osteoblast cells by MTT assay protocol.

146

4.3.1. DETERMINATION OF DEGREE OF DEACETYLATION (DD) OF CHITOSAN

Several procedures and equations have been described in literature for calculation of degree of deacetylation with FTIR spectroscopy. Such equations are based on absorbance ratios of various spectral bands. In the present study following equation was used for the determination of percentage degree of deacetylation (Czechowska-Biskup et al., 2012).

$$DA(\%) = A_{1655}/A_{3450} \times 100/1.33$$

DA = Degree of deacetylation

A_{1655} = Absorbance at 1655 cm^{-1}

A_{3450} = Absorbance at 2870 cm^{-1}
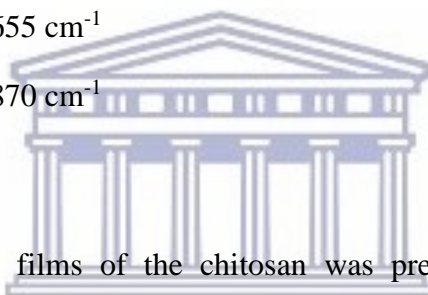
For FTIR spectroscopy films of the chitosan was prepared by dissolving 50mg of chitosan (0.25% wt/v) in 20mL of 1% acetic acid solution and stirred at 300 rpm until a homogenous solution was abstained. The resultant solution was poured into moulds and dried at 37°C in drying oven. The films were washed with methanolic ammonia for 10 min and dried again at 37°C. The measurements were done in transmission mode and spectra were obtained within a frequency range of 400-4000 cm^{-1}, each spectrum was an average of 64 scans with a resolution of 2 cm^{-1}.

The degree of seacetylation of various batches was from 70-80%.

4.3.2. FOURIER TRANSFORM INFRARED SEPCTROSCOPY (FTIR)

Characteristic functional groups of copolymer and copolymer/Si-HA (all concentrations) were identified using Fourier Transform Infrared Spectroscopy (Thermo Nicolet 6700, USA) with diamond Attenuated Total Reflectance (ATR) accessory. Spectra were collected over the region 400-625 cm^{-1} at a resolution of 8 cm^{-1} and averaging 256 scans. The data was analysed using OMINIC software.

Figure 4.5 shows the FTIR unit used.
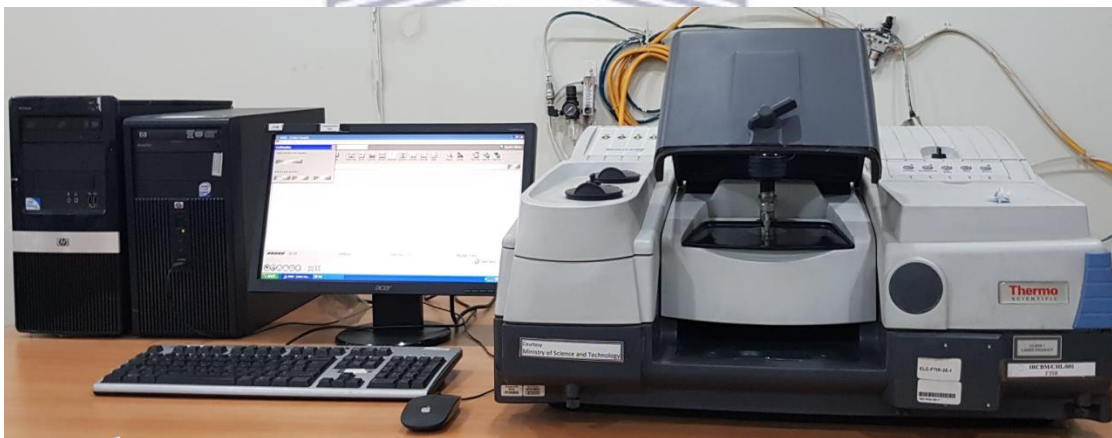
Fig: 4.5. Fourier Transform Infrared Spectroscopy (Thermo Nicolet 6700, USA) with diamond Attenuated Total Reflectance (ATR) accessory

4.3.3. SCANNING ELECTRON MICROSCOPY (SEM) & ENERGY-DISPERSIVE X-RAYS SPECTROSCOPY (EDS)

Surface morphology and elemental composition was studied using TESCAN Vega3 LMU Scanning electron microscope (SEM) with built-in Energy dispersive X-ray detector (EDX) (X-Act, Oxford Instrument). For SEM, samples were precoated using

148

gold targets for 90s using a sputter coater from Quorum Technologies while EDX analysis was carried out on uncoated samples. SEM images were acquired using an acceleration voltage of 15 kV with a beam intensity of 4 pA, while for EDX analysis an acceleration voltage and beam intensity of 20 kV and 10 pA were used, respectively. Figure 4.6 shows the SEM used.

Figure: 4.6. TESCAN Vega3 LMU Scanning electron microscope (SEM) with built-in Energy dispersive X-ray detector (EDX) (X-Act, Oxford Instrument

149

4.3.4. MECHANICAL PROPERTIES

The tensile mechanical test was chose to determine the maximum strength and elongation at break. For mechanical testing TIRA test 2810 E6 universal testing machine (UTM) with a 1kN load cell from TIRA GmbH, Germany was used. Figure 4.7 shows the universal testing machine used.

Fig: 4.7. Universal testing machine (TIRA test 2810 E6)

150

4.3.5. SWELLING BEHAVIOUR

The swelling behavior of the coplolymer and composite scaffolds was studied by determining the percentage of medium uptake by each specimen.

Samples measuring 10mm by 10mm were completely dried and weighed (electronic balance ATX 224, capacity 220g, readability 0.1mg, Shimadzu Corporation, Japan) before immersing into PBS solution pH 7.4 in a pre-weighed container at 37°C to allow any water uptake to occur. At given intervals (30 mintes, 1hour, 3hours, 5hours and 7hours) the solutions were carefully withdrawn from the containers. Any residual medium was removed by gently pressing the specimen between two filter papers. The percentage of medium uptake was calculated using the following formula for five replicates of each sample.
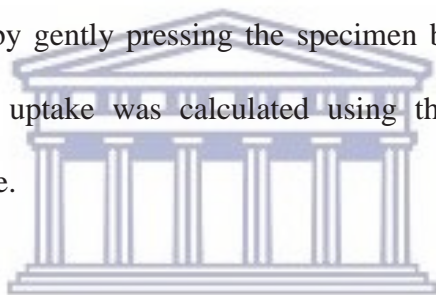
$$\text{Percentage of medium uptake} = \frac{final\ weight - \text{Initial weight}}{Initial\ weight} \times 100\%$$

4.3.6. CYTOTOXITY AND CELL PROLIFERATION

In order to investigate the cell proliferation behavior and rule out any cytotoxic effect of the materials used for the generation of nano-fibers on cell growth, samples were made as described earlier in the section of systhesis. One set of the samples was coated with BMP-2 to assess the potential of the material to act as a carrier system for growth factors

151

and to evaluate outcome of BMP-2 addition in terms of cell proliferation and differentiation. Samples were cut in 5mm x5mm diameter.

4.3.6.1. COATING OF SAMPLES WITH BMP-2

For coating, 100ng of BMPs were added in 100µL of phosphate buffered saline (PBS) (Phosphate Buffered saline tablets, Merk, Germany). Solution was prepared by dissolving one tablet in 1L of deionized water which yielded 140mM NaCl, 10mM Phosphate Buffer, and 3mM KCl, pH 7.4 at 25°C. The specimens were placed in 24 well plates and BMPs/PBS solution was coated to the surface of specimens. The specimens were incubated at 37°C (WiseVen Dry Oven, Daihan Scientific.co.Ltd, Korea) for about 3 hours and any extra solution left was carefully removed from the surface of the specimen.

4.3.6.2. CELLS

Mouse pre-osteoblast cell line MC3T3-E1 sub-clone 14, purchased from ATCC cell bank (USA), was used in this study. MC3T3-E1 cells were maintained in complete culture medium containing MEM-α, supplemented with 10% fetal bovine serum and 1% Penicillin-Streptomycin in T25 flasks. 1mL Trypsin-EDTA solution was used to detach the cells for sub-culturing. During sub-culturing, cells were washed with sterile phosphate buffered saline (PBS) to ensure a total removal of medium and cell debris. Cells were grown under standard cell culture conditions (37 °C and a humidified atmosphere of 5% CO_2).

4.3.6.3. CELL COUNT BY HAEMOCYTOMETER

Cells were counted using haemocytometer. Each square of the hemacytometer characterized a total volume of 0.1 mm. Subsequently cells were calculated using the following formula:

Cells/Ml = average count per square $\times$ dilution factor $\times 10^4$ (count 10 squares)

4.3.6.4. MTT ASSAY PRPTPCOL

The samples were washed with ethanol and sterilized with ultraviolet rays (UV) for one hour. Specimens were cut into 5mm x 5mm diameter and placed in 96 well tissue culture plates. All the specimens were used in triplicates.

A total of 1x104 MC3T3-E1 cells were seeded in each well with 100µL media containing 10% Fetal Bovine Serum. Cells were treated with Zno (1-4) and Nio (1-5) in triplicates. Control contained only cells and no Zno or Nio. The culture plates were incubated at 37°C in CO_2 incubator. Readings were taken at day 1, 3 and 7.

Briefly, 10µL of solution AB (3-(4,5-dimethylthiazol-2-yl)-2,5-diphenyl tetrazolium bromide/MTT reagent and PBS pH 7.4) was added to the cells and mixed well by tapping gently. For cleavage of MTT, cells were incubated at 37°C for 4 hours, followed by the addition of 100µL of solution C (isopropanol with 0.04 N HCl). Mixed thoroughly by repeated pipetting and incubated for another hour. Samples were then rendered to a plate

153

reader and took measurements at wavelength of 570 nm and a reference wavelength of 630 nm. This process was similar for day 1, 3 and day 7.

4.3.6.5. CELL MORPHOLOGY

For cell morphology the cells were washed with PBS and subjected to light microscope. SEM was not performed due to the early degradation of scaffolds.

4.4. STATISTICAL ANALYSIS

Statistical analysis of cell culture and mechanical properties data was performed using SPSS and results were calculated by 1- way ANOVA with Bonferroni's post-test with $P<0.05$.
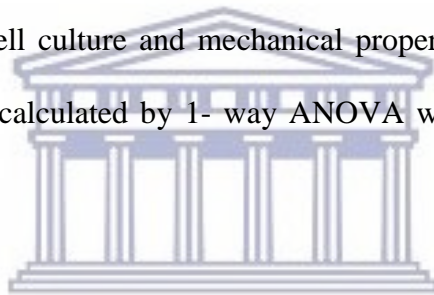
For swelling behaviour statistical analysis was performed using Friedman test to assess the statistically significant difference between the groups while Wilcoxon Signed Rank test was used to evaluate significant difference within the groups with $P< 0.05$.

REFERENCES:

- Czechowska-Biskup, R., Jarosińska, D., Rokita, B., Ulański, P., Rosiak, J.M. (2012). Determination of degree of deacetylation of chitosan- comparision of methods. *Progress on Chemistry and Application of Chitin and its Derivatives,* XVII: 5-20.

- Kulig, D., Zimoch-Korzycka, A., Jarmoluk, A., Marycz, K. (2016). Study on Alginate–Chitosan Complex Formed with Different Polymers Ratio. *Polymers*, 8:167.

- Puvvada, Y.S., Vankayalapati, S., Sukhavasi, S. (2012). Extraction of chitin from chitosan from exoskeleton of shrimp for application in the pharmaceutical industry. *International Current Pharmaceutical Journal*, 1(9): 258-263.

- Rødde, R.H., Einbu, A., Kjell M., Vårum, K.M. (2008). A seasonal study of the chemical composition and chitin quality of shrimp shells obtained from northern shrimp (Pandalus borealis). *Carbohydrate Polymers,* 71: 388–393.

- Soares, J., Santos, J., Chierice, G., Cavalheiro, E. (2004). Thermal behavior of alginic acid and its sodium salt. *Eclética Química,* 29:57-64.

155

CHAPTER 5

RESULTS

UNIVERSITY *of the*

WESTERN CAPE
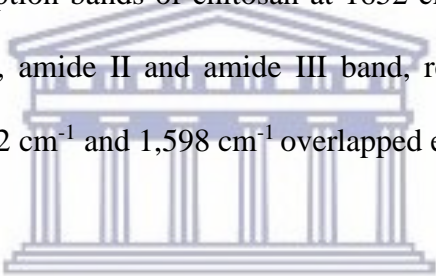
5.1. FOURIER TRANSFORM INFRARED SEPCTROSCOPY (FTIR)

FTIR analysis of all the base materials such as chitosan, alginate, HA, Si-HA and end products including copolymer and composite membranes and nanofibrous scaffolds were done to chacterize the intermolecular intersctions between components in system.

5.1.1. FTIR OF CHITOSAN FILM

The characteristic absorption bands of chitosan at 1652 cm^{-1}, 1598 cm^{-1}, and 1320 cm^{-1} represented the amide I, amide II and amide III band, respectively. The characteristic absorption bands at 1,652 cm^{-1} and 1,598 cm^{-1} overlapped each other.

The peaks between 4000 cm^{-1} to 3000 cm^{-1} represented the OH and NH stretching vibrational peaks. At 2907cm^{-1} CH$_2$ bending occurred and at 1145 cm^{-1} C-O-C stretching took place. Chitosan showed C-O stretching and C-O skeletal vibrations at 1085 cm^{-1} and 1035 cm^{-1} respectively as shown in figure 5.1.

157

Fig: 5.1. FTIR of Chitosan film

5.1.2. FTIR OF ALGINATE FILM

The alginate spectrum showed the characteristic peak at 1623 cm^{-1}, which corresponded to the carboxylate group (C=O). The absorption bands in sodium alginate at 1,620 cm^{-1} and 1,416 cm^{-1} were due to the respective asymmetric and symmetric stretching vibrations of carboxylate anions. The symmetric stretching frequency of the carboxyl group was observed at 1418 cm^{-1}, whereas 1098 cm^{-1} –1026 cm^{-1} showed the asymmetric stretching frequency. Figure 5.2 shows the FTIR spectra of alginate.
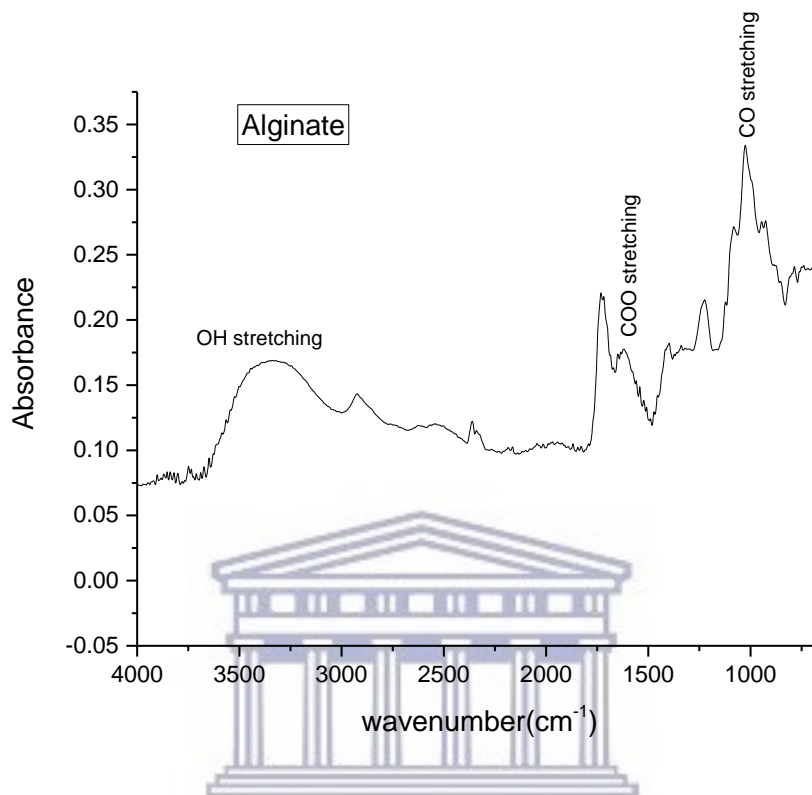
Fig: 5.2. FTIR of Alginate film

5.1.3. FTIR OF HYDROXYAPATITE (HA) & SILICON SUBSITUTED HYDROXYAPATITE (Si-HA)

IR spectrum of Hydroxyapatite represented a broad band from 1300 cm^{-1} to 834 cm^{-1}. Shape of this band suggested that it may contain a number of peaks indicating the presence of symmetric and asymmetric stretching of P-O bond in phosphate groups and/or asymmetric stretching vibrations of Si-O-Si in the case of Si-HA.

159

The FTIR spectrum of both HA and Si-HA showed the phosphate (PO_4) peak. For Si-HA peak appeared at $1016cm^{-1}$ while in case of HA characteristic peak occurred at $1029cm^{-1}$. In addition to the above mentioned peaks, $868\ cm^{-1}$ peak is attributed to the Si-O bending vibration. The band at $1653cm^{-1}$ represented OH bending vibration of absorbed water. FTIR spectra of HA and Si-HA are shown in figures 5.3 and 5.4 respectively.
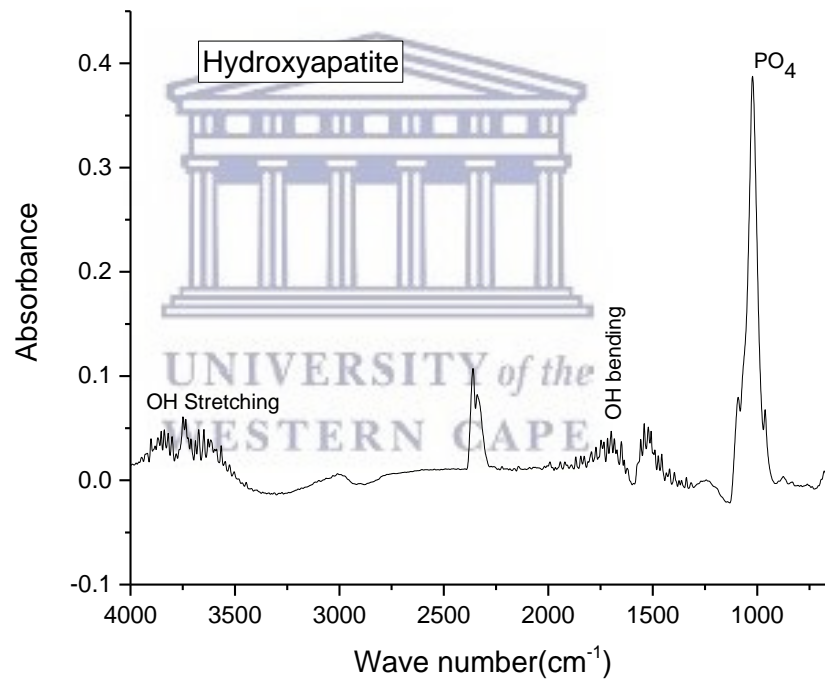
Fig: 5.3. FTIR of HA
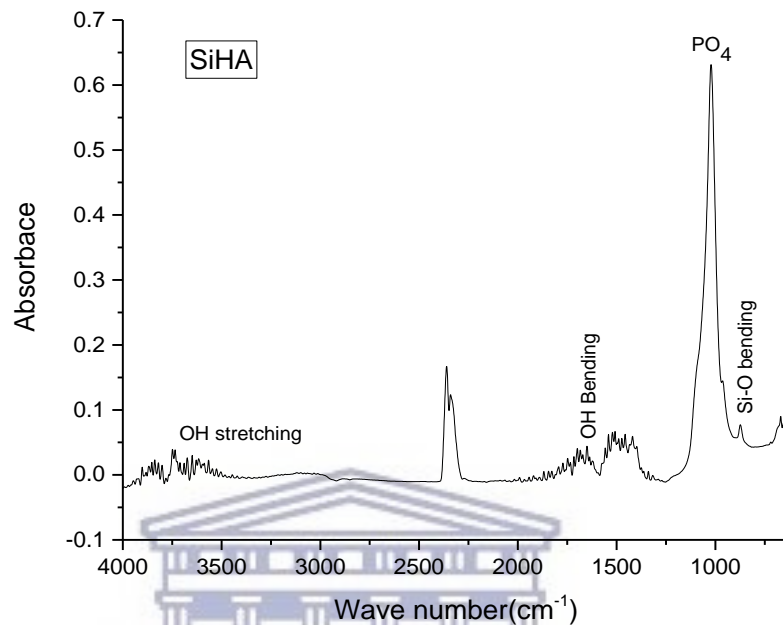
Fig: 5.4. FTIR of Si-HA

5.1.4. FTIR OF COPOLYMER OF CHITOSAN & ALGINATE FILM

The FT-IR spectrum of blend membrane (chitosan/alginate 1:1) presented in figure 5.5 revealed differences from pure Chitosan and Sodium Alginate membranes. The blend film presented amide I absorption margined with characteristic absorption band of amide N–H group and showed a wide absorption at 1,635 cm^{-1}. For alginate the absorption bands at 1,620 cm^{-1} and 1,416 cm^{-1} were due to the respective asymmetric and symmetric stretching vibrations of carboxylate anions. The absorption band at 1,620 cm^{-1} shifted to

161

1,641 cm^{-1} and 1,416 cm^{-1} shifted to 1,403 cm^{-1} after alginate reacted with –NH$_2$ groups via hydrogen bonds. An intense peak was also observed at 1613 cm^{-1}, corresponding to the superposition of the bands assigned to the carboxylate group of Alginate and the amine group of Chitosan. The amide III at 1320 cm^{-1} disappeared. Chitosan, alginate and their blend displayed characteristic absorption bands between 3400 cm^{-1} and 3450 cm^{-1}, which represent the –OH and –NH$_2$ groups in free as well as in amide form in chitosan. The –OH and –NH$_2$ groups in chitosan may form hydrogen bonds with –C=O and –OH groups of alginate. The characteristic absorption band 3350 cm^{-1} in chitosan membrane shifted to 3328 cm^{-1}
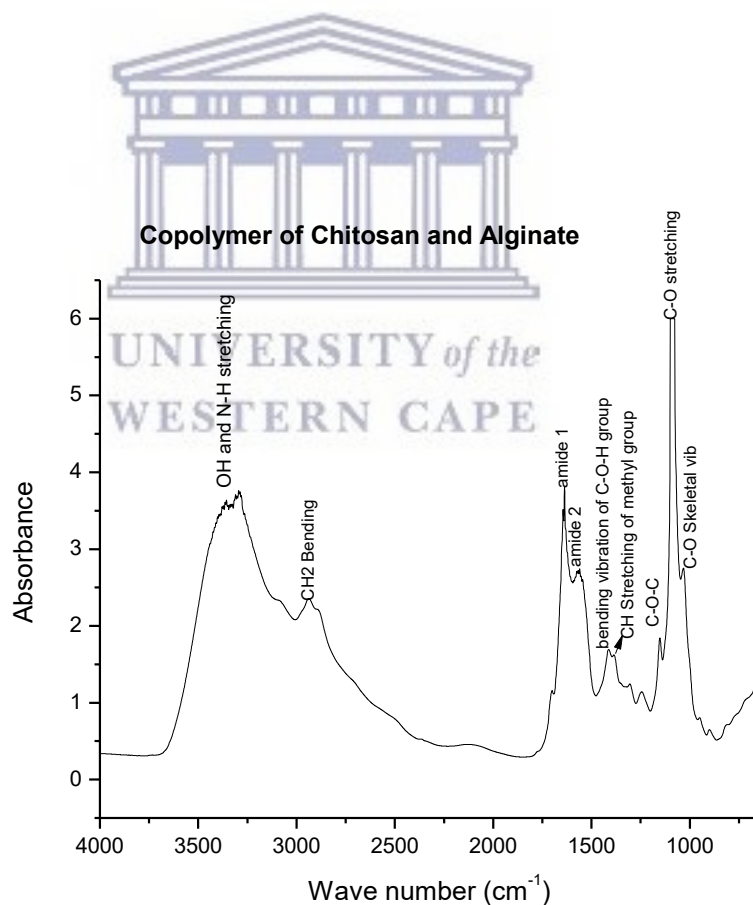
Fig: 5.5. FTIR of Copolymer of alginate & Chitosan film

162

5.1.5. FTIR OF CHITOSAN-ALGINATE-20% HA MEMBRANE

When hydroxyapatite (HA) was added into the copolymer of chitosan and alginate some peaks reduced, added or disappeared. In the FTIR spectra as shown in Figure 5.6 bands at 1034 cm^{-1} is the characteristic band of phosphate bending vibration in HA while the absorption band at 3570 cm^{-1} is assigned to a hydroxyl group in HA.
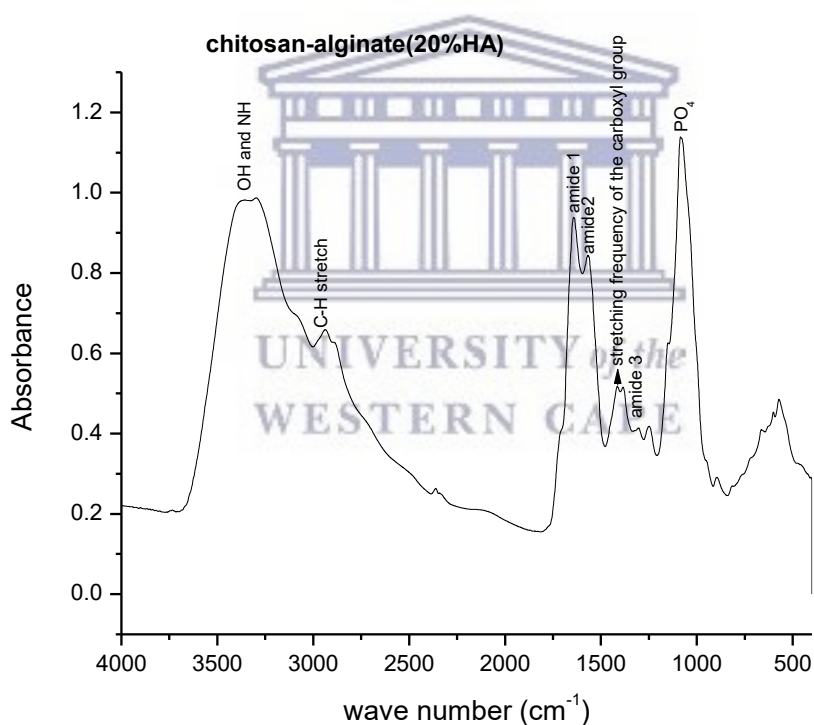
Fig: 5.6. FTIR of Chitosan-Alginate-20% HA membrane

163

In the spectrum of composite of chitosan-alginate-HA, the amide-I peak shifted from 1635 cm^{-1} to 1641 cm^{-1}, whereas amide-II was shifted from 1557 cm^{-1} to 1573 cm^{-1} and the peak of the amide-III was negligibly small. These changes would be suggestive of the formation of the chitosan-alginate copolymer complex as a result of the ionic interactions between the negatively charged carbonyl group (–COOH) of alginate and the positively charged amino group (–NH2) of chitosan.
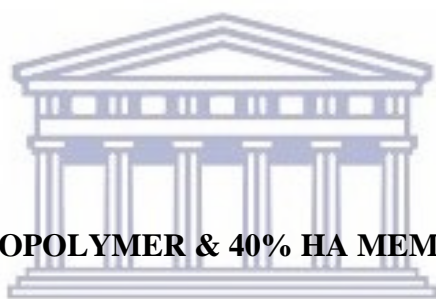
5.1.6. FTIR OF 60% COPOLYMER & 40% HA MEMBRANE

When the amount of HA was increased up to 40%, the HA-chitosan-alginate composite spectrum showed the shift of amide-II from 1557 cm^{-1} to 1581cm^{-1} while there was no significant change in the amide-I peak. There was no significant change in the other peaks. Figure 5.7 shows the spectra of copolymer-40% HA composite membrane.
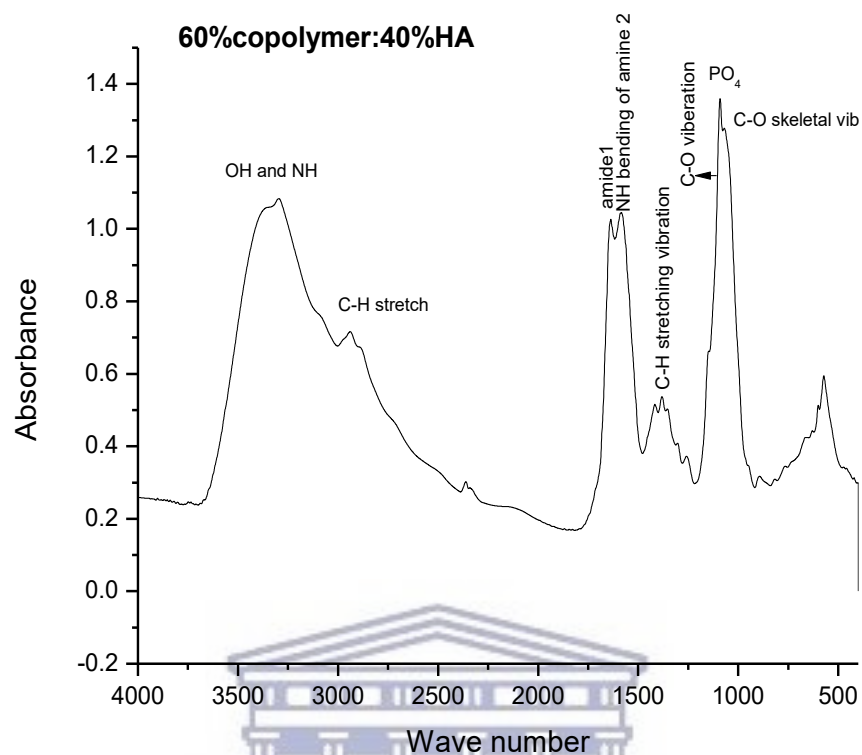
Fig: 5.7. FTIR of 60% copolymer & 40% HA membrane

5.1.7. FTIR OF 40% COPOLYMER & 60% HA MEMBRANE

As the amount of HA was further increased up to 60%, the amide-1 overlapped with the amide-II. The peak shifted at 1599 cm^{-1} which is evident in figure 5.8.
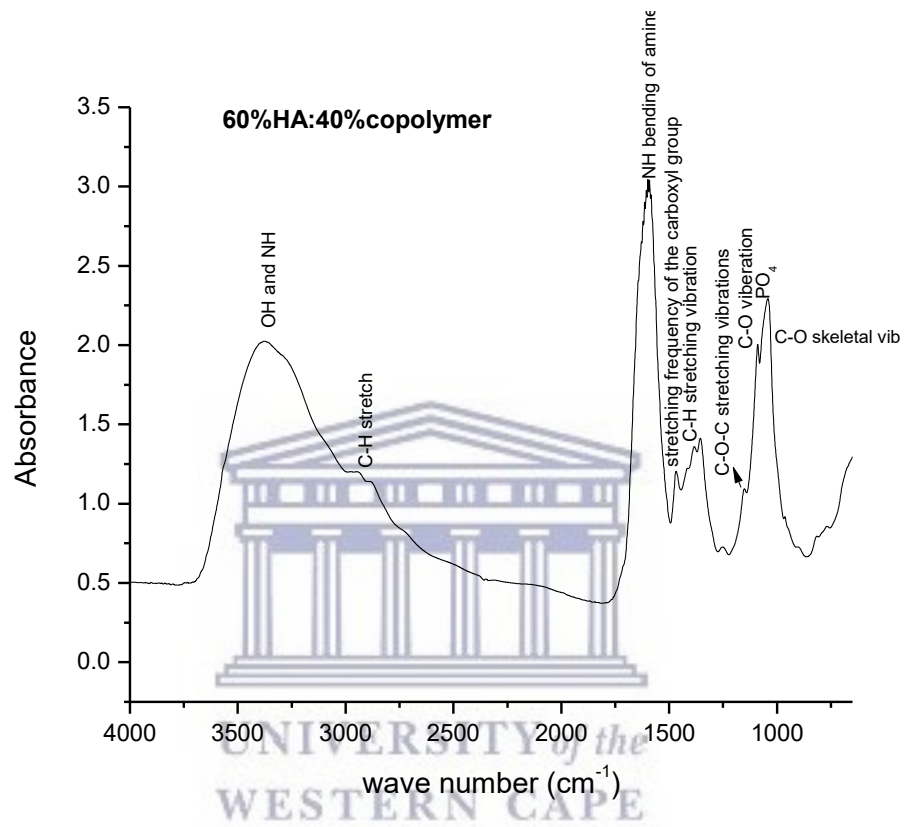
Fig: 5.8. FTIR of 40% copolymer & 60% HA membrane
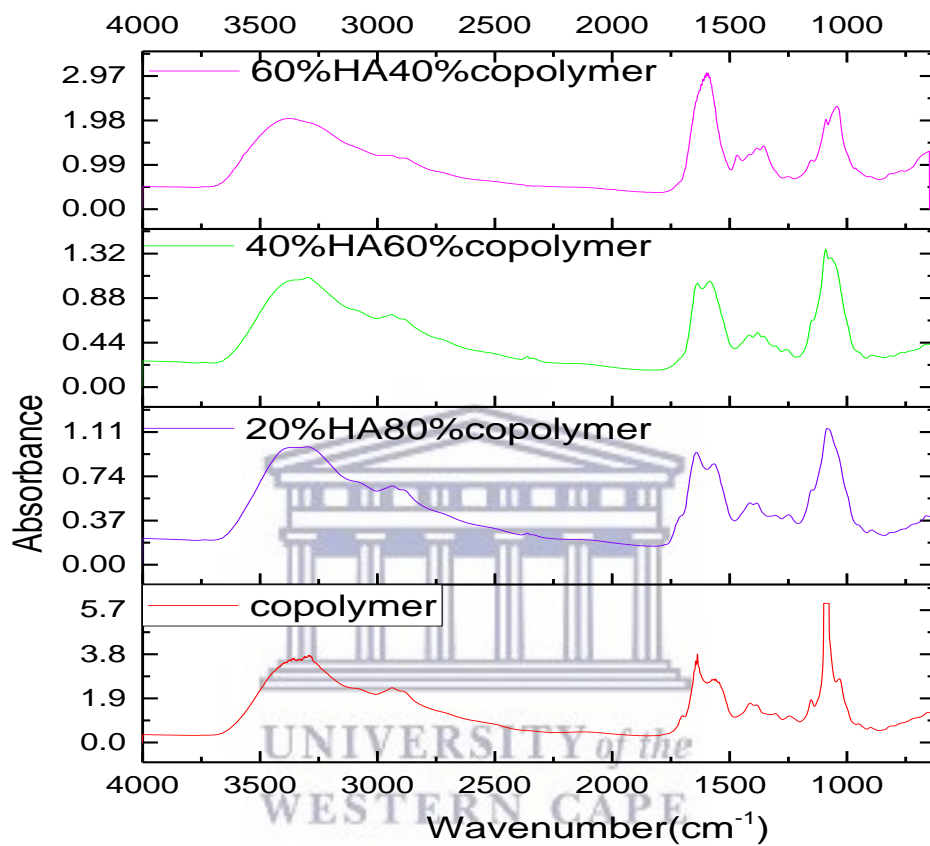
Fig: 5.9. Comparative spectra of Copolymer, Copolymer with 20, 40, 60% HA

Figure 5.9 shows the comparative spectra of copolymer, copolymer with 20, 40 & 60%

HA respectively.

5.1.8. FTIR OF NANOFIBERS

FTIR spectra of the nanofibrous scaffolds composed of copolymer-gelatin-Si-HA composite were also obtained using the same parameters as used for copolymer–HA membranes.

5.1.9. FTIR OF NANOFIBERS WITH 20% Si-HA

The nanofibers also showed the characteristic absorption bands of chitosan just like FTIR of films at 1652 cm^{-1}, 1534 cm^{-1}, and 1322 cm^{-1} representing the amide-I, amide-II and amide-III band, respectively. The peaks between 4000 cm^{-1} to 3000 cm^{-1} were because of the -OH and -NH stretching vibrations. CH$_2$ bending occurred at 2907cm^{-1}. At 1145cm^{-1} C-O-C stretching took place in saccharide structure of chitosan.

Chitosan showed C-O stretching and C-O skeletal vibrations at 1085 cm^{-1} and 1035 cm^{-1} respectively. Characteristic band of C-H stretching vibration of methyl group presented at 1380 cm^{-1} was due to the residual acetylamido groups of the chitosan, because of the incomplete deacetylation of the parent chitin. Fibers also showed the peak of gelatin. The spectrum had C–H bending vibration at 2935 cm^{-1} for the amide in gelatin.

The bands at 1035 cm^{-1} to 1040 cm^{-1} were the characteristic band of phosphate bending vibration in Si-HA while the absorption band at around 4000 cm^{-1} was assigned to a hydroxyl group in Si-HA.

168

Figure 5.10 shows the spectra of composite nanofiber of copolymer and 20% Si-HA.
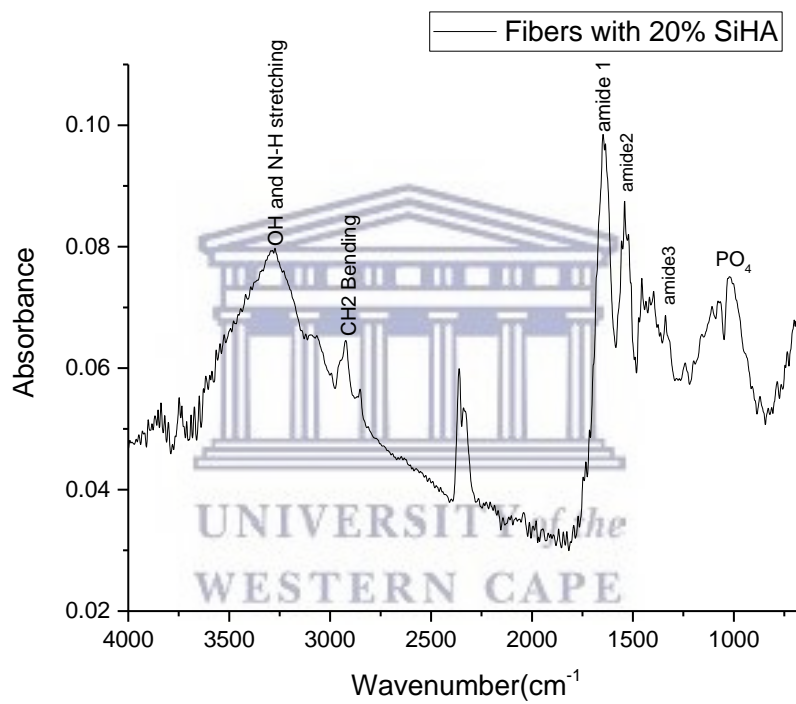
5.10. FTIR of Nanofibers with 20% Si-HA

5.1.10. FTIR OF NANOFIBERS WITH 40% Si-HA

With increase in Si-HA concentration, the amide-I and II peaks shifted to higher wave number, and the peak of the amide-III was negligibly small as shown in figure 5.11. A shoulder at 930 cm-1 showed the Si-O stretching of non-bridging oxygen is deformed due to bonding.
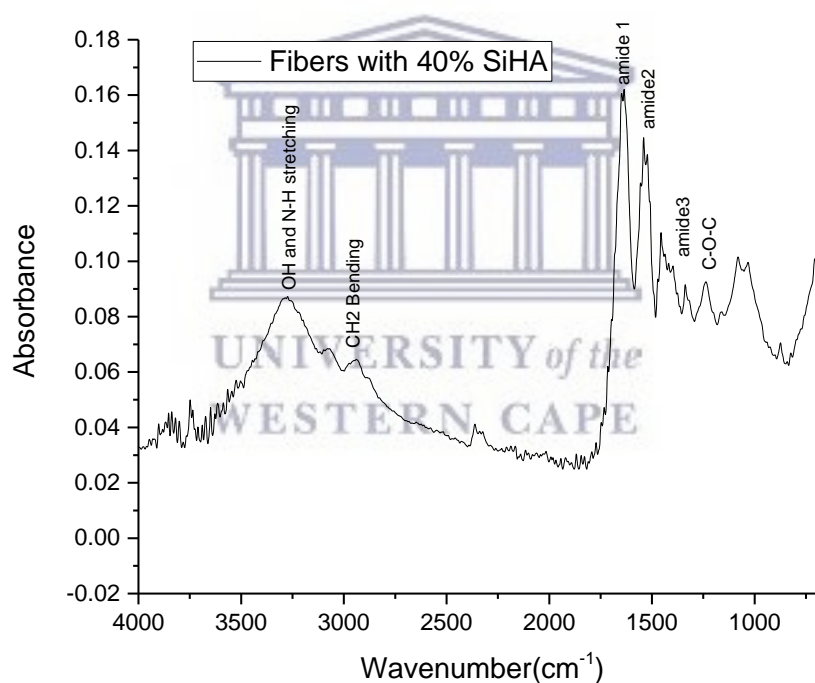
Fig: 5.11. FTIR of Nanofibers with 40% Si-HA

5.1.11. FTIR OF NANOFIBERS WITH 60% Si-HA

Fibers with 60% Si-HA showed the highest intensity of PO_4 whereas the fibers with 40% and 20% Si-HA showed the low intensity peaks of PO_4. Figure 5.12 shows the spectra of nanofibers with 60% Si-HA.
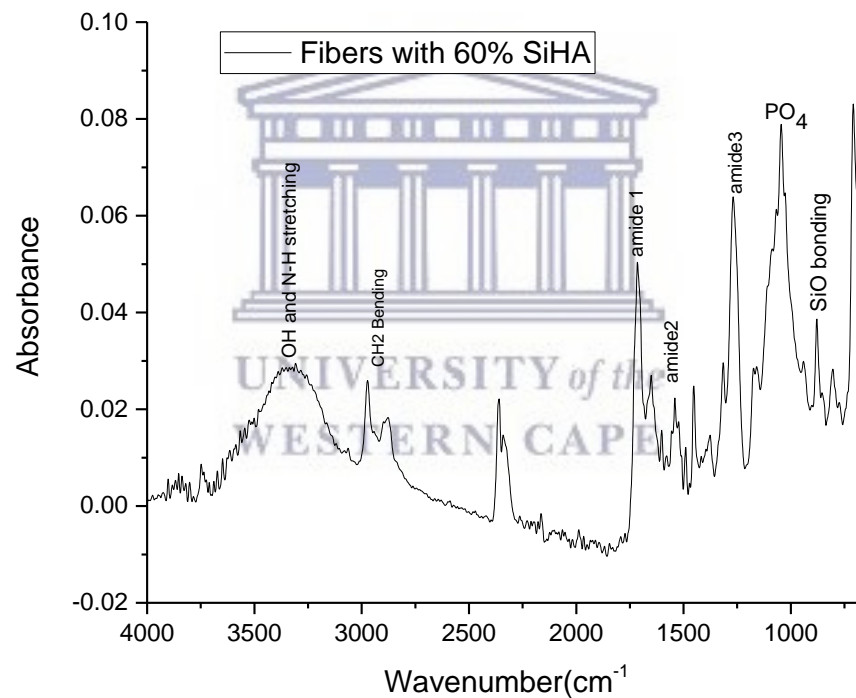
Fig: 5.12. FTIR of nanofibers with 60% Si-HA

171
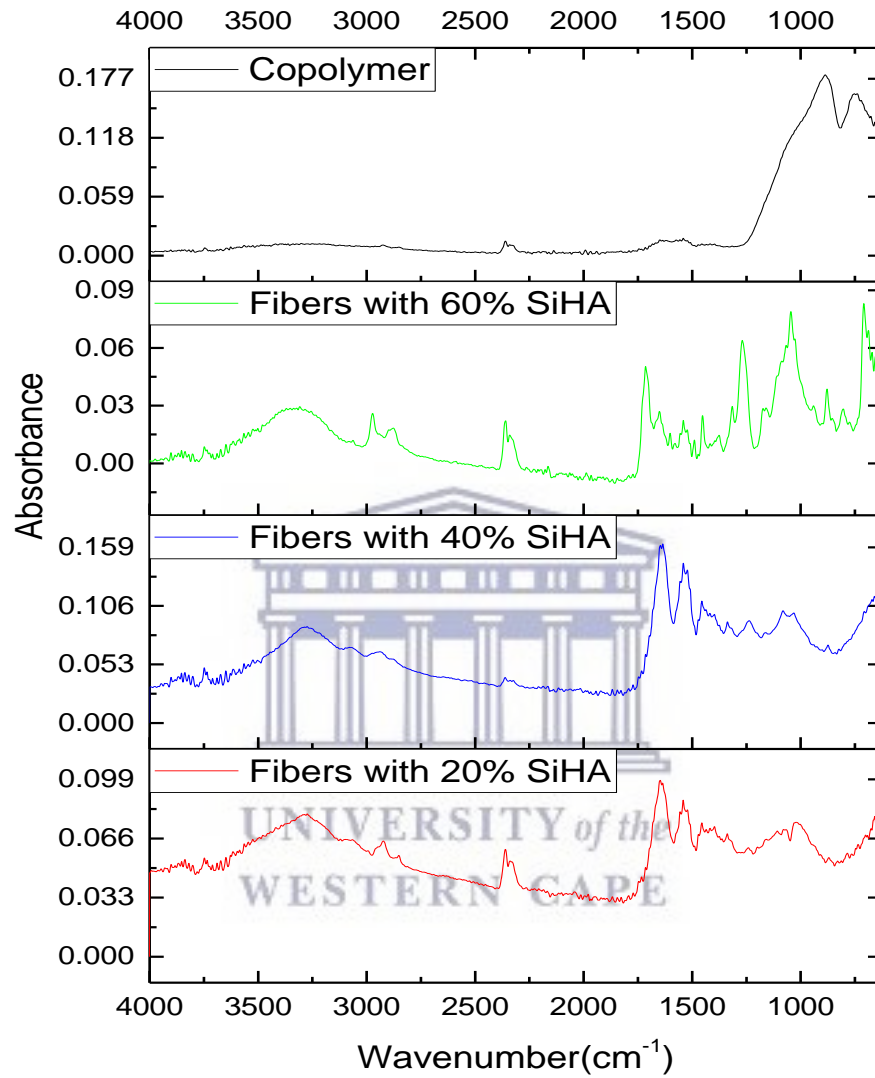
Fig: 5.13. Comparative spectra of nanofibers

Figure 5.13 shows the comparative spectra of composite nanofibers with different concentration of Si-HA.

5.2. SCANNING ELECTRON MICROSCOPY (SEM) & ENERGY-DISPERSIVE X-RAYS SPECTROSCOPY (EDS)

Scaning Electron Microscopy (ECM) images of copolymer and composite membranes and nanofibrous scaffolds showed the surface morphology and Energy dispersive X-ray (EDS) analysis showed the presence of HA and Si-HA in polymeric network and with the increase in the concentration of bioactive fillers, change in intensity with EDX spectra was observed.

5.2.1. SEM OF HYDROXYAPATITE (HA)

The Figures 5.14 and 5.15 shows the SEM images of the synthesized HA powder obtained after heat treatment. The powder appears to be of crushed angular shape. Higher magnification revealed that particles of AH are made of agglomeration of nano sized grains. These grains may be agglomerated due to the formation of the gel during the synthesis process.

173
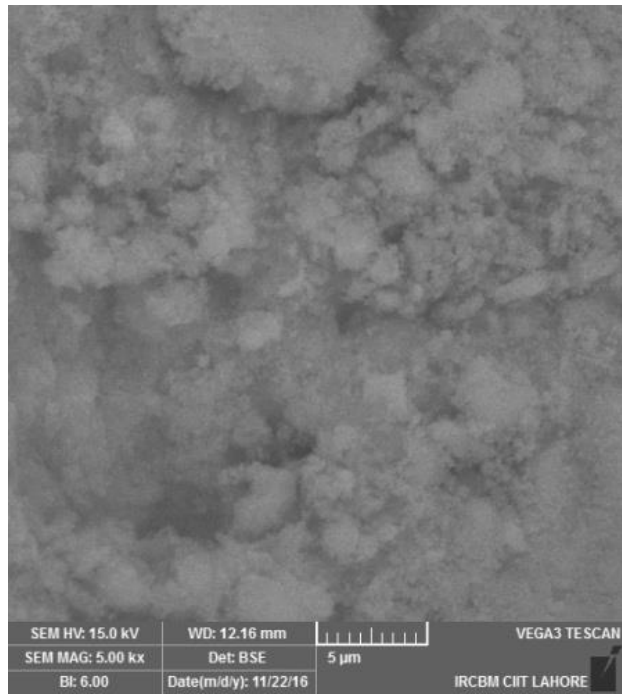
Fig: 5.14. SEM images of HA at scale bar 5µm
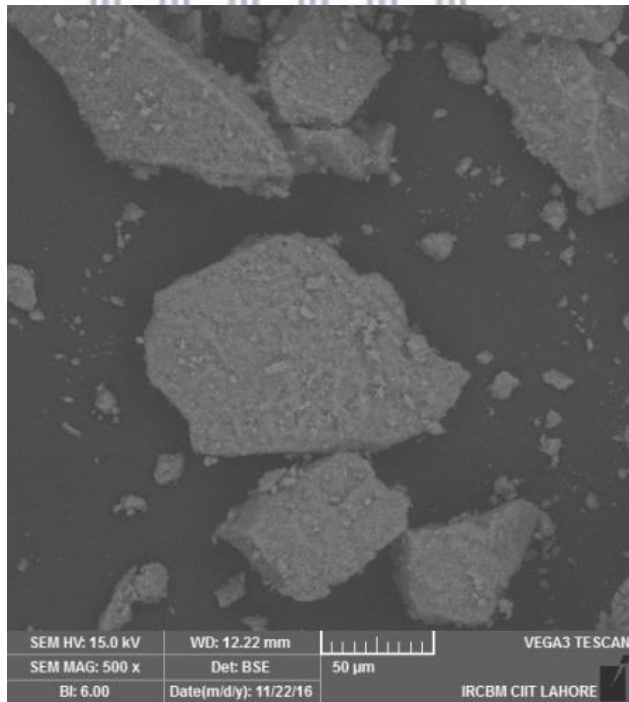
Fig: 5.15. SEM images of HA at scale bar 50µm

5.2.2. SEM OF SILICON-SUBSTITUTED HYDROXYAPATITE (Si-HA)

SEM images of the Si-HA as shown in figures 5.16 and 5.17 revealed that the particles have rough surfaces and irregular shape and consists of multiple particles fused together. The average size of the particles was 441.37±130.84 nm.

SEM HV: 8.0 kV	WD: 8.20 mm		VEGA3 TESCAN
SEM MAG: 25.0 kx	Det: SE	1 µm	
BI: 4.00	Date(m/d/y): 09/20/16		IRCBM CIIT LAHORE
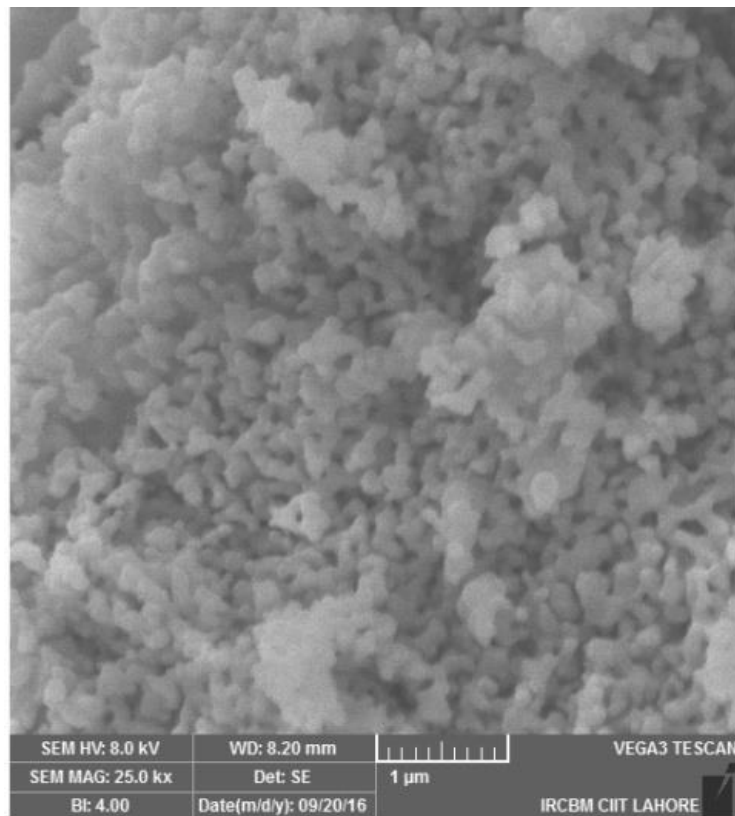
Fig: 5.16. SEM images of Si-HA at scale bar 5µm

175
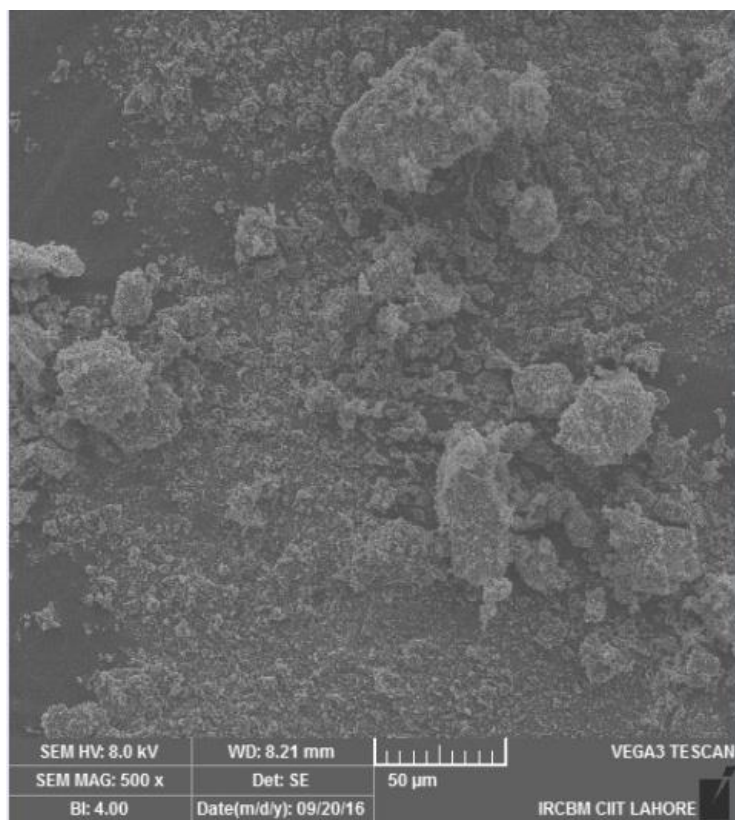
Fig: 5.17. SEM images of Si-HA at scale 50µm
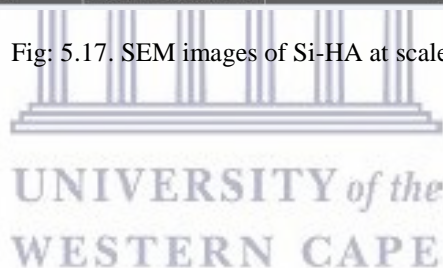
5.2.3. SEM OF COPLYMER MEMBRANES

SEM micrographs of copolymer membranes are shown in figure 5.18 and 5.19. SEM image of copolymer membranes revealed a homogenous surface morphology having striated surface. These are typical morphological structure found in chitosan-alginate coplymer because these are oppositely charged polymers. Similarly, the chitosan-alginate-gelatin membranes also showed a homogenous smooth surface.

176
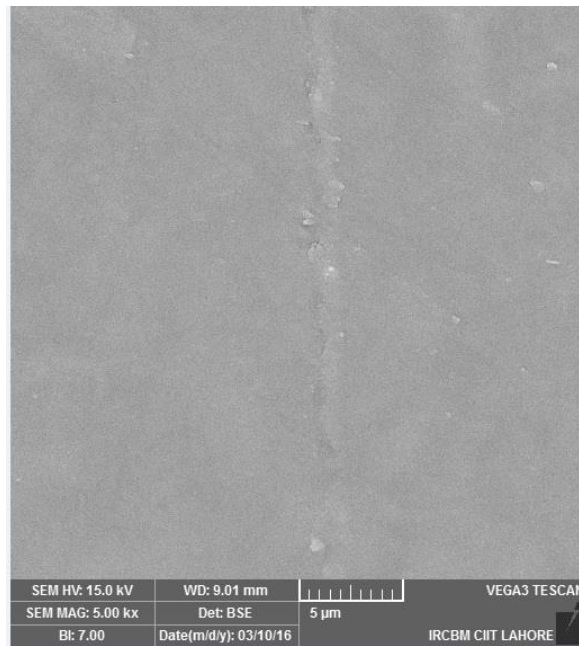
Fig: 5.18. SEM image of chitosan-alginate copolymer membrane (Bar scale 5µm)
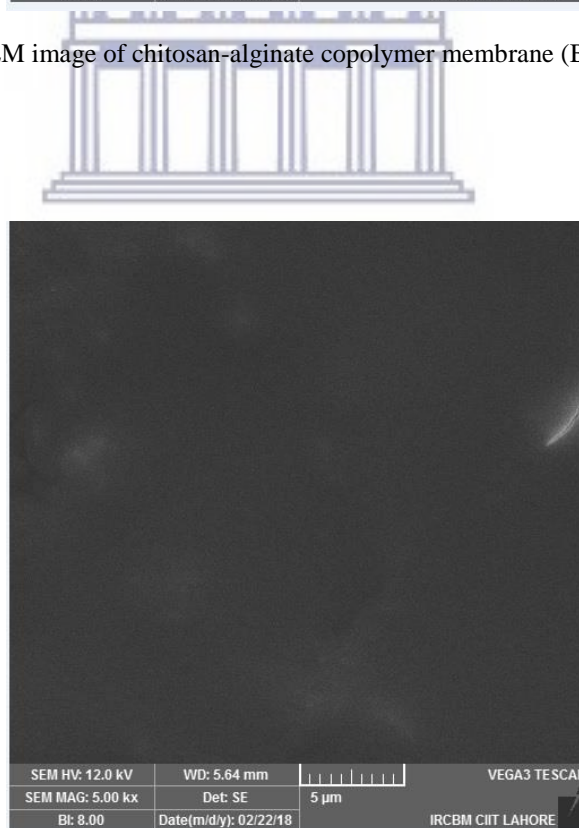
Fig: 5.19. SEM image of chitosan-alginate-gelatin copolymer membrane (Bar scale 5µm)

5.2.4. SEM OF COMPOSITE MEMBRANES

The morphology of composite membranes with different concentrations of HA and Si-HA are shown in figrures 5.20, 5.21, 5.22, 5.23, 5.24, 5.25. Composite membranes showed a less homogenous suface compared to copolymer membranes.

Membranes having varying amount of HA (20%, 40%, 60% wt/v) exhibited irregular, fibrous structures of surface and rough cross-section morphology, with pores and clusters of sodium alginate–chitosan aggregated particles. It was observed that complex aggregates appear in micrographs as segments with elongated structures having the HA particles distributed on the surface. It was found that with increasing ratio of hydroxyapatite more complex aggregates were formed, which can be seen as an increase in the structure's irregularity.
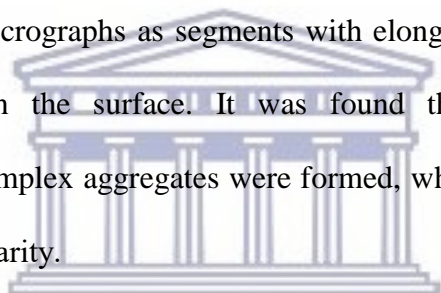
The chitosan-alginate-gelatin and Si-HA composite membranes presented more irregularities and aggregates of Si-HA on the surface compared to chitosan-alginate HA membranes with increasing concentrations of Si-HA.
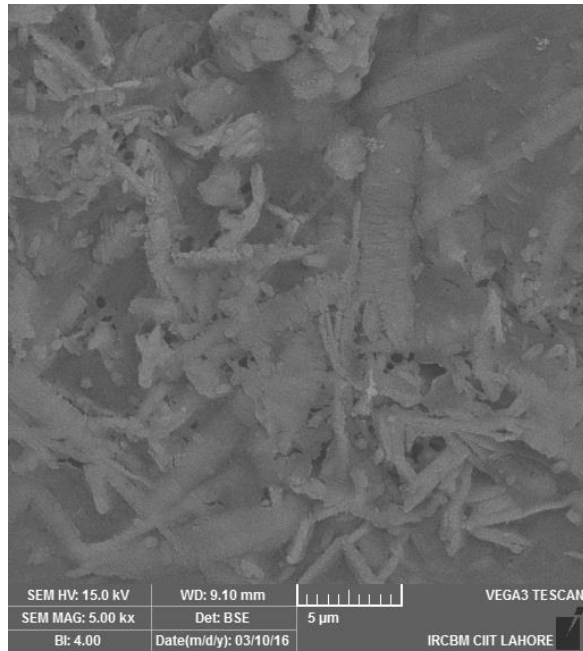
178

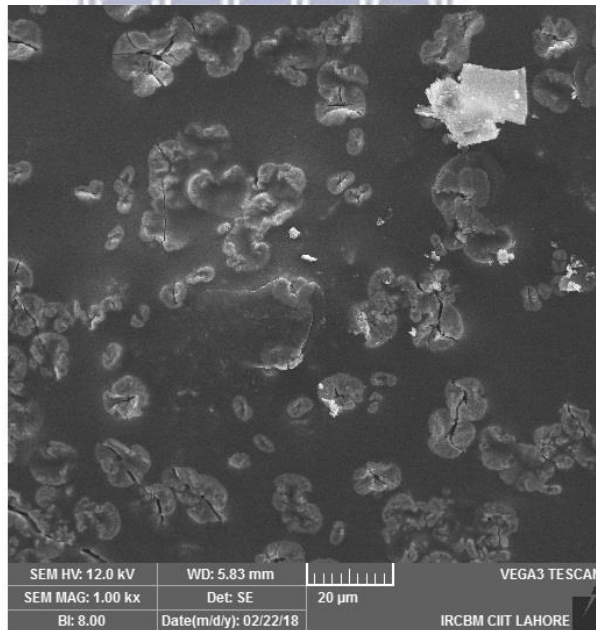Fig: 5.20. SEM image of chitosan-alginate-20% HA membrane (Bar scale 5µm)

Fig: 5.21. SEM image of membranes chitosan-alginate-gelatin-20% Si-HA (Bar scale 20µm)
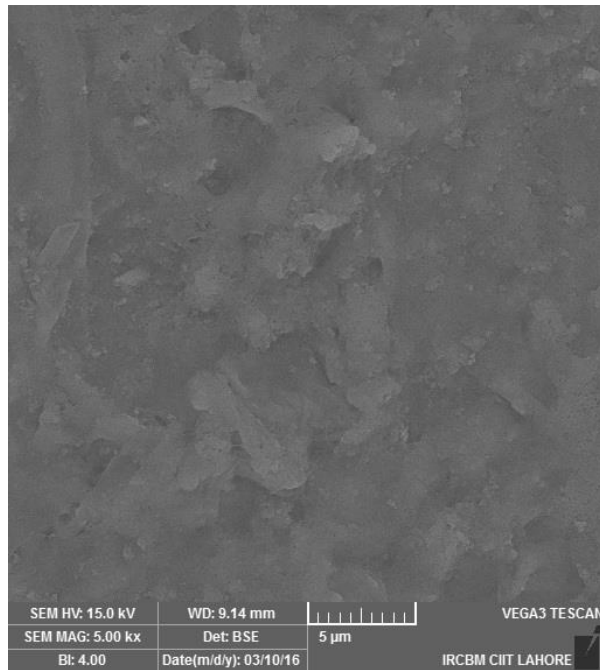
179

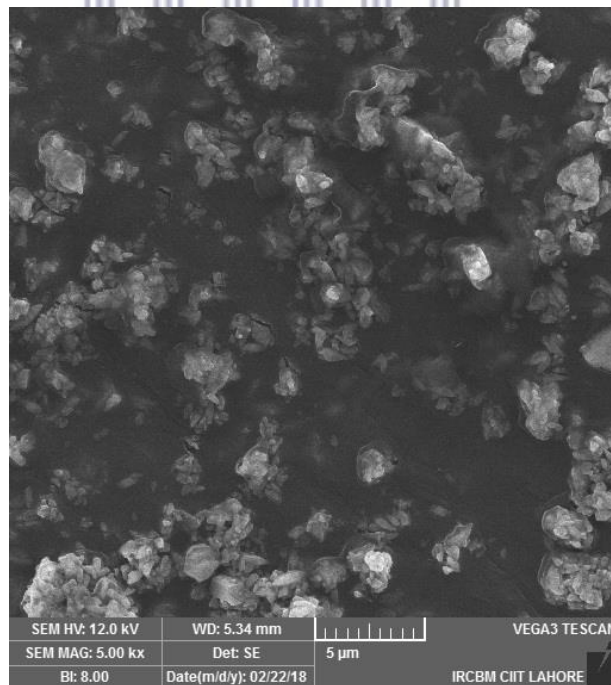Fig: 5.22. SEM image of chitosan-alginate-40% HA membrane. (Bar scale 5µm)

Fig: 5.23. SEM image of chitosan-alginate-gelatin-40% Si-HA membrane (Bar scale 5µm)
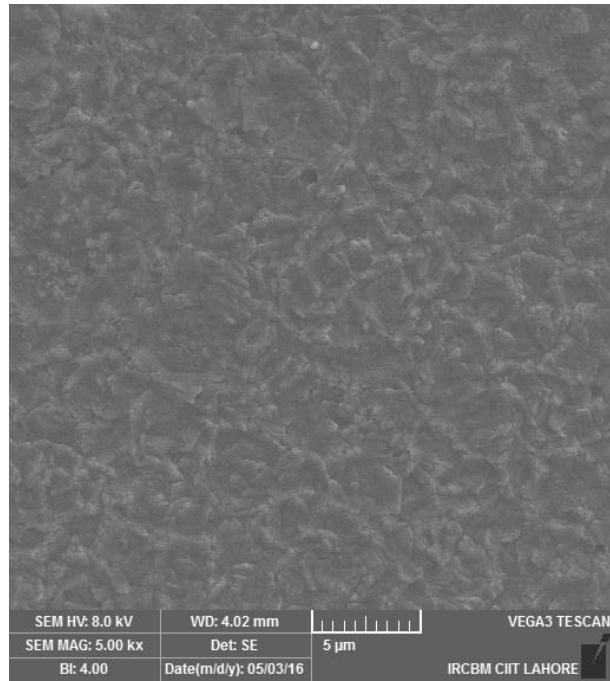
180

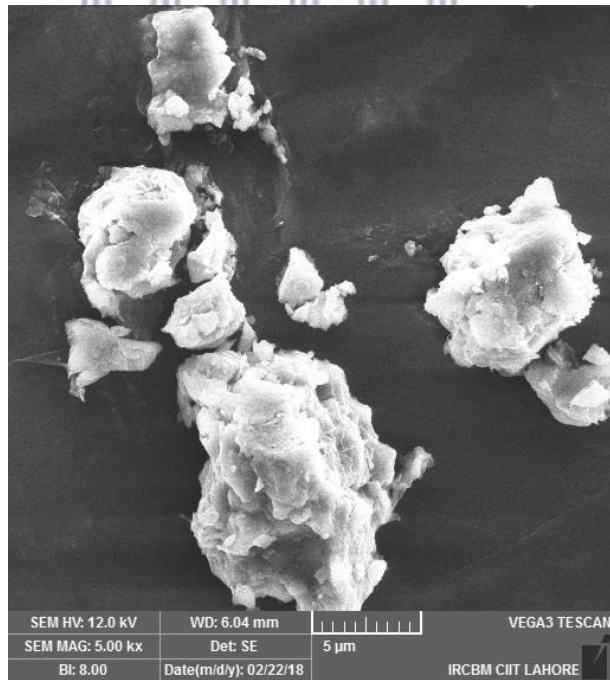Fig: 5.24. SEM images of chitosan-alginate-60% HA membrane (Bar scale 5µm)

Fig: 5.25. Chitosan-alginate-gelatin-60% Si-HA (Bar scale 5µm)

181

5.2.5. SEM & EDS OF NANOFIBROUS SCAFFOLDS

SEM images of copolymer electrospun nanofibrous scaffolds are shown in figures 5.26 and 5.27. The nanofibers were randomly oriented and diameter raneged from 61.75nm to 546.72nm with an average diameter of 242.41±158.12.
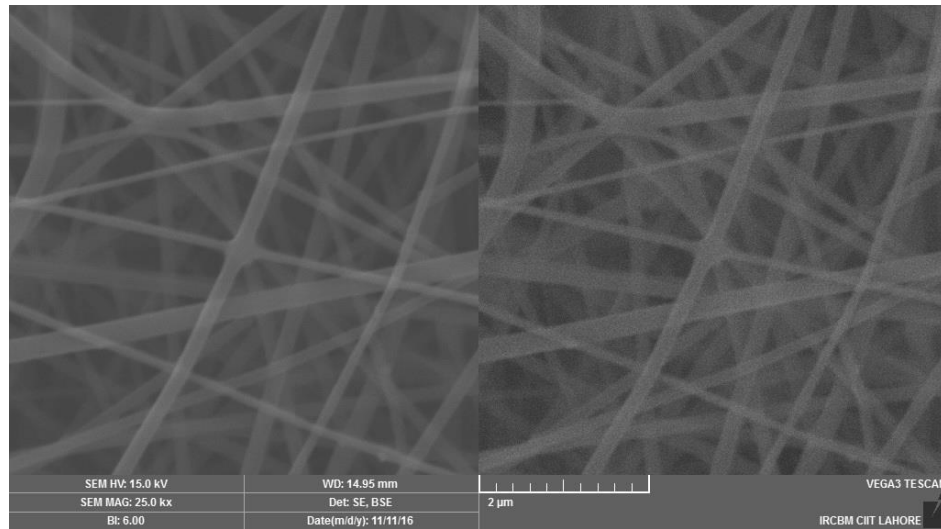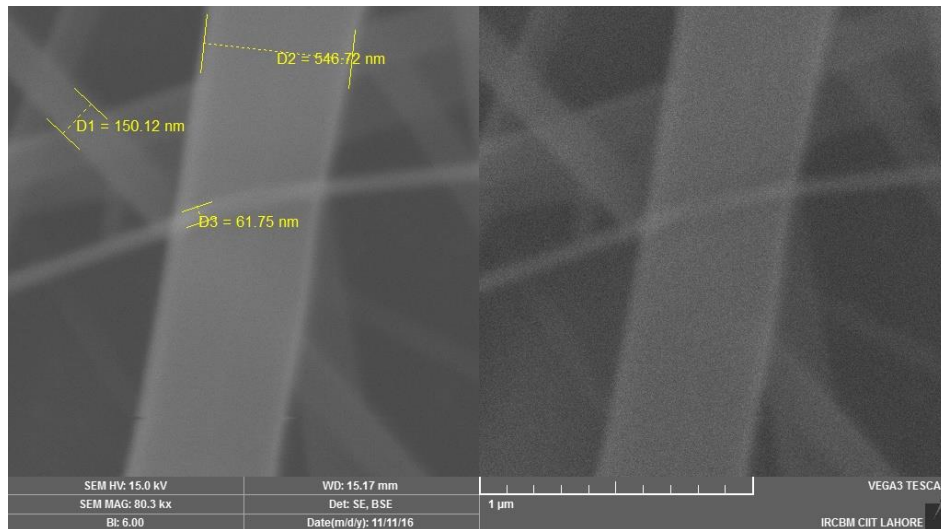

Fig: 5.26. SEM image of copolymer nanofibrous scaffold, showing randomly oriented fibers of different diameter (Bar scale 2µm)

182
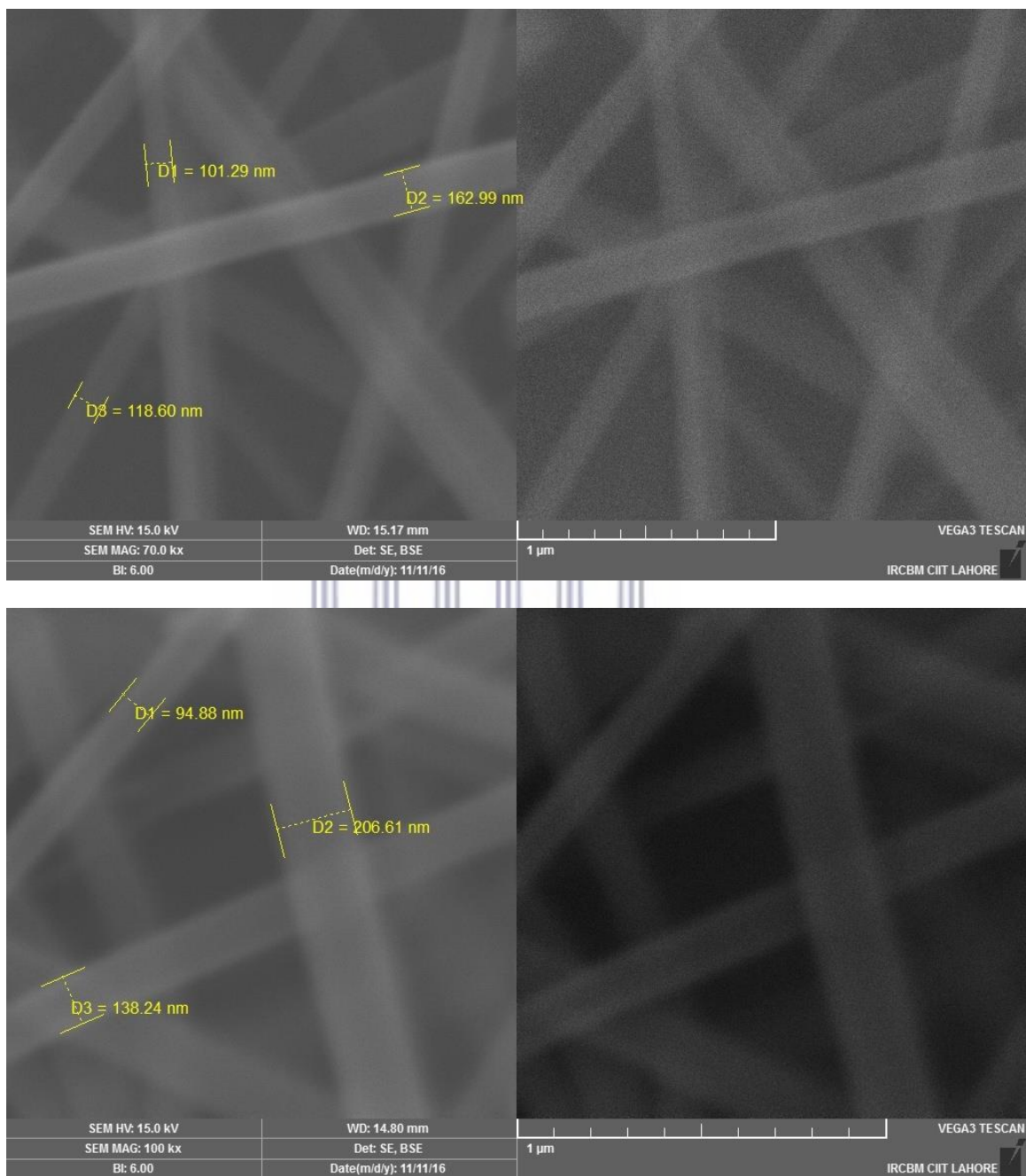
Fig: 5.27. SEM image of copolymer scaffold showing different diameters of fibers (Bar scale 1µm)

The EDS of copolymer fibers revealed its elemental composition. The EDS spectra of copolymer fibers showed the peaks of Carbon and Oxygen suggestive of the presence of copolymer, while no peak of Calcium (Ca), Phosohrous (P) and Silicon (Si) was apparent which indicate the absence of Si-HA in these fibers. Figure 5.28 shows the EDS spectra of copolymer fibers.

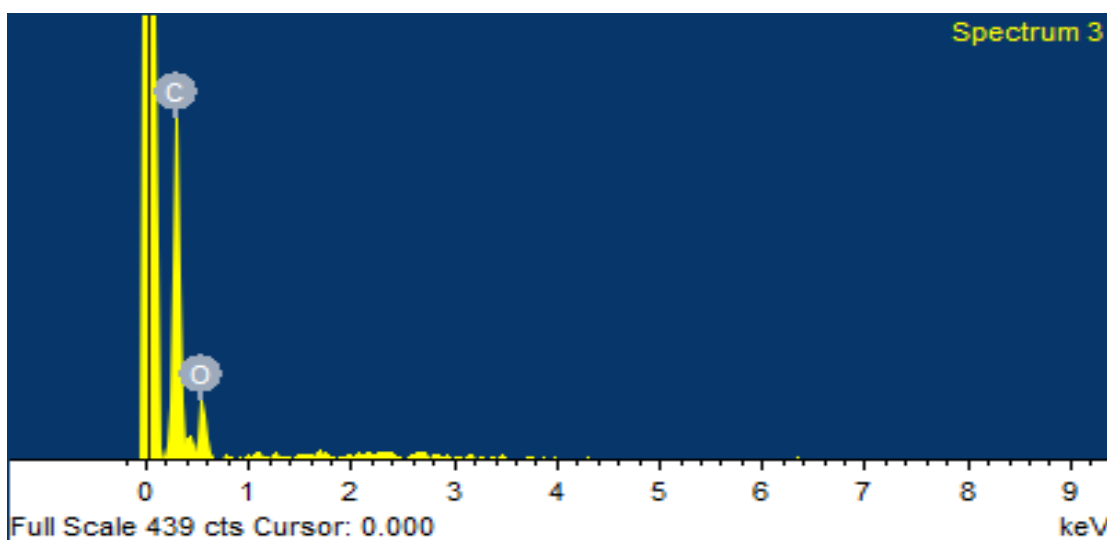Fig: 5.28. EDS spectra of copolymer nano-fibers

5.2.6. SEM & EDS OF COMPOSITE NANOFIBROUS SCAFFOLDS

SEM images of the composite nanofibrous scaffolds showed Si-HA particles dispersed on the surface as well as embedded into randomly oriented copolymer nanofibers. The EDS spectra of composite nanofibrous scaffolds confirmed the presence of Si-HA in the fibers in the form of peaks for Ca, P and Si.

184

Figures 5.29 and 5.30 show the SEM images of the composite nanofibrous scaffolds containing 20% Si-HA. The Si-HA particles were visble on the surface as well as embedded into copolymer nanofibers.

Fig: 5.29. SEM images of copolymer nanofibers with 20% Si-HA (Bar scale 1µm)
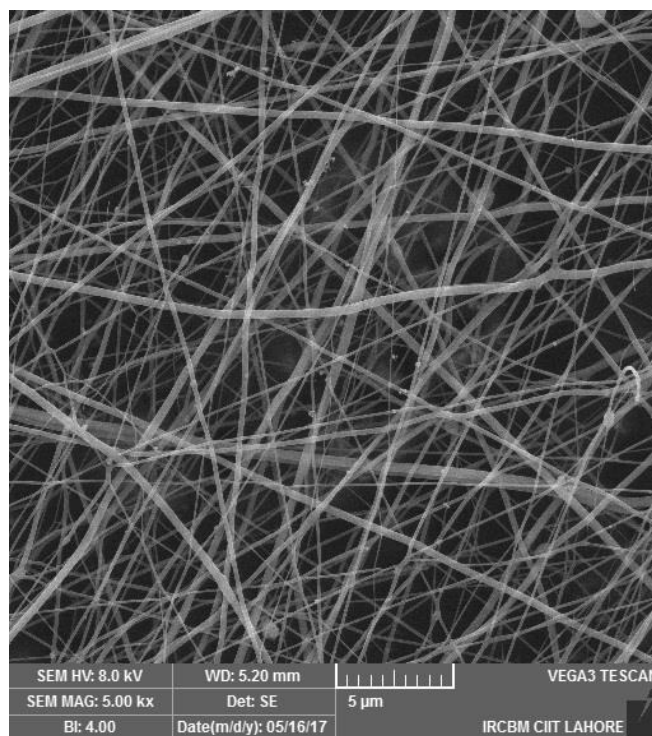
Fig: 5.30. SEM images of copolymer nanofibers with 20% Si-HA (Bar scale 5µm)

The EDS spectra of nanofibrous scaffold with 20% Si-HA confirmed the presence of Si-HA in the fibers in the form of peaks for Ca, P and Si. Figure 5.31 shows the EDS spectra of nanofibrous scaffold with 20% Si-HA.
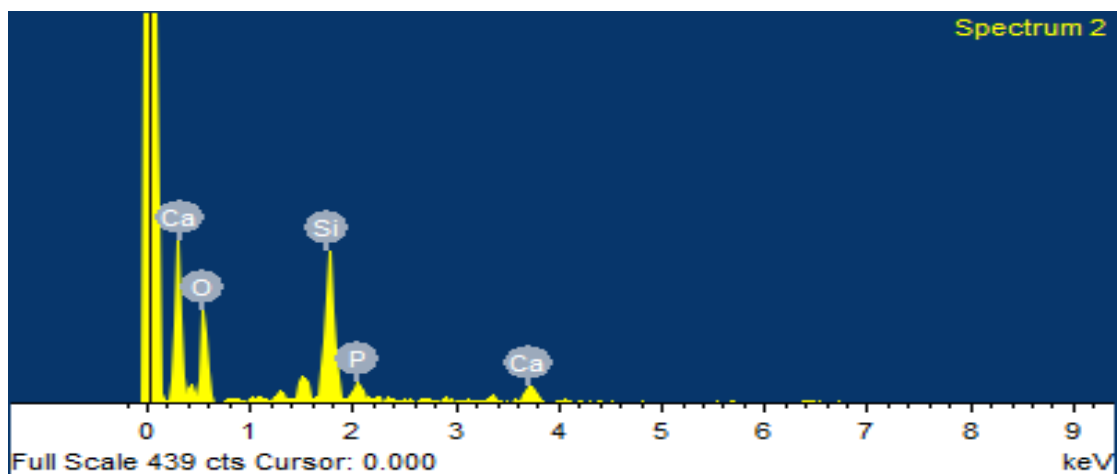
Fig: 5.31. EDS spectra of copolymer-20% Si-HA nanofibrous scaffold

186

Figures 5.32 and 5.33 show the SEM images of copolymer-40% Si-HA nanofibrous scaffold. Si-HA particals evenly dispersed as well as embedded in randomly oriented nanofibers.
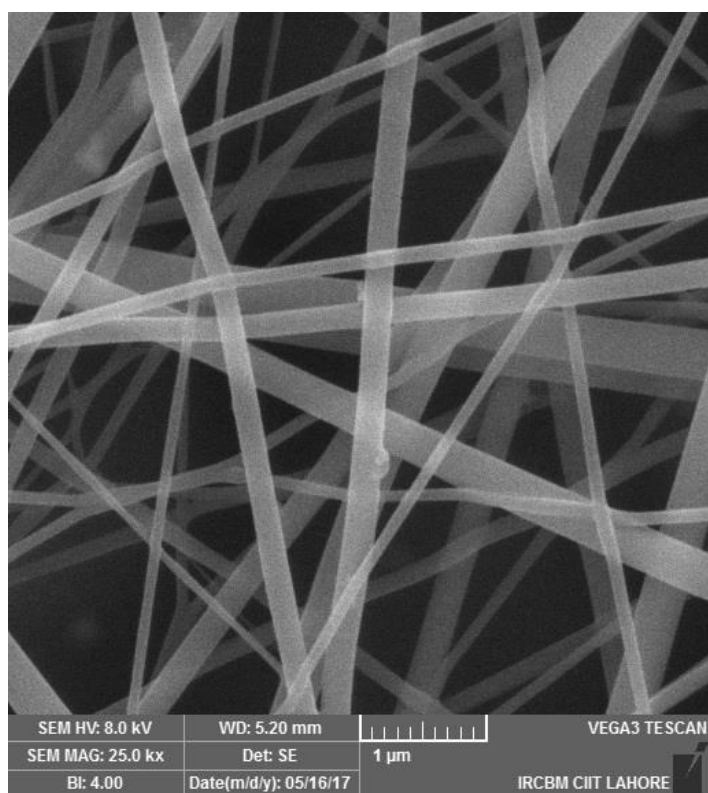

Fig: 5.32. SEM images of copolymer with 40% Si-HA (Bar scale 2µm)
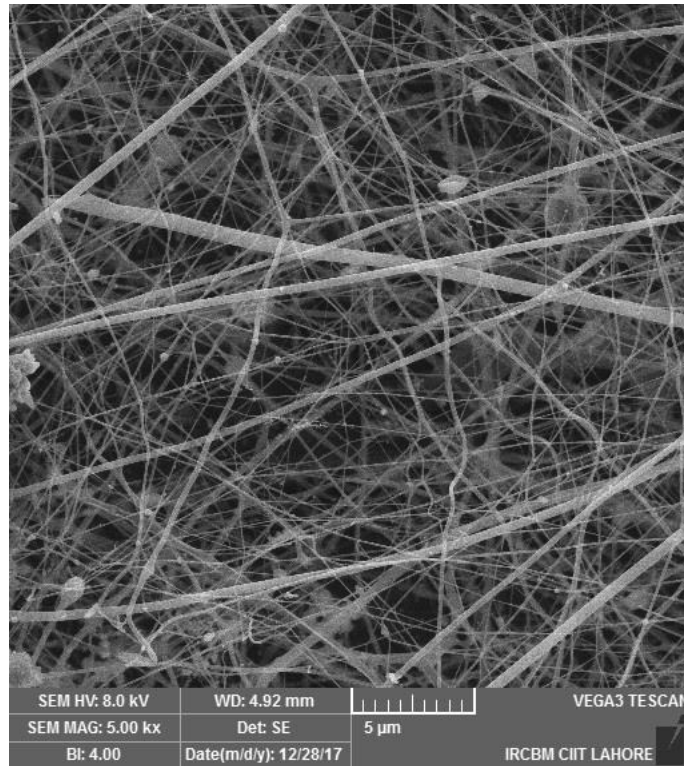
Fig: 5.33. SEM images of copolymer with 40% Si-HA (Bar scale 5µm)

EDS spectra of the composite nanofibrous scaffold with 40% Si-HA as shown in figure 5.34 exhibited higher quantity of Si-HA in the form of elevated Si peak compared to 20% Si-HA composite scaffold.
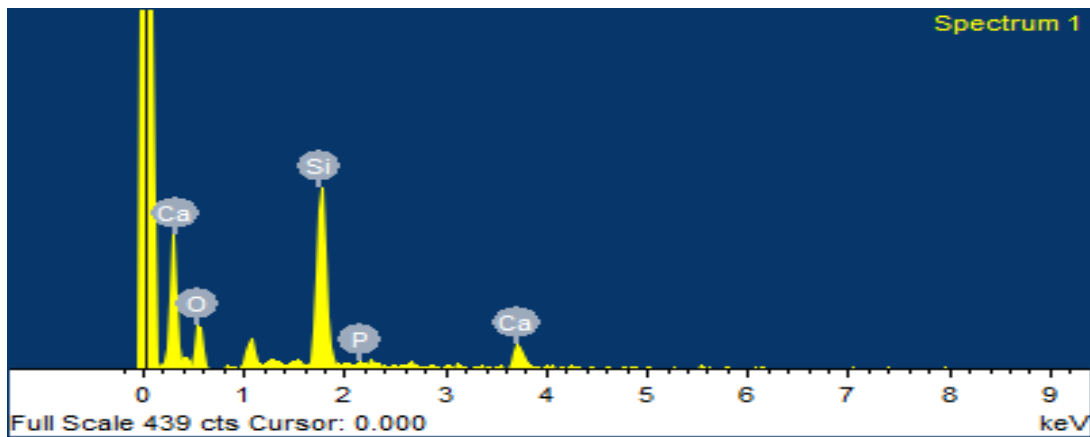
Fig: 5.34. EDS spectra of copolymer-40% Si-HA nanofibrous scaffold

188

SEM images of composite scaffold containg 60% Si-HA shows higher quantity of Si-HA particles on the surface of randomly oriented fibers (figure: 5.35 and 5.36).
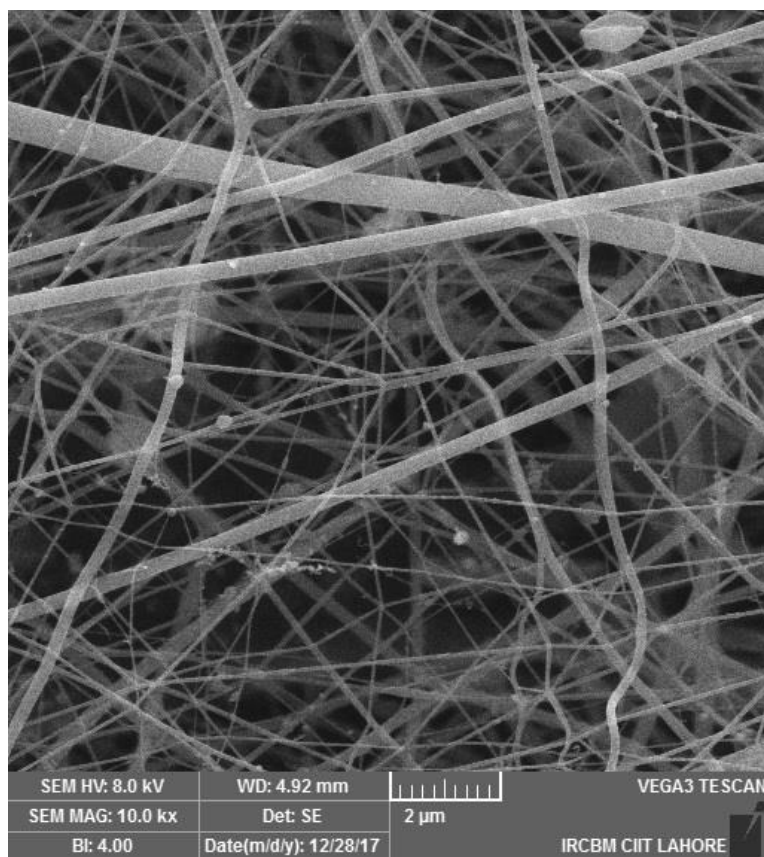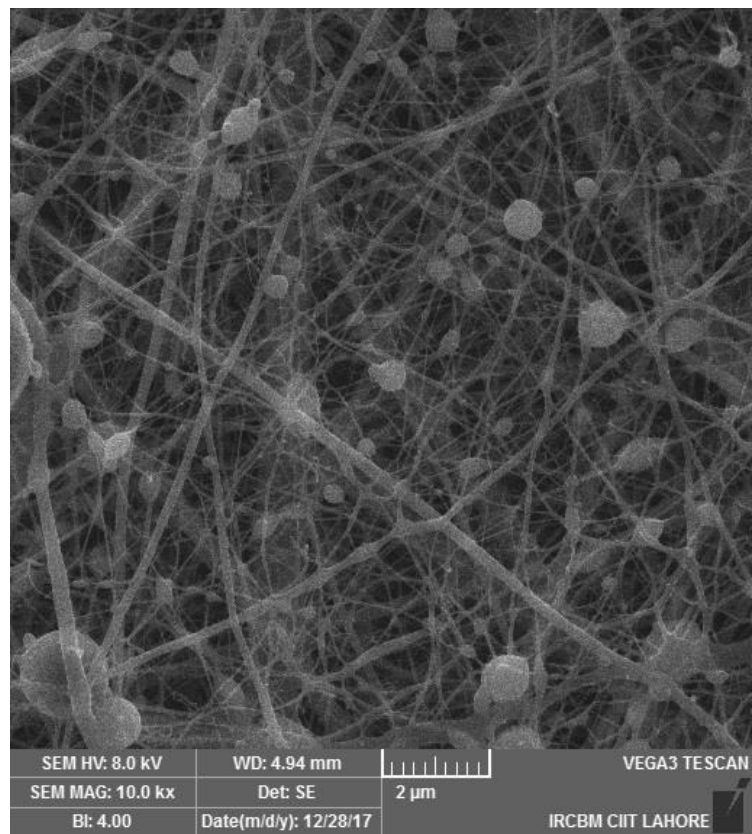

Fig: 5.35. SEM images of copolymer fibers with 60% Si-HA (Bar scale 2µm)
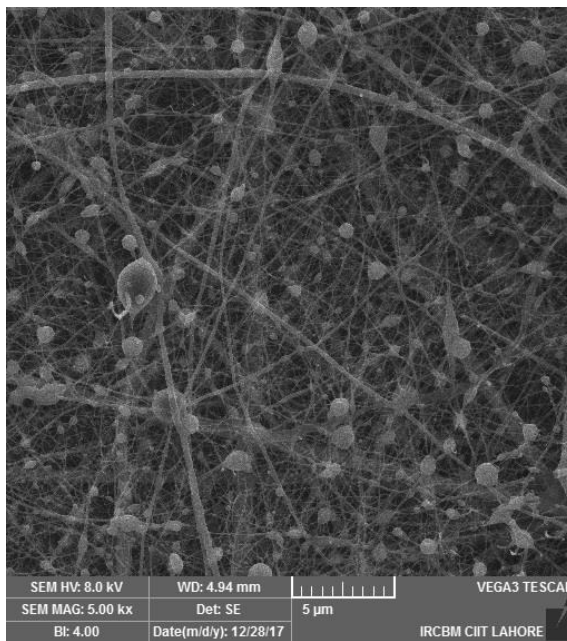
Fig: 5.36. SEM images of copolymer fibers with 60% Si-HA (Bar scale 5µm)

Figure 5.37 shows the EDS spectra of composite nanofibrous scaffold with 60% Si-HA as evident by much higher peak of the Si in the spectra.
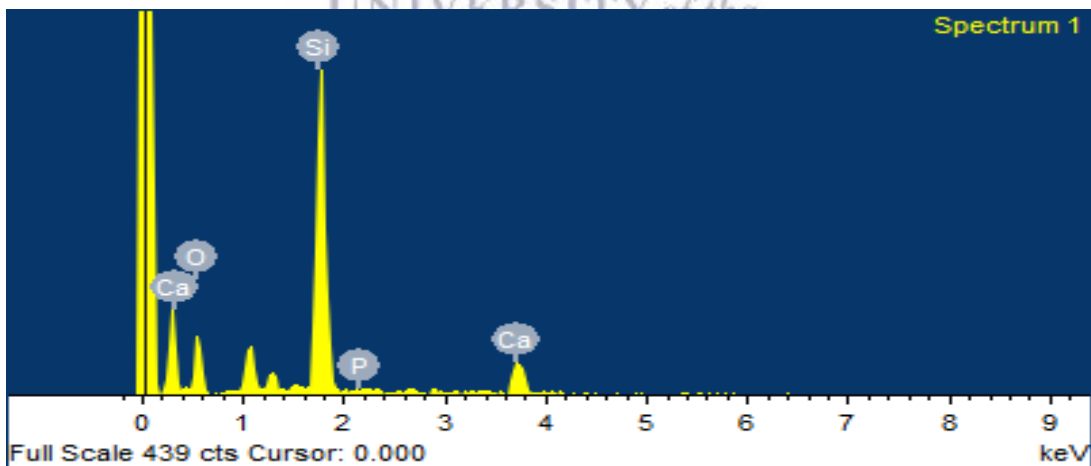
Fig: 5.37. EDS spectra of copolymer-60% Si-HA

190

5.3. MECHANICAL PROPERTIES

Tensile tests had been used as a first approach to get information about the mechanical performance of the scaffolds. Figure 5.38 shows the typical tensile stress-strain curve used to assess the mechanical properties.
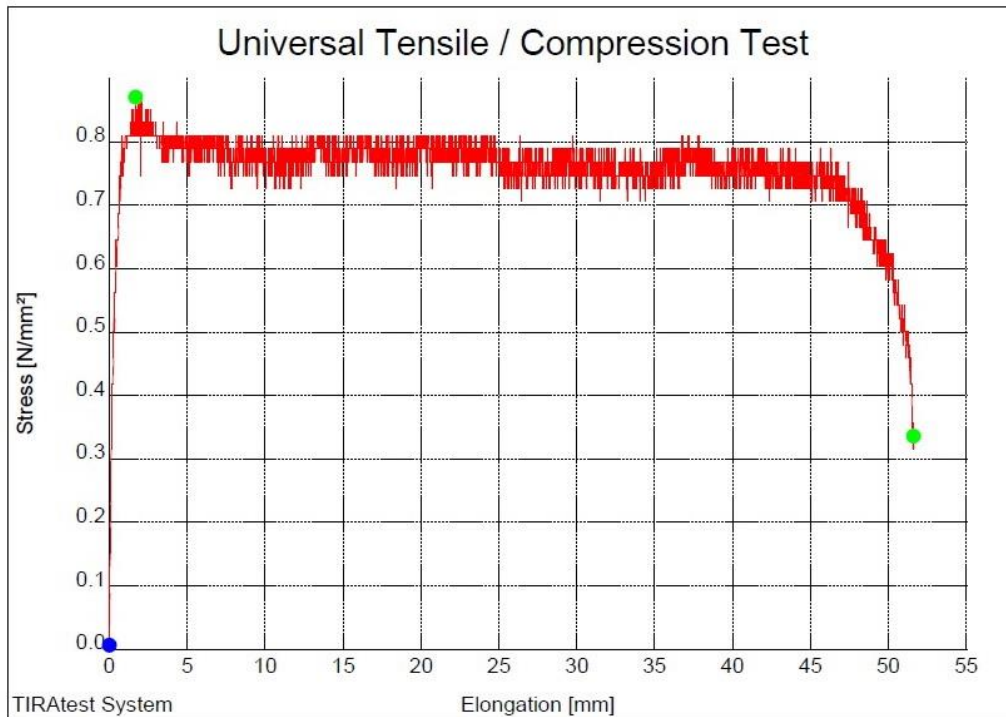
Fig: 5.38. Stess-strain curve used to determine mechanical properties

The tensile strength of copolymer, copolymer 20% Si-HA, copolymer 40% Si-HA and copolymer 60% Si-Ha was 0.493±0.04, 0.825±0.32, 1.08±0.20 and 1.5945±0.35 while % elongation was 183.3±23.13, 103.3±5.35, 77.6±9.05 and 41.4±1.89 respectively. Figure 5.39 (A) demonstrates the tensile strength while figure 5.39 (B) represents the % elongation at break of specimens that was dictated from stress-strain curve.

191
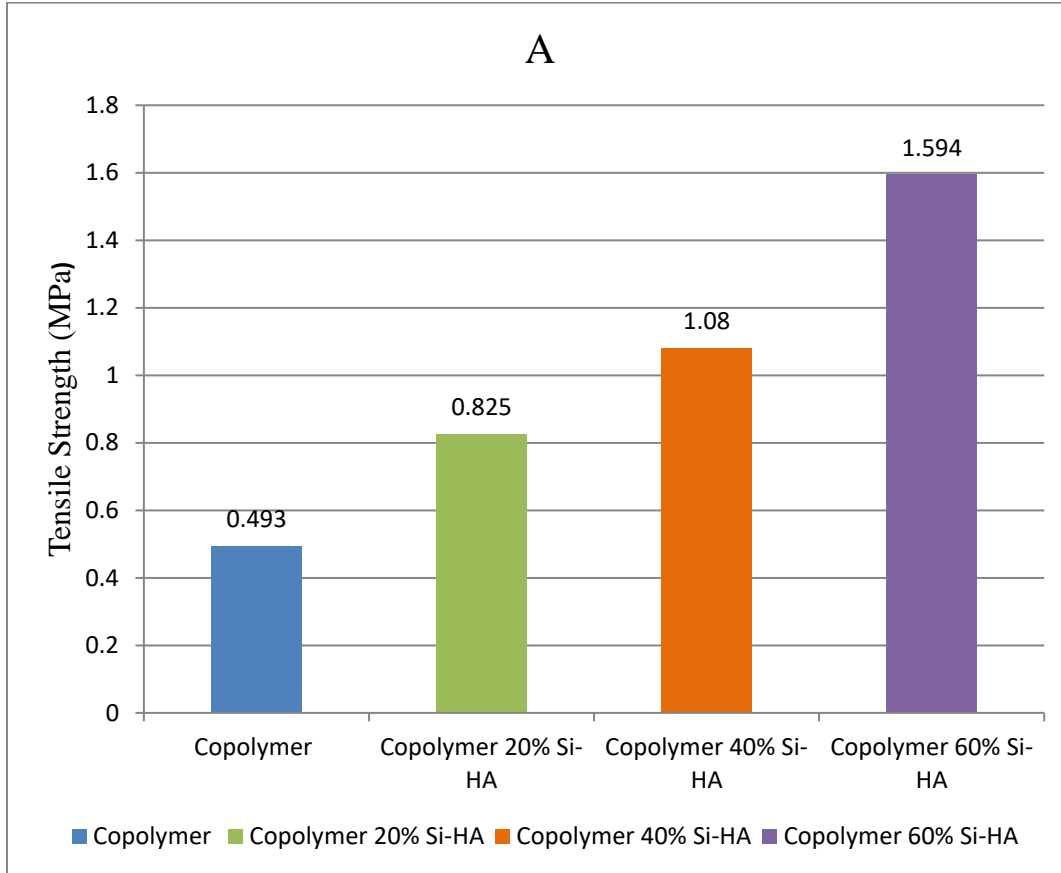
Fig: 5.39. (A): The tensile strength of scaffolds

As compared to simple copolymer scaffolds tensile strength of composite scaffolds was increased while % elongation was decreased as expected. The tensile strength was increased with the increase of Si-HA wt%. The tensile strength of the composite scaffold with 60% Si-HA was three times greater compared to simple copolymer scaffolds. Among composite scaffolds, the lowest strength (0.825 MPa) was observed in 20% Si-HA scaffold while highest strength (1.595 MPa) observed in 60% Si-HA composite scaffolds.

192
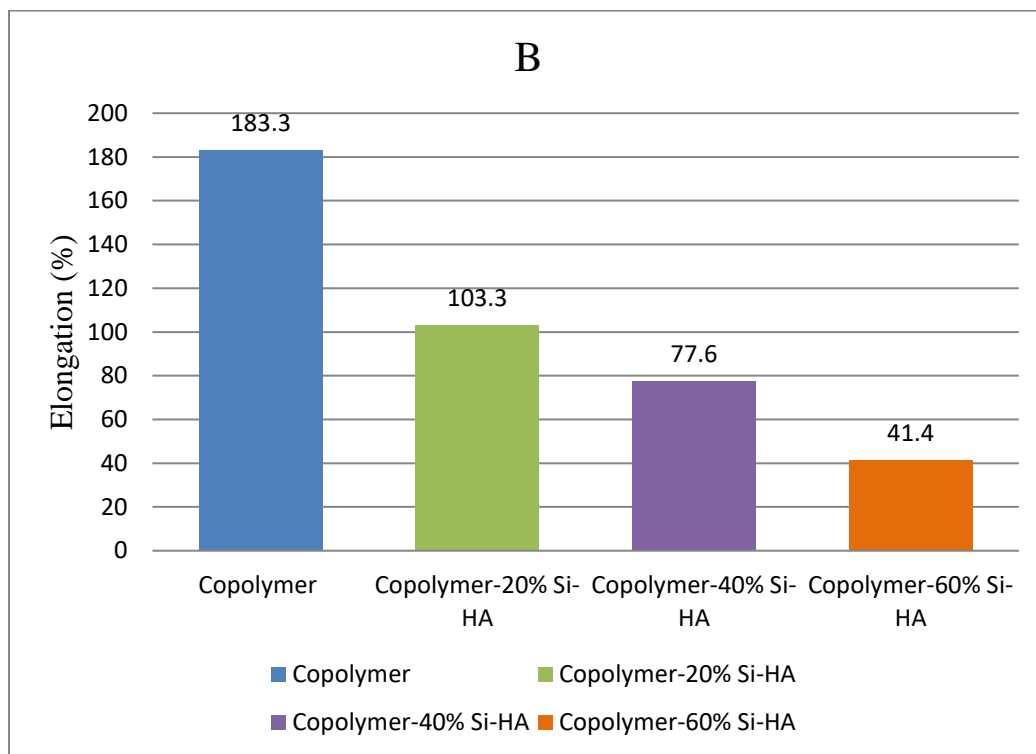
Fig: 5.39. (B): % elongation at break

In contrast to tensile strength, the % elongation at break was decreased with the addition of Si-HA. There was a significant difference ((P< 0.05) in % elongation between copolymer and composite scaffolds with 60% Si-HA, which suggested that by increasing Si-HA content elongation was declined.

193

5.4. SWELLING BEHAVIOUR

The mean swelling ratio calculated on copolymer and composite scaffolds up to 7hours is shown in table 5.1.

Time Intervals	Mean Swelling Ratio			
	Copolymer	Copolymer 20% Si-HA	Copolymer 40% Si-HA	Copolymer 60% SI-HA
0.5 hrs	22.17±0.514	13.61±0.415	9.30±1.145	0.398±0.476
01 hrs	30.95±1.228	17.56±0.715	12.17±1.111	0.43±0.600
03 hrs	37.65±1.269	23.39±0.343	16.17±0.826	2.91±0.993
05 hrs	39.43±0.559	25.56±0.850	18.26±0.387	3.52±0.432
07 hrs	44.48±0.371	29.47±0.433	19.65±0.304	6.478±0.589

Table: 5.1. Mean swelling ratio of copolymer & composite scaffolds at different time intervals

Copolymer nanofibrous scaffolds showed considerably higher water uptake behaviour compared to composite scaffold. Figure 5.40 illustrates the swelling behaviour of copolymer and composite scaffolds.

194
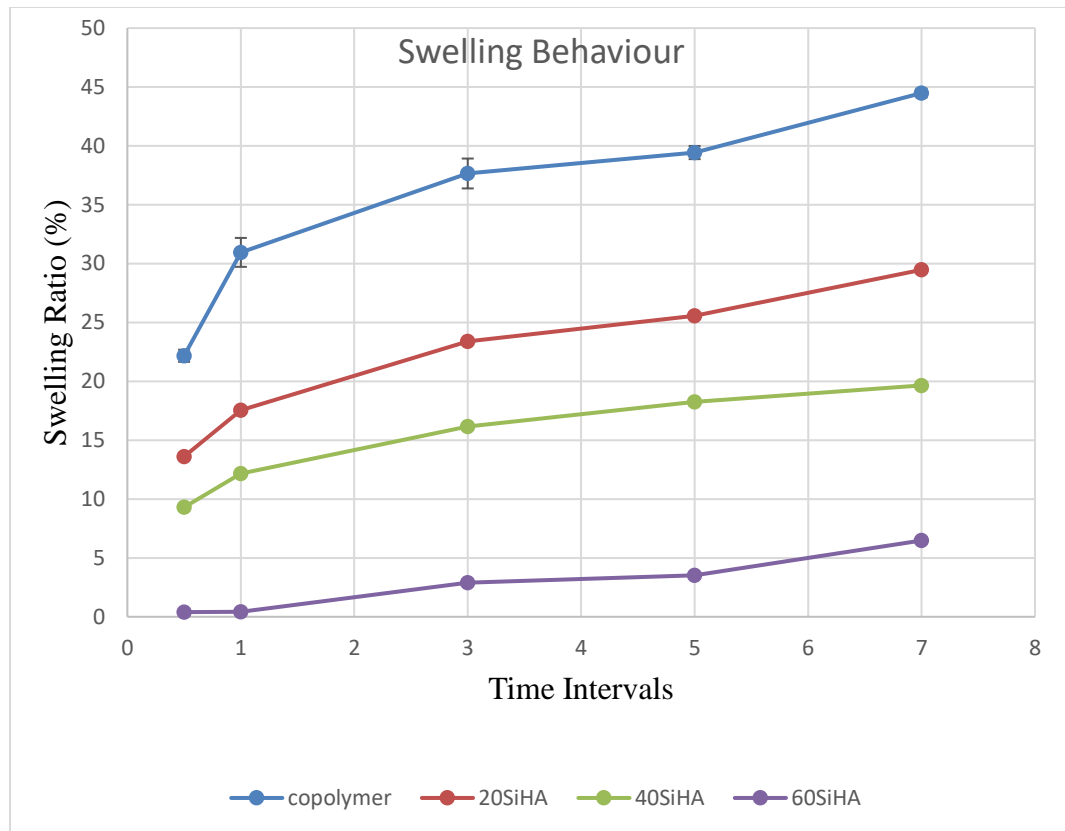
Fig: 5.40. Swelling behaviour of copolymer & composite scaffolds at different time intervals

Results also showed that percentage swelling started to decrease with the addition of Silicon substituted hydroxyapatite into the copolymer. The composite scaffolds exhibited a noticeably less water uptake as the concentration of Si-HA increased. Copolymer scaffolds showed 44.48±0.371% swelling ratio at 7 hrs while composite scaffold with 60% Si-HA revealed only 6.478±0.589% swelling ratio at 7 hrs. However, the difference in swelling ratio among copolymer and composite scaffolds was not statistically significant (P< 0.05). All the specimens showed almost same pattern of water uptake. Overall percentage swelling of copolymer and composite scaffolds was found to increase

195

with time and maximium ratio was achieved in the 1st half an hour by all the specimens while in the remaining times intervals the water uptake was notably low except the scaffolds containing 60% Si-HA, which showed only 0.398±0.476% swelling ratio in the 1st half an hour.

5.5. CYTOTOXITY AND CELL PROLIFERATION

For the potential use of any material to synthesize scaffolds for GTR/GBR the structure and chemical composition of material must ensure a normal growth and morphology of cells, with no toxic effect on the cellular machinery and biological pathways

5.3.1. CELL MORPHOLOGY

Normal morphology of the MC3T3-E1 cells was observed under light microscope as shown in the figure 5.41.
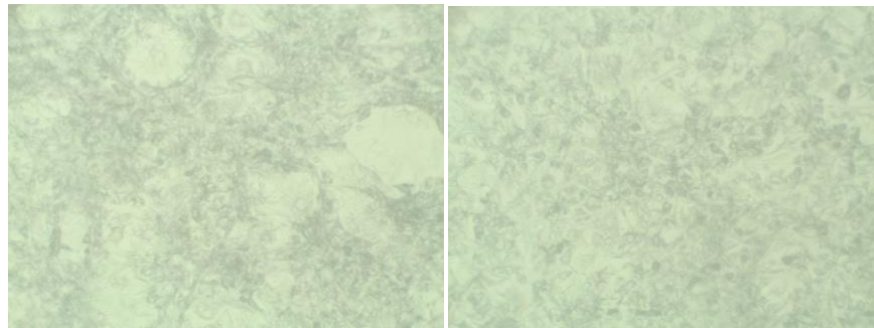
Fig: 5.41. Light microscopic view of cells attached to scaffold

196

In this experimental study, MC3T3-E1 cells exhibited a normal morphology and growth in the presence of copolymer and copolymer with different concentrations of Si-HA as compared to control. MTT assay showed no toxic effect, and cells were found viable which demonstrates this material provide a normal environment in which osteoblasts can grow and proliferate.

Cell proliferation on different samples at various intervals is shown in figures 5.42, 5.43 and 5.44. BMPs coated composite scaffolds with 60% Si-HA showed slightly higher proliferation rate compared to other scaffolds on day 1 and 7. Similarly, non- coated scaffolds with 20% Si-HA showed slightly higher proliferation rate on day 1, 3 and 7, however, there was a decrease in proliferation rate with the increase of Si-HA concentration in non-coated membrane on day 1 and 3. On the other hand, BMPs coated membrane showed slightly increased proliferation rate with increase in Si-HA concentrations on day 1 and 3.

The experiment showed similar results in triplicates.
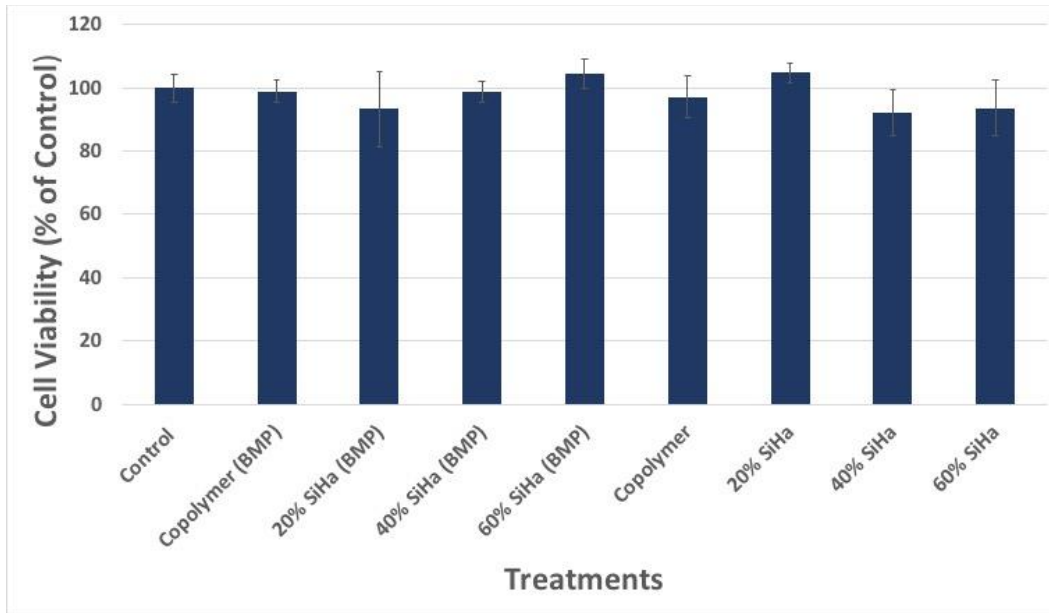
Fig: 5.42. Proliferation of cells on different scaffolds (Day 1)
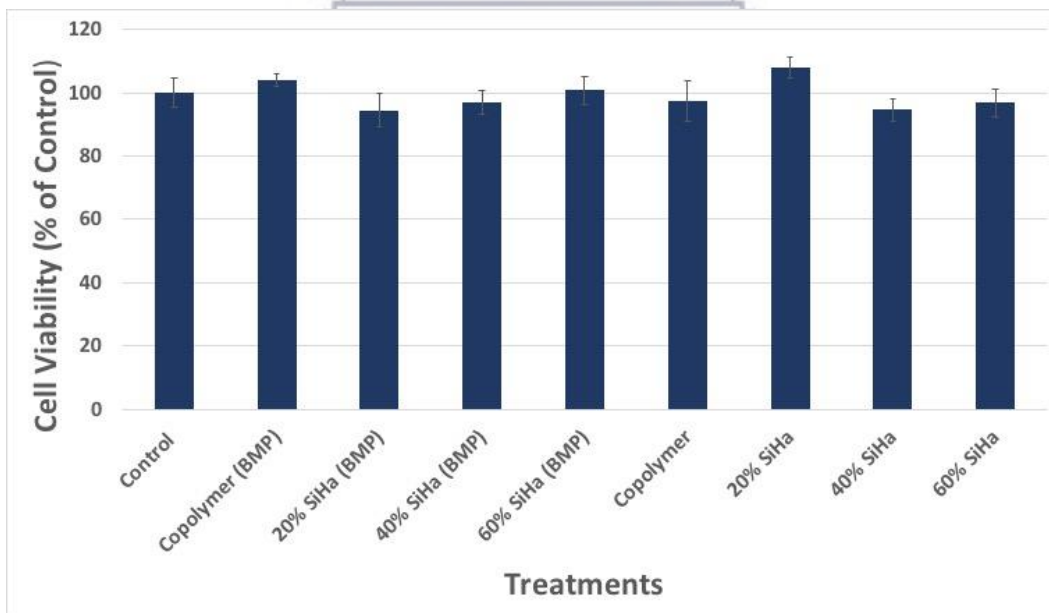
Fig: 5.43. Proliferation of cells on different scaffolds (Day 3)

198
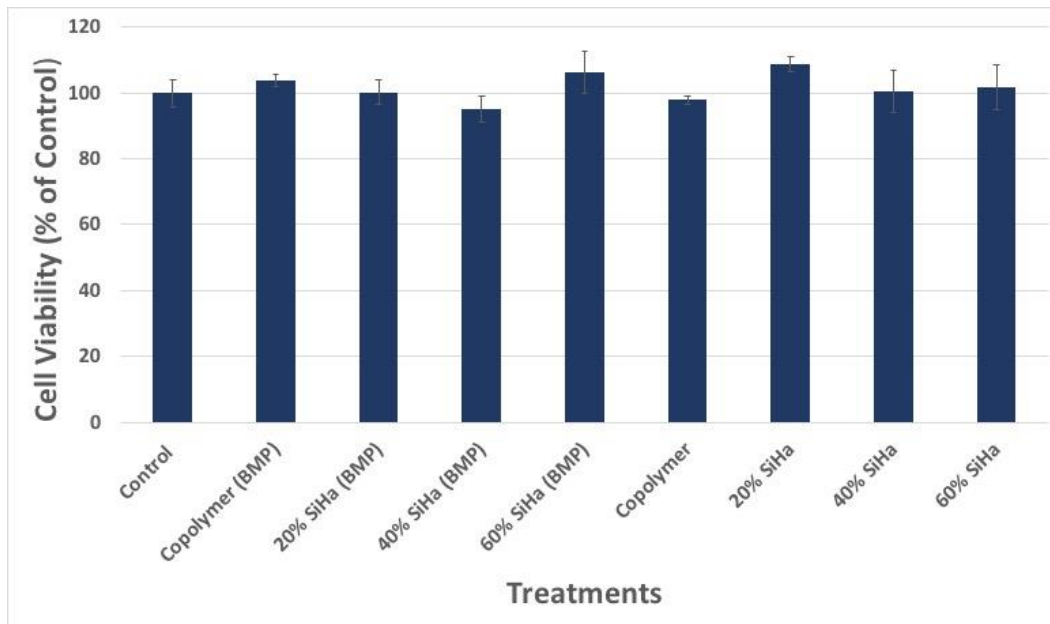
Fig: 5.44. Proliferation of cells on different scaffolds (Day 7)

There was no statistically significant difference between BMPs coated and non-coated set of samples. Comparatively all the specimens showed ample cell proliferation rate with a slight difference in various samples, which showed that polymer and composite nanofibrous scaffolds provided a compatible environment for the adherence and proliferation of cells.

199

CHAPTER 6

DISCUSSION
&
CONCLUSIONS

6.1. DISCUSSION

Several synthetic and natural polymers are currently being used for the synthesis of GTR/GBR membranes to treat the periodontal defects; however the regenerative potential of these membranes remains unpredictable. Consequently there is substantial interest in further developments in regenerative techniques to improve outcomes and predictability (Bottino & Thomas, 2015). New materials are being investigated for their potential and bone substitutes such as HA and β-TCP has also been incorpoarted in order to increase the regenerative potential and to improve the mechanical properties (Wang et al., 2016; Gentile et al., 2011). Another possible enhancement is the addition of growth factors in the membranes for their release at the site to enhance regeneration (Shimauchi et al., 2013).

A further significant factor in tissue engineering is the production of 3D environment that mimics the ECM. This characteristic may be a crucial feature in determining the success or failure of a tissue engineering scaffold. In the recent past, scientists have shown huge interset in nanotechnology, specifically nanofibers, as a solution to develop tissue engineering scaffolds (Deitzel et al., 2002). At present, only a few processing techniques can successfully produce fibers, and subsequent scaffolds, on the nanoscale. Conventional polymer processing techniques have difficulty in producing fibers smaller than 10 μm in diameter. Of the three commonly used techniques, electrospinning is considered the most effective and friendly method to generate nanofibers. For this reason electrospinning has extensively been used by the researchers to more adequately simulate the ECM geometry (Barnes et al., 2007).

201

Chitosan a natural occurring polymer has gained enormous interest as future material for the synthesis of GTR/GBR scaffolds. Although to date the chitosan based GTR/GBR membranes are still in the animal trial phase, however, the results showed great potential of this material in GTR/GBR procedures (Xu et al., 2012; Wang et al., 2016). A number of *in vitro* and animal studies have evaluated the regenerative potential of chitosan based membranes (Yeo et al., 2005; Kuo et al., 2006; Hong et al., 2007; Ho et al., 2010). In recent times, a few attempts have been made to prepare chitosan-based nanofibrous scaffolds by electrospinning, with very promising results (Ohkawa et al., 2004; Duan et al., 2004; Bhattaraia et al., 2005). Alginate alone has not been used commonly for the development of GTR/GBR membranes however; it has extensively been blended with other polymers to produce GTR/GBR scaffolds (Ueyama et al., 2002; Han et al., 2010). Elctrospinning of alginate alone (Nie et al., 2008) and alginate and chitosan has also been attempted with considerably good results (Chang et al., 2012; Jeong et al., 2011).

HA is considered the material of choice for various biomedical applications and has been incorporated into natural and synthetic polymers by many researchers to produces GTR/GBR scaffolds (Yang et al., 2008; Yang et al., 2009; Liao et al., 2015). Nevertheless Si-HA has not been used by any researcher for the synthesis of GTR/GBR scaffold, however, a range of recent studies have reported that Si-substituted HA has superior bioactivity both *in vitro* and *in vivo*. Thus making Si-substituted HA an attractive and innovative material for enhancing bone growth (Patel et al., 2002; Thian et al., 2005; Hing et al., 2006; Balamurugana et al., 2008).

202

Therefore, in the present study a 3D GTR/GBR scaffold was succesfully fabricated from the combination of Silicon substituted hydorxyapatite (Si-HA) and natural polymers (chitosan-alginate-gelatin) by electrospinning. Chitosan (DD 70 to 80%) was extracted from a local source and purified. FTIR of the resultant chitosan confirmed its elemental composition. The characteristic absorption bands of chitosan at 1652 cm^{-1}, 1598 cm^{-1}, and 1320 cm^{-1} represented the amide I, amide II and amide III band, respectively. The characteristic absorption bands at 1,652 cm^{-1} and 1,598 cm^{-1} overlapped each other. The peaks between 4000 cm^{-1} to 3000 cm^{-1} represented the OH and NH stretching vibrational peaks. At 2907cm^{-1} CH_2 bending occurred and at 1145 cm^{-1} C-O-C stretching took place. Chitosan showed C-O stretching and C-O skeletal vibrations at 1085 cm^{-1} and 1035 cm^{-1} respectively as shown in figure 5.1.

Copolymer of alginate and chitosan was prepared by chemical reaction in order to combine the beneficial properties of both natural polymers. The FT-IR spectrum (Fig: 5.5) of blend membrane (chitosan/alginate 1:1) revealed differences from pure Chitosan (Fig: 5.1) and Sodium Alginate (fig: 5.2) membranes spectra. Chitosan, alginate and their blend displayed characteristic absorption bands between 3400 cm^{-1} and 3450 cm^{-1}, which represent the –OH and –NH_2 groups in free as well as in amide form in chitosan. The –OH and –NH_2 groups in chitosan may form hydrogen bonds with –C=O and –OH groups of alginate. The characteristic absorption band 3350 cm^{-1} in chitosan membrane shifted to 3328 cm^{-1}. It can be observed that the chemical reaction completely changed the nature of both chitosan and alginate. Such modification of the alginate was desired because alginate is naturally non-adhesive to cells. Chemical bonding of alginate with chitosan in the form of a copolymer was expected to exihibit better cell adhesion due to the ability of

203

the positively charged chitosan to absorb serum proteins. In addition, due to the interaction between the amine group in the chitosan and carboxyl group in alginate the resultant polysaccharide ionic complex becomes insoluble in water (Jeong et al., 2011). This phenomenon makes the GTR/GBR scaffolds more stable in the wet environment of the oral cavity.

When silicon subsituted hydroxyapatite (Si-HA) was added into the copolymer of chitosan and alginate the FTIR spectra of composite scaffolds showed various changes (fig: 5.10, 5.11, and 5.12). The amide-I peak shifted from 1635 cm^{-1} to 1641 cm^{-1}, whereas amide 2 was shifted from 1557 cm^{-1} to 1573 cm^{-1} and the peak of the amino 3 was negligibly small. Shifting of the bands in IR spectra of composite nanofibrous scaffolds suggested that there may be some chemical bonding between polymer and Si-HA interface. Such interaction between HA and chitosan-alginate-gelatin polymer has previously been reported (Sharma et al., 2016). Addition of inorganic nanostructures in biodegradable polymers could be an important option to increase and modulate mechanical, electrical and degradation properties. The interface adhesion between nanoparticles and polymer matrix is the major factor affecting the properties of resultant composite (Armentano et al., 2010; Li et al., 2008).

Synthesis of nanofibers of chitosan-alginate copolymer and Si-HA was the main aim of the present study, however, there are enormous challenges in converting a bulk Si-HA/copolymer nanocomposite or hybrid into a fibrous form by electrospinning owing to poor electrospinnability of the chitosan itself as well as the adverse effect of the non-electrospinnable Si-HA nanoparticles (and their aggregates) contained in the spinning dope (Venugopal et al., 2010). As a result of these reported obstacles in electrospinning,

204

until now few attempts have been made to generate nanofibrous scaffolds using HA/Chitosan for bone tissue engineering (Rusu et al., 2005; Yang et al., 2008; Yang et al., 2009). Addition of an ultra-high-molecular-weight polyethylene oxide (PEO) as the fibre-forming aiding agent, (Zhang et al., 2008; Jeong et al., 2011) established that nanofibres could be generated easily with a minimum PEO loading ratio of up to 5 wt%. This made it possible to develop HA/Chitosan composite nanofibres for potential application in GTR/GBR.

In the current study, gelatin was used instead of PEO as electrospinning aiding agent because the aim of the study was to use natural polymers. Moreover, addition of high molecular weight fiber aiding agent could restrain multi-layer growth of cells. Conditions were optimized using different concentrations of the gelatin in copolymer solution until the nano scale fibers were produced. Optimization included systematically adjusting the solute concentration, flow rate; working distance and voltage of the electrospinning platform to yield electrospun fibers that were continuous, uniform in shape and without beading (Frohbergh et al., 2012). In the current study 3.5g (17.5% wt/v) of gelatin was added to 1.497g (7.48% wt/v) of copolymer, which makes the 70:30 ratio of gelatine and copolymer respectively in the resultant solution used for electrospinning to generate nanofibers. Effect of gelatin concentration on the morphology of the chitosan–gelatin blend electrospun fibers has previously been investigated by Jafari et al., (2011) and reported that 30% chitosan and 70% gelatine sample formed the smallest amount of beads and droplet and generated fibers with the highest morphological uniformity due to the decreased viscosity of the chitosan-gelatin blend. Low viscosity improves the capability of the electric field to form Tayler cone and polymer jet, thus making bead free

205

nanofibers. In this study one step electrospinning was performed by completely dissolving the copolymer and gelatin and dispersing the Si-HA homogenously which allowed the formation nanofibers with Si-HA particles incorporated on the surface of nanofibers.

SEM micrographs of membranes of copolymer (chitosan-alginate) (fig: 5.18) revealed a homogenous surface morphology having striated surface. These are typical morphological structure found in chitosan-alginate because these are oppositely charged polymers (Yan et al., 2001). Similarly, the chitosan-alginate-gelatin copolymer (fig: 5.19) membranes also showed a homogenous smooth surface. SEM images of the composite membranes with different concentrations of HA (20%, 40%, 60% wt%) showed that addition of HA and Si-HA significantly altered the surface morphology of composite membranes. The surface of the composite membranes as shown in figures 5.20 to 5.25 became rougher with the increasing concentration of HA and Si-HA contents and some small irregular pores appear on the surface. The porous structure of the chitosan-alginate/HA composite membranes would be likely to increase the number of cells adhering to the membranes on implantation at defect sites as GTR/GBR barrier and improve the membrane-tissue attachment by allowing the tissue to infiltrate. In addition, the interconnecting porous network in the membranes may be helpful to the circulation of body fluid and blood (Karageorgiou & Kaplan, 2005). However, the porous structure of the composite membranes could result in reduced mechanical properties compared to pure copolymer membranes (Teng et al., 2009; Xianmiao et al., 2009). The chitosan-alginate-gelatin and Si-HA composite membranes showed more irregularities and aggregates of Si-HA on the surface with increasing ratio of Si-HA compared to

206

copolymer-HA membranes most probably due to the larger particle size of the Si-HA used (441.37±130.84 nm).

SEM of fibrous scaffolds showed randomly oriented fibers with diameter ranging from 61.75 nm to 546.72 nm (fig: 5.26, 5.27). This huge inconsistency and heterogenecity in the size of ectrospun nanofibers has been reported before and may be caused by the inhomogenecity of the different batches of the solutions prepared at different times (Cai et al., 2010). The nanofibers exhibited high porosity and high spatial interconnectivity. High porosity means a high surface area/volume ratio, consequently supporting cell adhesion and proliferation. This property of the scaffold favors and promotes bone tissue regeneration (Thien et al., 2013). In composite scaffolds Si-HA particles were also evident embedded into the fibers and dispersed homogenously on the surface of the scaffold making the suface of the scaffold rougher compared to copolymer scaffold. This roughnes and presence of biological active Si-HA particles are vital features to make the scaffold suitable for GTR/GBR (Sharma et al., 2016).

The EDS spectra of copolymer (fig: 5.28) and composite nanofibers with 20%, 40% and 60% Si-HA (fig: 5.31, 5.34, 5.37) established the presence of main elemental components of chitosan (i.e, Carbon, Oxygen). Moreover, peaks of Calcium, phosphorous and silica were also detected which confirmed the presence of Si-HA in composite scaffolds. In the FTIR spectra of composite nanofibers as shown in figure 5.10 bands at 1035cm^{-1} to 1040cm^{-1} were characteristic band of phosphate bending vibration in Si-HA while the absorption band at around 4000 cm^{-1} was assigned to a hydroxyl group in Si-HA.

Mechanical properties of GTR/GBR scaffolds play essential role in clinical outcomes. Ideally, a GTR/GBR scaffold should be able to withstand the overlaying tissue and masticatory forces. This property becomes more decisive when GTR/GBR scaffold is used to cover a large defect without bone graft. Natural polymers have an inborn limitation of poor mechanical properties. The strength and stiffness of the natural polymer based scaffolds could be increased by incorporating inorganic fillers. It has been observed that mechnanical strength of natural polymer based scaffolds was significantly improved when bone ceramics were integrated into the fibrous scaffolds (Muzzarelli, 2011; Thien et al., 2013; Sharma et al., 2016). However, the addition of the inorganic fillers may increase the stiffness of the scaffolds but at the same time could make it more brittle and less adaptable. Furthermore, due to the brittleness of the HA and lack of interaction with polymer, the HA nanoparticles may cause harmful effects on the mechanical properties of composite scaffold when added in high concentrations (Armentano et al., 2010).

In order to appropriatory transfer the masticatory load to the adjacent tissue; the mechanical properties of the GTR/GBR scaffold should closely match the host bone. The mechanical properties of the natural bone vary considerably depending upon the type of the bone. The compressive strength of cortical bone ranges from 100 to 200 Mpa whereas the cancellous bone possesses compressive strength of 2 to 20 Mpa (Saravanan et al., 2016). Chitosan and alginate have low to moderate compressive strength therefore, to overcome the inherent low mechanical properties Si-HA was incorporated in the nanofibrous scaffold. In the present study tensile strength and % elongation of copolymer and composite scaffolds were assessed. The results revealed that the tensile strength of

208

the composite scaffolds showed great dependence on the Si-HA contents. The tensile strength was increased from 0.825 MPa to 1.595 MPa as the concentration of Si-HA was amplified from 20 % to 60% by weight. The interaction among Si-HA, chitosan, alginate and gelatin might also have played a role in the improvement of tensile strength. Alginate and gelatin is anionic while chitosan is cationic in nature at physiological pH, therefore, they demonstrate an electrostatic interaction. In addition, the possible interactions among the NH_3+ group of chitosan with Ca^{2+} and PO4 $^{3-}$ ions and –OH group of HA had already been reported by a number of investigators (Pramanik et al., 2009; Sharma et al., 2016). This interaction is evident from the shifting of the bands in IR septra as mentioned earlier and might be responsible for the formation of more compact and mechanically stable scaffold structure. Another reason of the increased tensile strength of the composite scaffolds could be the decrease in porosity due to the addition of Si-HA particles.

In contrast to tensile strength, the % elongation at break was decreased in composite scaffolds. There was a significant difference in % elongation between copolymer and composite scaffolds with 60% Si-HA. The copolymer showed 4 times increased elongation compared to composite scaffold with 60% Si-HA. However, in case of 20% Si-HA composite scaffold the difference in % elongation was reduced to 1.5 times, which suggested that at low concentrations the particles of Si-HA could disperse homogenously in copolymer (Teng et al., 2009; Li et al. 2012). While at high concentrations Si-HA may reduce the hydrogen bond interaction among chitosan molecules and breaks the structure and crystallinity of chitosan. In addition, due the larger particle size (441.37±130.84) of the Si-HA used for the synthesis of composite scaffold more aggregates (fig: 5.35, 5.35) of Si-HA particles were formed at high concentration which resulted in increased

209

brittleness of composite scaffolds. Over all the scaffolds exhibited modest mechanical properties which may be due the abscence of high molecular weight fiber aiding agents (PEO) and lack of cross-linking between chitosan and gelatin. On top, incorporation of Si-HA particles into the molecular structure of copolymer might have disrupted the molecular chain leading to reduced mechnanical strength of scaffolds.

Water uptake is an important phenomenon in the field tissue engineering particularly when the scaffold has to perform in the oral cavity. A biopolymer matrix containing an adequate amount of water shows similar properties to living tissue in terms of physiological stability, low interfacial tension, and permeability. A controlled rate of swelling of GTR/GBR scaffolds is always desired. Uptake of the fluids by scaffold makes it more pliable and adaptable, increases the pore size and total porosity, maximize the surface area/volume ratio. The swelling behavior of the GTR/GBR scaffolds also help to understand the absorption and diffusion of medium and nutrients into the scaffold which are essential for cell viability. However, excessive fluid contents could lead to poor mechanical properties.

Swelling behaviour of copolymer and composite scaffolds was assessed. The results uncovered that composite scaffolds exhibited considerably less water uptake as the concentration of Si-HA increased with lowest percentage swelling was demonstrated by the composite scaffolds containing 60% Si-HA. The swelling behaviour of polymers is dependent on the ionisable groups in the structure of polymer and surrounding medium. Chitosan chains swell due to the mechanical relaxation of coiled chains as a result of protonation of amine groups. Chitosan can also form hydrogen bond with water. This decrease in water uptake by composite scaffolds may be ascribed to the lower

210

hydrophilicity of the inorganic phase as compared to the polymer matrix. In addition the likely interaction between chitosan and Si-HA as evident by the shifting of the bands in FTIR could also reduce the hydrogen bonding between water and chitosan thus decreasing the water uptake (Li et al., 2012).

The effect of the nanofibrous scaffolds with different concentrations of Si-HA on cell proliferation and differentiation was tested. It is known that the initial cell adhesion to a material is important, because it greatly influences the succeeding processes of cell proliferation and differentiation (Dalby et al., 2002; Verrier et al., 2004). In this experimental study, MC3T3-E1 cells showed a normal morphology and growth in the presence of copolymer and composite scaffolds with different concentrations of Si-HA as compared to control. MTT assay showed no toxic effect, and cells were found viable which demonstrates this material provide a normal environment in which osteoblasts can grow and proliferate. However, results failed to show any significant difference in cell proliferation on copolymer and composite scaffolds containing Si-HA. These results match with the other studies which reported no significantly higher cellular response in composite scaffolds containing HA (Song et al., 2007; Kino et al., 2007; Kareem et al., 2019). However, some investigators have reported higher cellular activity on composite scaffolds containing nanoparticles of HA (Tetteh et al., 2014; Bianco et al., 2009; Fu et al., 2017; Peng et al., 2012). Current study was unable to demonstrate that the presence of bioactive Si-HA could promote the cell proliferation may be due to the detachment of the Si-HA particles from the surface of nanofibers and early degradation of nanofibers making it impossible to make the exact cell count in the presence of Si-HA particles.

A set of specimen was coated with BMPs to see the effects of growth factors adsorbed on the surface of nanofibers. The retention of the BMPs in a delivery system may be performed by various methodologies by means of adsorption, entrapment or immobilization, or by covalent binding. The easiest way to deliver the growth factor is adsorbing BMPs to the surface of the scaffold (Begam et al., 2017). Although BMPs coated composite scaffolds with 60% Si-HA showed highest cell proliferation rate on day 1 and 7, however, almost similar rate of proliferation was also observed in non-coated samples with 20% Si-HA. Therefore, BMPs could not exhibit any significant effect on cell proliferation in the present study.

BMPs have extensively been investigated in periodontal regeneration. Among synthetic polymers PCL, PEG and PLGA are extensively used as BMPs delivery systems and are also combined with other osteoinductive materials such as HA and TCP. The results indicated an enhanced cellular attachment and proliferation in BMPs loaded scaffolds (Kaito et al., 2005; Fu et al., 2008; Zhang et al., 2010; Schofer et al., 2011). Chitosan based scaffolds have previously been investigated as BMP delivering strategy, particularly in composites with other synthetic or natural polymers and bone ceramics and had revealed enormous regenerative potential (Yilgor et al., 2009; Soran et al., 2012; He et al., 2014). BMPs could not show any significant effect on cell proliferation in the present study. These results are in contrast to the previous studies as mentioned earlier that reported a significantly higher cell proliferation. One of the reasons could be the method of incorporating BMPs, although adsorbing proteins on the surface of scaffold may be the easiest way to deliver growth factors and nanofibrous scaffolds had demonstrated a higher amount of adsorbed growth factors due to larger surface area,

212

however, this method of BMPs addition may lead to poor control on release kinetics and could be unsuccessful to achieve the desired biological effects (Hu & Ma, 2011). In addition low stability and high hydrophilicity of the chitosan-alginate-gelatin copolymer could be another reason.

213

6.2. CONCLUSIONS

Chitosan was successfully extracted from indigenous source with a degree of deacetylation from 70 to 80%.

Co-biopolymer of chitosan and alginate was effectively created by hydrolysis method.

Membranes comprised of copolymer/hydroxyapatite (HA) and copolymer/silicon-substituted hydroxyapatite (Si-HA) were synthesized, where the concentration of HA and Si-HA was 20%, 40%, and 60% wt/v.

Nanofibrous composite scaffolds based on coopolymer and Silicon-substituted HA were successfully generated by electrospinning.

Spectroscopic analysis i.e. FTIR confirmed the synthesis of chitosan and biopolymer-based composite.

SEM and EDS analysis showed the presence of HA and Si-HA in polymeric network and with the increase in the concentration of bioactive fillers, change in intensity with EDS spectra were observed.

The composite scaffolds exhibited a noticeably less water uptake as the concentration of Si-HA was amplified.

Compared to copolymer scaffolds tensile strength of composite scaffolds was increased by increasing the concentration of inorganic filler while % elongation was decreased. Overall, the nanofibous scaffolds synthesized in the present study exhibited modest mechanical properties.

214

Cytocompatibility was confirmed when biopolymers were treated with Mouse pre-osteoblast cell line MC3T3 and it was observed that copolymer and composite nanofibrous scaffolds provided a compatible environment for the adherence and proliferation of cells. However, addition of bioactive fillers and growth factors (BMPs) could not increase cell viability.

Although the overall results of the study suggests that chitosan-alginate-Si-HA based nanofibrous scaffols could be good candidates for GTR/GBR applications, however, further work needs to be done in order make it suitable for clinical use.

6.3. FUTURE WORK

The ultimate potential of the GTR/GBR scaffolds can be tested effectively in animal models and human clinical trials. Therefore, a number of studies are required to further test these scaffolds in clinical settings. At the same time some aspects of *in vitro* testing also needs to be addressed.

Additional work is needed to improve the reliability in the manufacturing of nanofibrous scaffolds particularly the parameters which can be used to produce scaffolds with uniform nanofibers. Studies are required to optimize the processing parameters in order to control the variations in fibers diameters and dispersion of the inorganic filler.

The ability of nanofibrous scaffolds to carry and release growth factors needs to be investigated further. Multilayered scaffolds consisting of different surfaces may be fabricated to test the controlled and directional release of growth factors.

215

Long term degradation studies are required to assess the stability of the scaffolds in oral environment. In addition, effects of temperature and pressure on degradation should be analyzed.

Mechanical properties of the scaffolds should be optimised by adjusting the concentration of inorganic fillers and crosslinking the biopolymers.

Finally, the suitability of scaffolds for GTR/GBR procedures needs to be evaluated *in vivo* clinical trials.

REFRENCES

- Armentano, I., Dottori, M., Fortunati, E., Mattioli, S., Kenny, J.M. (2010). Biodegradable polymer matrix nanocomposites for tissue engineering: A review. *Polymer Degradation and Stability,* 95: 2126-2146.

- Bhattaraia, N., Edmondsona, D., Veiseha, O., Matsenb, F.A., Miqin Zhanga, (2005). Electrospun chitosan-based nanofibers and their cellular compatibility. *Biomaterials,* 26: 6176–6184.

- Bianco, A., Federico, D.I., Moscatelli, E., Camaioni, I., Armentano, A., Campagnolo, I., Dottori, L., Kenny, M., Siracusa, G., J.M., Gusmano, G., 2009. Electrospun poly(ε-caprolactone)/Cadeficient hydroxyapatite nanohybrids: Microstructure, mechanical properties and cell response by murine embryonic stem cells. *Material Science and Engineering: C,* 29: 2063–2071.

- Bottino, M.C., Thomas, V., Schmidt, G., Vohra, Y.K., Chu, T.G., Kowolik, M.J., Janowski, G.M. (2012). Recent advances in the development of GTR/GBR membranes for periodontal regeneration—A materials perspective. *Dental Materials,* 28: 703–721.

- Cai, Z.X., Mo, X.M., Zhang, K.H., Fan, L.P., Yin, A.L., He, C.L. Wang, H.S. (2010). Fabrication of chitosan/silk fibroin composite nanofibers for wound dressing application. *International Journal of Molecular Science,* 11: 3529-3539.

- Chang, J.J., Leeb, Y.H., Wua, M.H., Yanga, M.C., Chienc, C.T., (2012). Electrospun anti-adhesion barrier made of chitosan alginate for reducing peritoneal adhesions. *Carbohydrate Polymers*, 88:1304– 1312.

217

- Dalby, M.J., Di Silvio, L., Harper, E.J., Bonfield, W. (2002). *In vitro* adhesion and biocompatability of osteoblast-like cells to poly(methylmethacrylate) and poly(ethylmethacrylate) bone cements. *Journal of Materials Science,* 13:311-314.

- Deitzel, J.M., Kosik, W., McKnight, S.H., Ten, N.C.B., Desimone, J.M., Crestte, S. (2002). Electrospinning of polymer nanofibers with specific surface chemistry. *Polymer,* 43(3):1025-1029.

- Duan, B., Dong, C.H., Yuan, X.Y., Yao, K.D. (2004) Electrospinning of chitosan solutions in acetic acid with poly(ethylene oxide). Journal of Biomaterial Science-Polymer edition, 15:797-811.

- Frohbergh, M.E., Katsman, A., Botta, G.P., Lazarovici, P., Schauer, C.L., Wegst, U.G.K., Lelkes, P.I. (2012) Electrospun hydroxyapatite-containing chitosan nanofibers crosslinked with genipin for bone tissue engineering. Biomaterials, 33: 9167-9178.

- Fu, C., Bai, H., Zhu, J., Niu, Z., Wang, Y., Li, J., Yang, X., Bai, Y. (2017). Enhanced cell proliferation and osteogenic differentiation in electrospun PLGA/hydroxyapatite nanofiber scaffolds incorporated with grapheme oxide. *PLoS One*, 12(11): e0188352.

- Fu, Y.C., Nie, H., Ho, M.L., Wang, C.K., Wang, C.H. (2008). Optimized bone regeneration based on sustained release from three-dimensional fibrous PLGA/Hap composite scaffolds loaded with BMP-2. *Biotechnology and Bioengineering*, 99(4): 996-1006.

- Gentile, P., Chiono, V., Tonda-Turo, C., Ferreira, A.M., Ciardelli, G. (2011). Polymeric membranes for guided bone regeneration. *Biotechnology Journal*, 6: 1187–1197.

- Han, J., Zhou, Z., Yin, R., Yang, D., Nie, J. (2010). Alginate-chitosan/ hydroxyapatite polyelectrolyte complex porous scaffolds: Preparation and characterization. *International Journal of Biological Macromolecules,* 46:199-205.

- He, X., Liu, Y., Yuan, X., Lu, L. (2014). Enhanced healing of rat calvarial defects with MSCs loaded on BMP-2 releasing Chitosan/Alginate/Hydroxyapatite scaffolds. *PLoS ONE,* 9(8):e104061.

- Ho, M.H., Hsieh, C.C., Hsiao, S.W., Thien, D.V.H. (2010) Fabrication of asymmetric chitosan GTR membranes for the treatment of periodontal disease. *Carbohydrate Polymers,* 79:955–963.

- Hong, H., Wei, J., Liu, C. (2007). Development of asymmetric gradational-changed porous chitosan membrane for guided periodontal tissue regeneration. *Composites: Part B,* 38:311–316.

- Hu, J., Ma, P.X. (2011). Nano-fibrous tissue engineering scaffolds capable of growth factor delivery. Pharmaceutical research, 28:1273-1281.

- Jafari, j., Hojjati, E.S., Ali, S., Ali, B.M., Fazel, G. (2011). Electrospun chitosan-gelatin nanofibrous scaffold: fabrication and *in vitro* evaluation. *Bio-Medical Materials and Engineering,* 21(2): 99-112.

- Jeong, S.I., Kerbs, M.D., Bonino, C.A., Samorezov, J.E., Khan, S.A., Alsberg, E. (2011). Electrospun chitosan-alginate nanofibers with in situ polyelectrolyte

219

complexation for use as tissue engineering scaffolds. *Tissue Engineering Part A,* 1-2:59-70.

- Kaito, T., Myoui, A., Takaoka, K., Saito, N., Nishikawa, M., Tamai, N., Ohgushi, H., Yoshikawa, H. (2005). Potentiation of the activity of bone morphogenetic protein-2 in bone regeneration by a PLA-PEG/hydroxyapatite composite, *Biomaterials,* 26:73–79.

- Karageorgiou, V., Kaplan, D. (2005). Porosity of 3D biomaterial scaffolds and osteogenesis. *Biomaterials,* 26: 5474-5491.

- Kareem, M.M., Hodgkinson, T., Sanchez, M.S., Dalby, M.J., Tanner, K.E. (2019). Hybrid core shell scaffolds for bone tissue engineering. *Biomedical Materials*, 14(2): 025008. doi: 10.1088/1748-605X/aafbf1.

- Kino, R., Ikoma, T., Yunoki, S., Nagai, N., Tanaka, J., Asakura, T., Munekata, M. (2007). Preparation and characterization of multilayered hydroxyapatite/silk fibroin film. *Journal of Bioscience and Bioengineering*, 103(6):514-520.

- Kuo, S.M., Chang, S.J., Chen, T.W., Kuan, T.C. (2006). Guided tissue regeneration for using a chitosan membrane: An experimental study in rats. *Journal of Biomedical Research*, 76(2):408-415.

- Li, J., Lu, X.L., Zheng, Y.F. (2008). Effect of surface modified hydroxyapatite on the tensile property improvement of HA/PLA composite. *Applied Surface Science,* 255:494-497.

- Liao, H., Shi, K., Peng, J., Qu, Y., Liao, J., Qian, Z. (2015). Preparation and properties of nano-hydroxyapatite/Gelatin /Poly(vinyl alcohol) composite membrane. *Journal of Nanoscience and Tecnology,* 15(6):4188-4192.

220

- Muzzarelli, R.A.A. (2011). Chitosan composite with inorganics, morphogenetic proteins for bone regeneration. *Carbohydrate Polymer,* 83: 1433-1445.

- Nie, H., He, A., Zheng, J., Xu, S., Li, J., Han, C.C. (2008). Effects of Chain Conformation and Entanglement on the Electrospinning of Pure Alginate *Biomacromolecules,* 9: 1362–1365.

- Ohkawa, K., Cha, D.I., Kim, H., Nishida, A., Yamamoto, H. (2004). Electrospinning of chitosan. *Macromolecular Rapid Communications*, 25: 1600-1605.

- Peng, H., Yin, Z., Liu, H., Chen, X., Feng, B., Yuan, H., Su, B., Quyang, H., Zhang, Y. (2012). Electrospun biomimetic scaffolds of hydroxyapatite / chitosan supports enhanced osteogenic differentiation of mMSCs. *Nanotechnology*, 23(48):485102 doi: 10.1088/0957-4484/23/48/485102.

- Pramanik, N., Mishra, D., Banerjee, I., Maiti, T.K., Bhargava, P., Pramanik, P. (2009). Chemical synthesis, characterization and biocompatibility study of hydroxyapatite/chitosan phosphate nanocomposite for bone tissue emgineering application. *International Journal of Biomaterials,* 53: 1-8.

- Rusu, V. M., Ng, C. H., Wilke, M., Tiersch, B., Fratzl, P. Peter, M. G. (2005). Size-controlled hydroxyapatite nanoparticles as self-organized organic–inorganic composite materials. *Biomaterials*, 26:5414–5426.

- Saravanan, S., Leena, R. S., Selvamurugan, N. Chitosan based biocomposite scaffolds for bone tissue engineering. *International Journal of Biological Macromolecules,* 93: 1354-1365.

- Schofer, M.D., Roessler, P.P., Schaefer, J., Theisen, C., Schlimme, S., Heverhagen, J.T., Voelker, M., Dersch, R., Agarwal, S., Fuchs-Winkelmann, S., Paletta1, J.R.J. (2011). Electrospun PLLA nanofiber scaffolds and their use in combination with BMP-2 for reconstruction of bone defects. *PLoS ONE,* 6(9):e25462.

- Sharma, C., Dinda, A.K., Potdar, P.D., Chou, C.F., Chandra, N. (2016). Fabrication and characterization of novel nano-biocomposite scaffold of chitosan-gelatin-alginate-hydroxyapatite for bone tissue engineering. *Material Science and Engineering:C,* 64: 416-427

- Shimauchi, H., Nemoto, E., Ishihata, H., Shimomura, M. (2013). Possible functional scaffolds for periodontal regeneration. *Japanese Dental Science Review,* 49(4): 118-130.

- Song, J.H., Kim, H.E., Kim, H.W. (2007). Collagen-apatite nanocomposite membranes for guided bone regeneration. *Journal of Biomedical Materials research Part B: Applied Biomaterials,* 83(B):248-257.

- Soran, Z., Aydm, R.S.T., Gümüşderedlioğlu, M. (2012). Chitosan scaffolds with BMP-6 loaded alginate microspheres for periodontal tissue engineering. *Journal of Microencapsulation,* 29(8): 770-780.

- Teng, S.H., Lee, E.J., Yoon, B.H., Shin, D.S., Kim, H.E., Oh, J.S. (2009). Chitosan/nanohydroxyapatite composite membranes via dynamic filtration for guided bone regeneration. *Journal of Biomedical Material Research*, 88A: 569–580.

- Tetteh, G., Khan, A.S., Delaine-Smith, R.M., Reilly, G.C., Rehman, I.U. (2014). Electrospun polyurethane/hydroxyapatite bioactive scaffolds for bone tissue engineering: the role of solvent and hydroxyapatite particles. *Journal of the Mechanical Behavior of Biomedical Materials,* 39:95-110.

- Thien, D.V.H., Hsiao, S.W., Ho, M.H., Li, C.H., Shih, J.L. (20130. Electrospun chitosan/hydroxyapatite nanofibers for bone tissue engineering. *Journal of Materials Science,* 48:1640-1645.

- Venugopal, B. J., Prabhakarani, M.P., Zhang, Y., Low, S., Choon, A.T., Ramakrishna, S. (2010). Biomimetic hydroxyapatite-containing composite nanofibrous substrates for bone tissue engineering *Philosophical Transactions of the Royal Society A,* 368: 2065–2081.

- Verrier, S., Blaker, J.J., Maquet, V., Hench, L.L., Boccaccini. A.R. (2004). Pdlla/bioglass composites for soft-tissue and hard-tissue engineering: An in vitro cell biology assessment. *Biomaterials,* 25:3013-3021.

- Wang, J., Wang, L., Zhou, Z., Lai, H., Xu, P., Liao, L., Wei, J. (2016). Biodegradable Polymer Membranes Applied in Guided Bone/Tissue Regeneration: A Review. *Polymers,* 8 (4): 115-135.

- Xianmiao, C., Yubao, L., Yi, Z., Li, Z., Jidong, L., Huanan, W. (2009). Properties and in vitro biological evaluation of nano-hydroxyapatite/chitosan membranes for bone guided regeneration. *Materials Science and Engineering C,* 29:29–35.

- Xu, C., Lei, C., Meng, L., Wang, C., Song, Y. (2012). Chitosan as a barrier membrane material in periodontal tissue Regeneration *Journal of Biomedical Materials Research Part B Applied Biomaterials*, 100(5):1435-1443.

- Yang, D. Z., Jin, Y., Ma, G. P., Chen, X. M., Lu, F. M., Nie, J. (2008). Fabrication and characterization of chitosan/PVA with hydroxyapatite biocomposite nanoscaffolds. *Journal of Applied Polymer Science,* 110: 3328–3335.

- Yang, F., Both, S.K., Yang, X., Walboomers, X.F., Jansen, J.A. (2009). Development of an electrospun nano-apatite/PCL composite membrane for GTR/GBR applications. *Acta Biomaterialia,* 5:3295-3304.

- Yeo, Y.J., Jeon, D.W., Kim, C.S., Choi, S.H., Cho, K.S., Lee, Y.K., Kim, C.K. (2005). Effects of Chitosan nonwoven membrane on periodontal healing of surgically created one-wall intrabony defects in Beagle dogs. *Journal of biomedical materials research Part B Applied Biomaterials,* 72(1):86-93.

- Yilgor, P., Tuzlakoglu, K., Reis, R.L., Hasirci, N., Hasirci, V. (2009). Incorporation of a sequential BMP-2/BMP-7 delivery system into chitosan-based scaffolds for bone tissue engineering. *Biomaterials,* 30: 3551–3559.

- Zhang, Y. Z., Su, B., Ramakrishna, S., Lim, C. T. (2008). Chitosan nanofibers from an easily electrospinnable UHMWPEO-doped chitosan solution system. *Biomacromolecules,* 9:136–141.

- Zhang, H., Migneco, F., Lin, C.Y., Hollister, S.J. (2010) Chemically-Conjugated Bone Morphogenetic Protein-2 on Three-Dimensional Polycaprolactone

Scaffolds Stimulates Osteogenic Activity in Bone Marrow Stromal Cells. *Tissue engineering Part A,* 16(11): 3441-3448.